Winter 2008

Evaluation of multiple small volume aquaculture cage systems

Ryan R. Despins
University of New Hampshire, Durham

EVALUATION OF MULTIPLE SMALL VOLUME AQUACULTURE CAGE SYSTEMS

BY

RYAN R. DESPINS
B.S., University of New Hampshire, 2007

THESIS

Submitted to the University of New Hampshire
in Partial Fulfillment of
the Requirements for the Degree of

Master of Science
in
Ocean Engineering

December, 2008

This thesis has been examined and approved.

Thesis Director, Barbaros Celikkol
Professor of Mechanical Engineering

Kenneth C. Baldwin
Professor of Mechanical and Ocean Engineering

M. Robinson Swift
Professor of Mechanical and Ocean Engineering

Igor I. Tsukrov
Associate Professor of Mechanical Engineering

Date

ACKNOWLEDGEMENTS

I would like to thank all of the people who have helped me throughout the course of my master's career. To my friends and family who have given me their continued support and guidance when I needed it most. To Jud DeCew for answering all my little questions day in and day out. And to Professors Rob Swift, Barbaros Celikkol, Ken Baldwin, and Igor Tsukrov for their assistance in strengthening my education.

To everyone I have listed above and anyone who I have failed to mention, please accept my sincere and gracious thanks for your support.

TABLE OF CONTENTS

LIST OF TABLES

LIST OF FIGURES

NOMENCLATURE

RAO	Response Amplitude Operator
RAO_{heave}	Heave RAO
RAO_{surge}	Surge RAO
RAO_{pitch}	Pitch RAO
RAO_{load}	Load RAO
η	Surface Elevation
H	Wave Height
k	Wave Number
x	Horizontal Position
σ	Wave Period
t	Time
Φ	Wave Slope
h	Water Depth
z	Depth from Water Surface
u	Horizontal Water Particle Velocity
ζ	Wave Excursion
To	Tension at the Origin
X_a	Horizontal Distance from Origin to Point A
Y_a	Vertical Distance from Origin to Point A
S_a	Length from the Origin to Point A
X_{ab}	Horizontal Distance from Point A to Point B
Y_{ab}	Vertical Distance from Point A to Point B
S_{ab}	Length from Point A to Point B
Φ_a	Angle of Vector T and T_{va}
T_{va}	Vertical Tension at Point A
T_{ha}	Horizontal Tension at Point A
T_{vb}	Vertical Tension at Point B
T_{hb}	Horizontal tension at Point B
P	Net Weight of Chain per Unit Length in Water

ABSTRACT

EVALUATION OF MULTIPLE SMALL VOLUME AQUACULTURE CAGE SYSTEMS

By

Ryan Despins

University of New Hampshire, December, 2008

The construction of the University of New Hampshire (UNH) American Soybean Association International Marketing (ASAIM) cage was documented and modifications were made to the original design. Testing included hydrostatics and solid modeling to ensure modifications would not violate cage parameters.

To test alternate mooring systems, the finite element package Aqua-FE was used. Five mooring designs (three for single cage, two for multi-cage systems) were reduced to two through an initial feasibility study. Results from AquaFE demonstrated that transverse loadings, loads applied perpendicular to the mooring, supplied higher anchor tensions and system motions than in-line loadings, loads applied parallel to the mooring.

The string mooring, a multi-cage design utilizing two main anchors at the fore and aft of the system and rope bridles to hold cages in-line, was identified as the best mooring configuration because it allowed for easy harvest, additional cages, and an even distribution of loads among the mooring lines.

CHAPTER I

INTRODUCTION

I.1. Background

In an effort to expand the domestic and international soybean market the American Soybean Association International Marketing (ASAIM) along with the U.S. Soybean Export Council (USSEC) pursued the use of soy based fish feed for use in aquaculture. One method to assist with soybean based product expansion was to develop a small volume fish cage for use in open ocean and high current environments. Soy based foods would then be utilized to feed the fish in the system. The cage was initially deployed three years ago off the coast of China. Since the near shore sites suffered from multi-use and environmental conflicts, the cage was deployed a few miles off shore in the South China Sea.

The University of New Hampshire's (UNH) Ocean Engineering Program partnered with ASAIM and began a series of studies on the ASAIM Ocean Cage Aquaculture Technology (OCAT) cage and mooring system. Risso (2007) investigated the operational limits which would aid in recommendations for improvements to the early designs. Risso determined through physical and numerical models that the ASAIM cage and single point mooring (SPM) cage

system was "appropriate for deployment at any variety of sites for which similar environmental parameters to those tested would be experienced." In December of 2007, UNH constructed a full scale OCAT system. Modifications to the original configuration were made during the building process to simplify the design while maintaining structural integrity. This cage is presently moored at the University of New Hampshire Open Ocean Aquaculture (OAA) site within its submerged mooring (Fredriksson et al. 2004).

One goal of ASAIM is to expand operations of the OCAT system to different countries and environments. This includes increasing biomass capacity as well as the versatility of the mooring. The original analysis, performed by Risso, was based on a single OCAT system in the SPM. Although the cage could submerge in high currents, the operations are mostly limited to areas of calmer seas. The SPM mooring allows only one cage to be moored. Thus, the OCAT system was investigated to determine if different mooring configurations could be used to allow for multi-cage systems to be deployed.

To perform the analysis, five mooring configurations were designed, three single cage and two multi-cage systems. A feasibility study was initiated utilizing a numerical modeling program called Aqua-FE. The cage response and mooring line loads were obtained. Based on these results, two mooring configurations, one single and one multi-cage, were modified and reanalyzed. In both cases, the OCAT cage was used as the net pen. Cage motion response in heave, surge, and pitch and critical mooring line tensions were of most importance.

I.2. Objectives

The objectives of this thesis were as follows:

- Document the design changes and construction of the OCAT cage performed by UNH personnel.
- Develop alternative mooring configurations for the ASAIM OCAT cage for single and multi-cage systems.
- Construct numerical models for the alternative mooring configurations utilizing the UNH OCAT cage as a blueprint.
- Perform an initial feasibility study on all mooring configurations using a "worst case scenario" loading in the UNH's finite element analysis (FEA) package, Aqua-FE.
- Analyze two mooring configurations for the single and multi-cage designs for motion and tension responses when subjected to a variety of dynamic loadings including currents and regular waves.
- Make final design recommendations.

I.3. Methodology

To better understand the OCAT cage dynamics, a hydrostatic analysis was performed using a mathematical software program MathCad. The hydrostatics determined key system parameters such as the OCAT's center of gravity (CG), center of buoyancy (CB), and overall system buoyancy. These results were utilized during the mooring configuration design process.

Three single cage and two multi-cage mooring configurations were then designed as alternatives to the SPM. A feasibility study was initiated analyzing the cage and mooring configurations under a "worst case condition", a 1.0 m/s current with the UNH storm wave condition. This study utilized a numerical modeling program developed at UNH specifically for aquaculture structures, Aqua-FE. The program is equipped to handle three dimensional models which may be subjected to large displacements and allow for stresses and displacements to be output for further investigation. Aqua-FE was used to determine key stresses in mooring and anchor lines as well as cage displacements for all tested mooring configurations.

To further describe the system's response to wave loadings, response amplitude operators (RAOs) were calculated. RAOs are a ratio of system response normalized by the forcing magnitude. These results were used to determine if the mooring designs performed adequately and could be used in the field.

CHAPTER II

UNH OCAT SYSTEM

II.1. ASAIM OCAT System

The ASAIM cage was designed as a high bio-mass density, small scale cage. The cage is a 4.5 meters tall truncated pyramid with a 7 by 7 meter base and a 2 by 2 meter top. The static waterline of the system was approximately half way up the top rim.

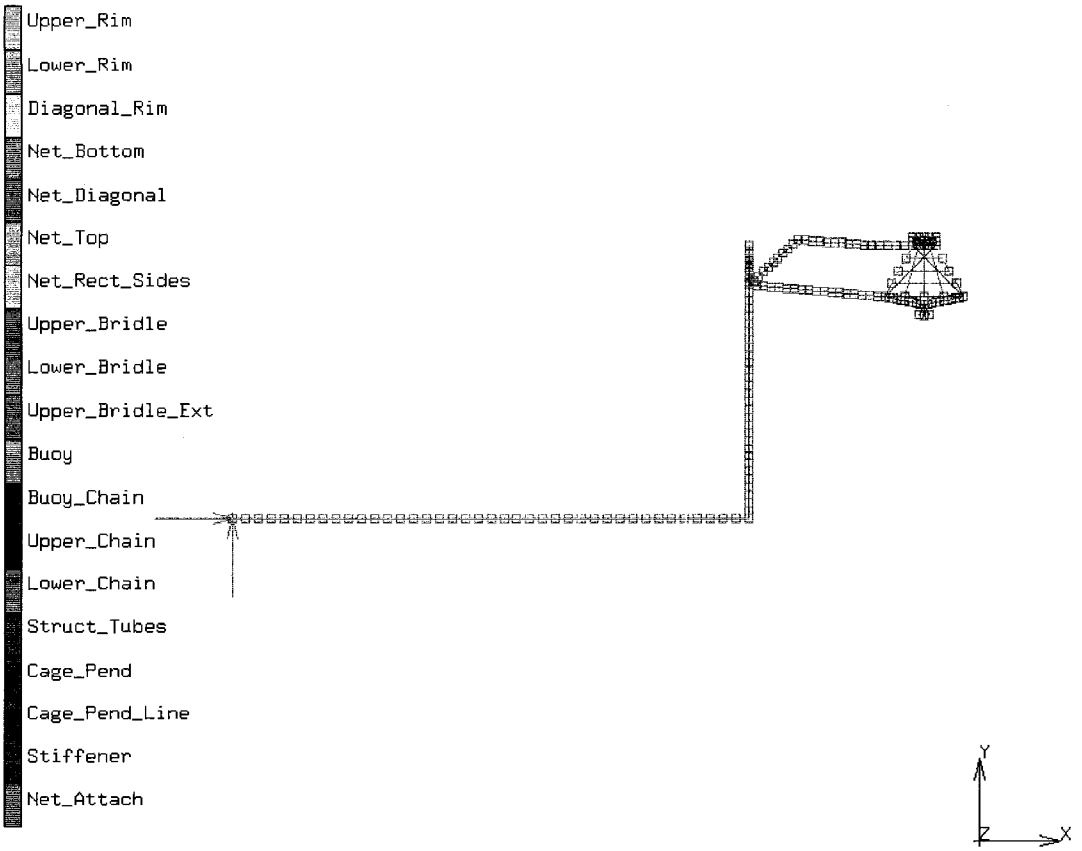

Figure 2.1: Original ASAIM OCAT System

The cage frame was constructed of high density polyethylene (HDPE) pipe and steel corner weldments. Cage rim segments connected to the corner weldments by sliding the HDPE pipe over an exposed section of the corner and securing it with bolts (see figure). All rim segments were plugged at the ends to allow for adjustment of the systems buoyancy. Water or air could be pumped in to raise or lower the cage to the proper waterline.

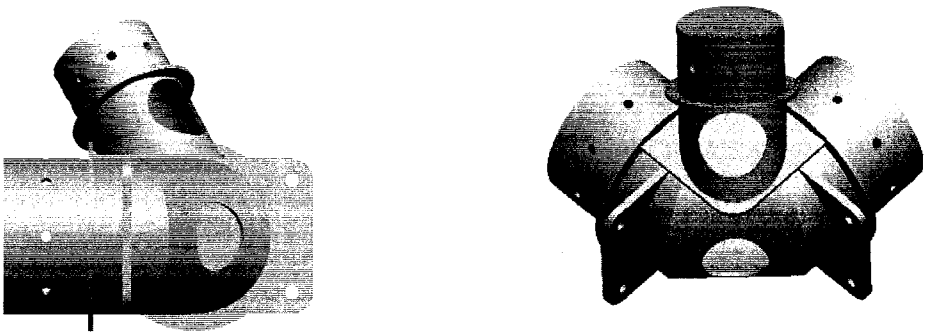

(a) (b)

Figure 2.2: Original ASAIM OCAT Corner Weldments

To add additional stability to the system, a ballast chain was connected via a rope bridle below the lower rim. The original cage can be seen in Figure 2.3.

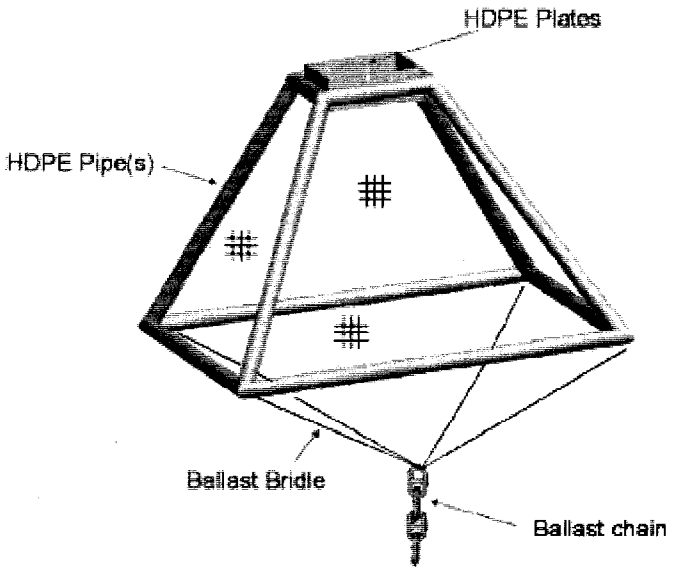

Figure 2.3: Original OCAT Cage
The small size allows for the cage to be utilized in small areas while the large internal area allows for a single farmer to raise a large stock.

Since this cage was originally designed for use in non-developed countries, fish feeding was performed by hand. To prevent food from floating away, HDPE splashboards were attached to the upper rim via HDPE handrails.

The splashboards were designed to extend to the top of the upper rim. The handrails were comprised of two vertical HDPE pipes and one longer horizontal pipe that was the length of an upper rim side.

To house the fish and keep predators out, netting was used. The net chamber was comprised of four trapezoidal sides and a large square for the bottom. The internal net volume measured 100 m^3. The net was attached to the eight corner weldments and was knotted 0.03 m stretch mesh with a twine diameter of 2.5 mm. The projected solidity of the net (defined as the ratio of projected area to outlined area) was calculated as 14.8%. Table 2.1 shows the cage components along with major dimensions quantities and material types.

Table 2.1: Original ASAIM Components

Original Cage Designed Components				
Component	**Quantity**	**Length**	**Diameter**	**Material**
Upper Rim	4	2 m	0.28 m	HDPE
Diagonal Rim	4	5.72 m	0.20 m	HDPE
Lower Rim	4	7 m	0.28 m	HDPE
Corner Weldments	8	----------	0.23 m / 0.15 m	Galv. Steel, Sch. 40 Pipe
Splashboards	4	2 m	0.3 m*	HDPE
Handrails	4	0.6 m/ 2 m	0.15 m	HDPE
Pendent Bridle	4	5 m	0.025 m	Polyester
Pendent Chain	3	1 m	0.032 m	Galv. Steel

Note: * Thickness listed, not diameter

The OCAT system utilized a single point mooring (SPM). A SPM is a mooring which utilizes a single anchor to hold the cage. Since the cage is connected to a single point, it is free to rotate around with the dominant current or weather direction. This allows for disposal of fish waste as well as provides for a self submergence feature in extreme current events (DeCew, 2006). A 5000 kg anchor was used to secure the system to the seafloor. From this, 27.4 meters of

20 mm diameter anchor chain connected to a 12.2 meter, 14 mm diameter, "suspended chain" The suspended chain extended from the ocean floor to a triangular connector plate. The connector plate also attached the cage bridle lines and the buoy chain. The buoy chain held a 180 kg buoy which kept the "suspended chain" vertical in the water column. The single point mooring configuration can be seen in Figure 2.4.

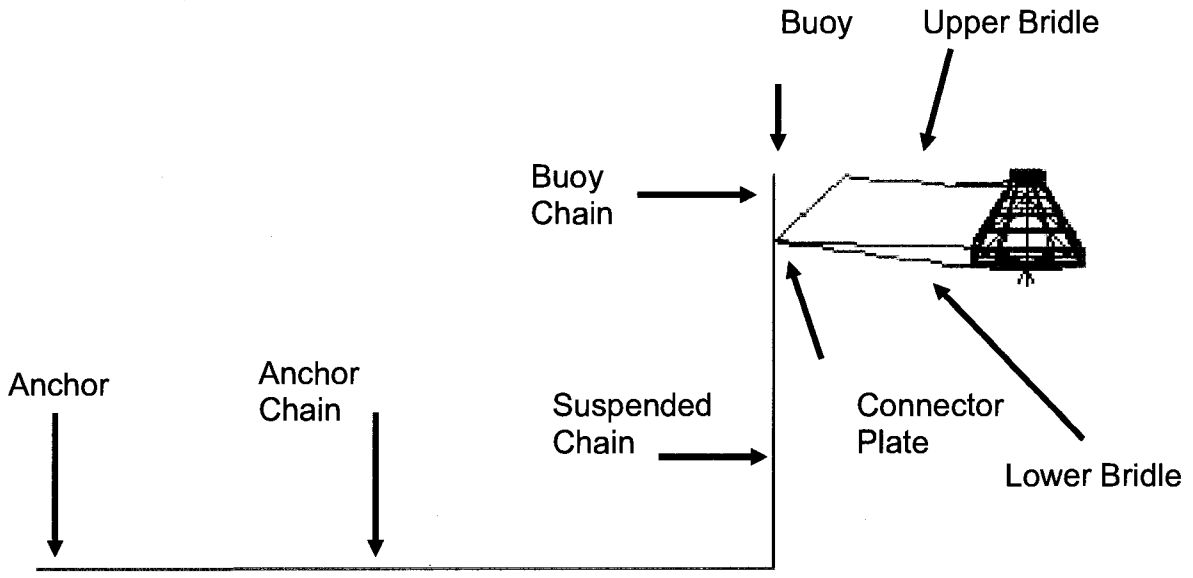

Figure 2.4: Original ASAIM Cage Single Point Mooring
The single point mooring allows for the cage to swing around the anchor weight in changing current profiles.

The upper and lower bridles secured the cage to the chain mooring. Both sections of line were polyester with a diameter of 18 mm. Table 2.2 contains all mooring components along with their quantities, lengths, diameters, and material types. Further details on the OCAT cage and mooring can be found in Risso (2007).

Table 2.2: Original Mooring Configuration Components

Original Cage Mooring Designed Components				
Component	**Quantity**	**Length**	**Diameter**	**Material**
Lower Mooring Chain	1	27.4 m	0.025 m	Galv. Steel
Upper Mooring Chain	1	12.2 m	0.019 m	Galv. Steel
Buoy Chain	1	3 m	0.013 m	Galv. Steel
Upper Bridle	2	3.57 m	0.018 m	Polyester
Lower Bridle	2	12.66 m	0.018 m	Polyester
Upper Bridle Extension	1	12.4 m	0.025 m	Polyester
Mooring Buoy	1	1 m	1 m	180 kg buoyancy

II.2. Modifications

One task of the collaboration work between ASAIM and UNH was the fabrication and assembly of an OCAT cage system. In an effort to reduce the OCAT component costs and ease fabrication and cage assembly, a few modifications to the original design were made. The first step in this process was to perform a full design review. The design review analyzed all facets of the system and several modification suggestions were made. The design changes were then verified to assure that system dynamics would not be greatly affected. To guarantee compatibility between system components, the solid modeling program ProEngineer was used. MathCad was employed to create a mathematical model of the cage. This model was changed with each modification to verify that key parameters such as center of gravity (CG), center of buoyancy (CB), and waterline would be acceptable. At the completion of the design review, it was determined that two major modifications would be made, one involving the

corner weldments and one involving the cage upper rim. As a result of these changes, the construction process was also modified from the original method.

II.2.1. Corner Weldments

The original corner weldments, shown in Figure 2.5, secured the HDPE pipe to create the cage frame. The HDPE piping was placed over the steel weldments and fastened by bolts. However, to make the original design fit properly, standard sized steel pipe could not be used. Instead, steel tubing which is usually more expensive and harder to acquire, was needed and had to be machined to fit. Due to the complex geometry, non-standard pipe sizing, and custom nature of the corners, it was found that they would each cost approximately $3,250. This would result in a total cost of $26,000 for the eight weldments needed to construct the cage.

The high price made the corner weldments a good candidate to be modified. Sliding the HDPE pipe over the metal fittings is not only a point of wear, but difficult to assembly and maintain. Field evidence on existing ASAIM systems has shown that the bolts wear the HDPE-metal interface away, causing failure. To fix this, flanges were attached to the rims allowing them to be bolted to the corner weldments as seen in Figures 2.5 and 2.6. All the steel tubing in the corner weldments were converted to standard 10" steel pipe fittings and were now constructed using one 90° tee, two 45° elbows and three flanges. Unlike the steel tubing which would have needed to be machined, these are standard piping sizes, readily available, and shipped prepped for welding.

The new corner modifications resulting in the HDPE pipe segments being upgraded. Two part flanges, consisting of a HDPE stub end and a steel backing ring, were fused onto the ends of each pipe rim. An HDPE stub end is a 12" piece of HDPE with a wide base which can hold on a backing ring, figure 2.5 (b). Once attached, the HDPE pipe was bolted directly onto the fittings.

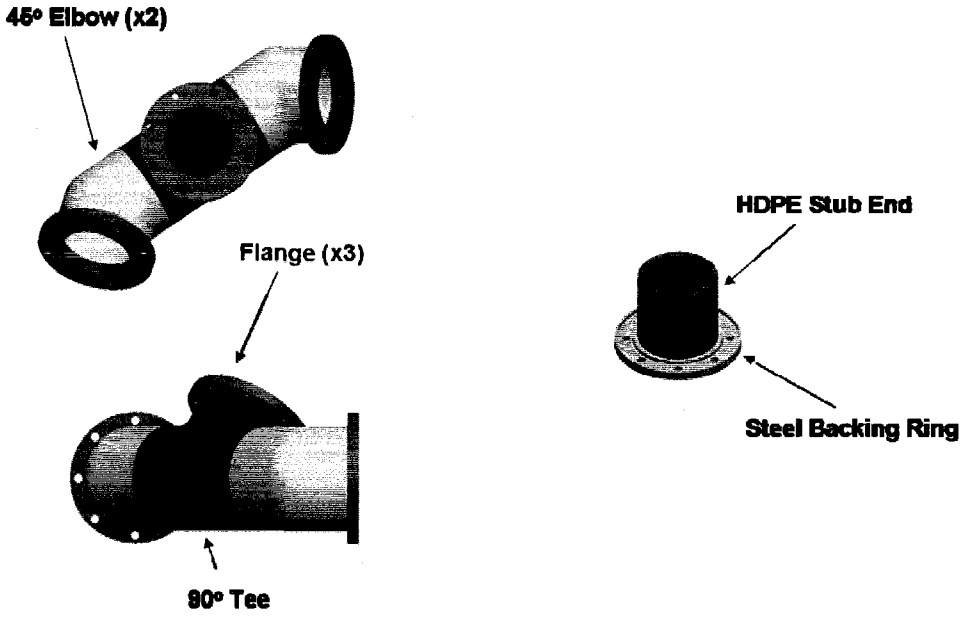

(a) (b)

Figure 2.5: Newly Designed Corner Weldments
(a). The new corners are made of standard 10 inch pipe fittings. (b). The HDPE pipe segments will have stub end fused on and the backing ring can be used to bolt the components together.

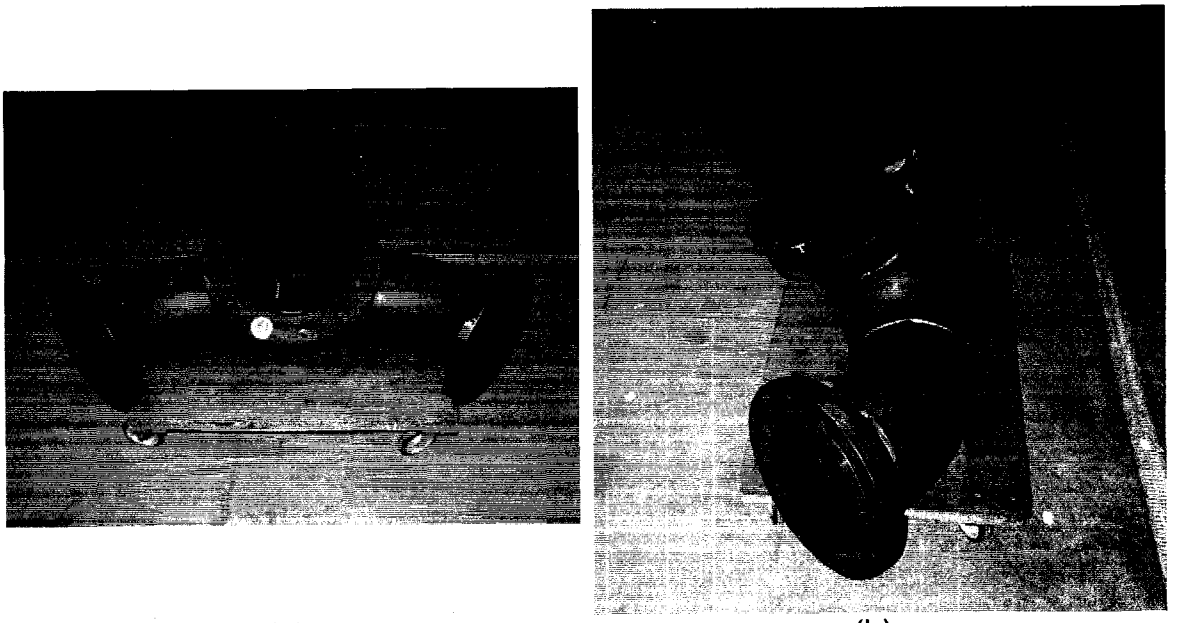

(a) (b)

Figure 2.6: New Corner Prototype
The HDPE rim sections are able to be bolted directly to the corner weldments

These modifications to the corner weldments simplified the corner weldment fabrication, reduced the overall cost, and eased the cage construction. The new corners reduced the cost per corner fitting by over 50% and saved over $13,000. Attachment of the rims to the corner was made easier since holes in the weldments and rims did not need to be matched up for bolting. Instead, the flanges could be rotated easily when in place and secured.

The one major drawback with the new corner design was its new weight of 338 lbs whereas; the original corners had a weight of just over 100 lbs, which allowed them to be easily moved. To resolve this issue, small supports with castors were built so the corner could rest on it and ease movement. A corner with one of these supports can be seen in Figure 2.7. These supports also aided during the construction processes as they held the lower rim off the ground.

Figure 2.7: Fitting Supports
The supports allowed the new, heavier corners to be moved with little effort and eased the construction process.

Drawings of the new corner weldment can be found in Appendix A, while drawings of the corner support can be found in Appendix B.

II.2.2. Upper Rim

After the new corner fittings were designed, it was determined that the corners could also be manufactured entirely out of HDPE, eliminating the steel entirely. This would lower the cost and overall weight of the system. This change would also allow UNH personal to determine the construction process of a cage built entirely out of HDPE piping for future projects.

Fabricating HDPE corners was skipped due to the high confidence of successes based on the lower, steel fittings. Similar parts are used in both designs, although made of different materials. The effort to determine the feasibility of making the cage entirely out of HDPE was taken a step further and the top corner pieces were removed. The top rim was then constructed out of HDPE in one piece, incorporating the fittings into the rim. The resulting rim section is seen in Figure 2.8.

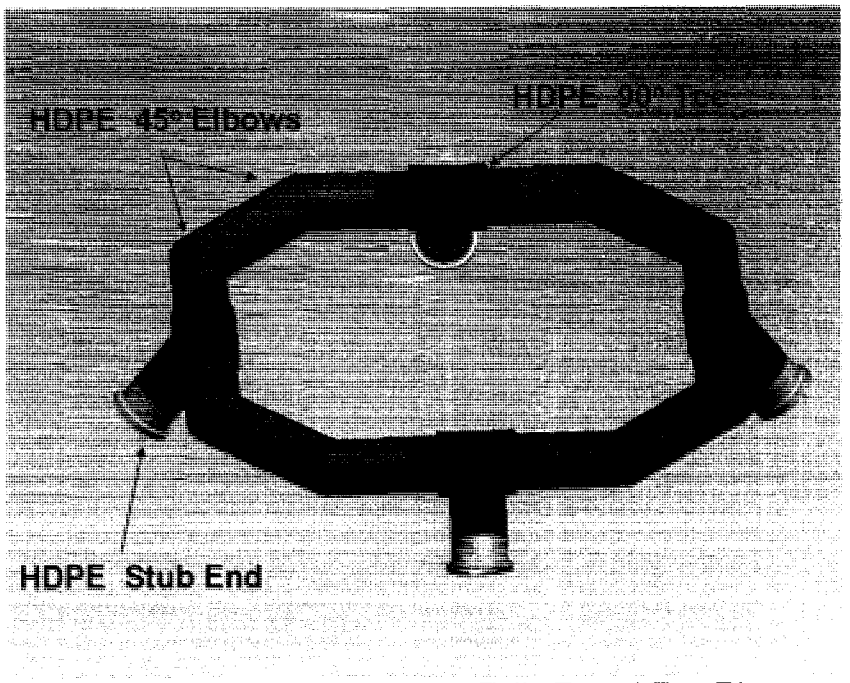

Figure 2.8: Depiction of the Fully Fused Top Rim

II.3. Effect of the Modifications

Changing the corner weldments and making the upper rim entirely out of HDPE caused some changes to the cage hydrostatics. Three critical parameters were analyzed, the center of gravity (CG), center of buoyancy (CB), and the water line level of the cage when under tow. Note that the cage is typically towed out of the water, with the lower rim at the surface. Once the cage is at the grow site, water is added to the various pipes, reducing the systems buoyancy until the proper waterline is reached. Table 2.3 below shows the changes in these parameters from the old to the new system. It can be seen that the new system's CG is lowered by 0.51 meter while the CB is raised by 0.39 meter. These changes are due to the added weight of the bottom corner weldments and the new, lighter, and larger HDPE upper rim. The added weight caused the cage to sit lower in the water when transported. A draft of 1.6 meters was calculated. To

lessen the depth of the draft, temporary floats were added to the lower rim when the cage was transported.

Table 2.3: Hydrostatic Differences Between the Original Model and New Model

Parameter	Original System	New System
Center of Gravity*	3.42 m	2.91 m
Center of Buoyancy*	2.95 m	3.34 m
Transportation water line	0 m	1.6 m

* Measured from the lower horizontal rim upwards.

The last small effect of the modifications was the orientation of the upper rim to the bottom rim. The new system has the fully fused top rim rotated 45° with respect to the lower rim as seen below in figure 2.9.

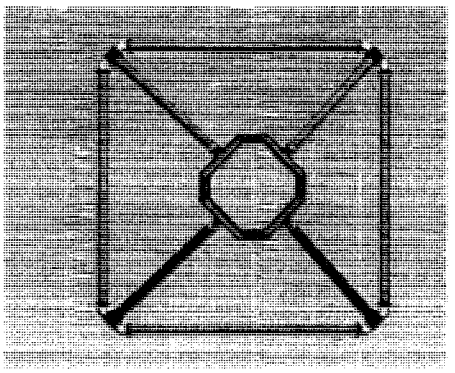

Figure 2.9: Top View of the New Cage
Due to the use of a single fused HDPE upper rim, it is 45° out of phase with the lower rim.

II.4. Construction

Construction of the UNH ASAIM cage took place in two phases. The first phase included fabrication of the top rim, fusing the end caps to all rim sections, painting the pre-fabricated corners, and building the handrail with splashboard attachments. This took place on November 15th and 16th at the University of New Hampshire Jere A. Chase Ocean Engineering Laboratory. Phase two of the cage

construction was performed at the State of New Hampshire Port Authority in Portsmouth New Hampshire on December 6th and 7th. Phase two included building the cage structure and all systems as well as deployment of the cage into the Piscataqua River.

II.4.1. Phase One

The first phase of the project consisted of component fabrication for the UNH OCAT system. General organization of the system parts was performed, including painting of the steel corners, arranging the air system, sealing the pipes with HDPE plugs, and assembling the handrail.

Since the delivered parts were not all built to the correct specifications (i.e. length tolerance of ± 2 inch), all parts were measured and a layout was produced to provide the best arrangement with the least amount of cutting required. The resulting upper rim with final dimensions is seen below.

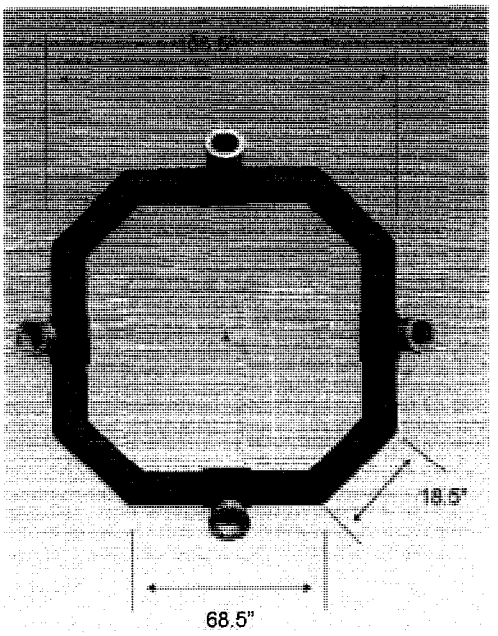

Figure 2.10: Top Rim Dimensions

To fuse the top rim together, pieces were placed in an HDPE fusing machine, shown in Figure 2.11. The fuser "faced" both pieces, squaring them for good contact. The pieces were then heated with a hot plate and pressed together. The two HDPE pieces melted together and the resulting connection had the same strength as a continuous pipe.

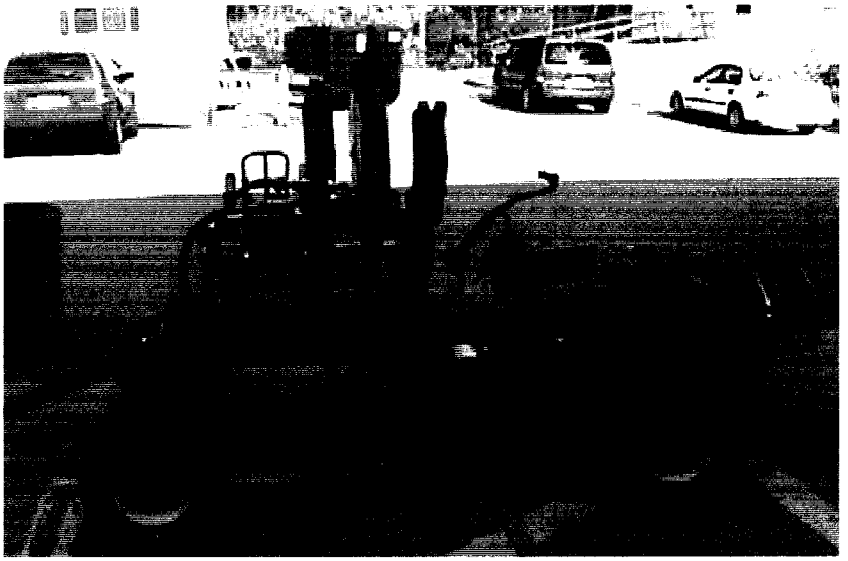

Figure 2.11: HDPE Fuser

The top handrail was made in similar fashion. Splashboards were bolted to the handrail and the unit was welded to the top rim. The top rim with splash boards and handrails attached can be seen in Figure 2.12.

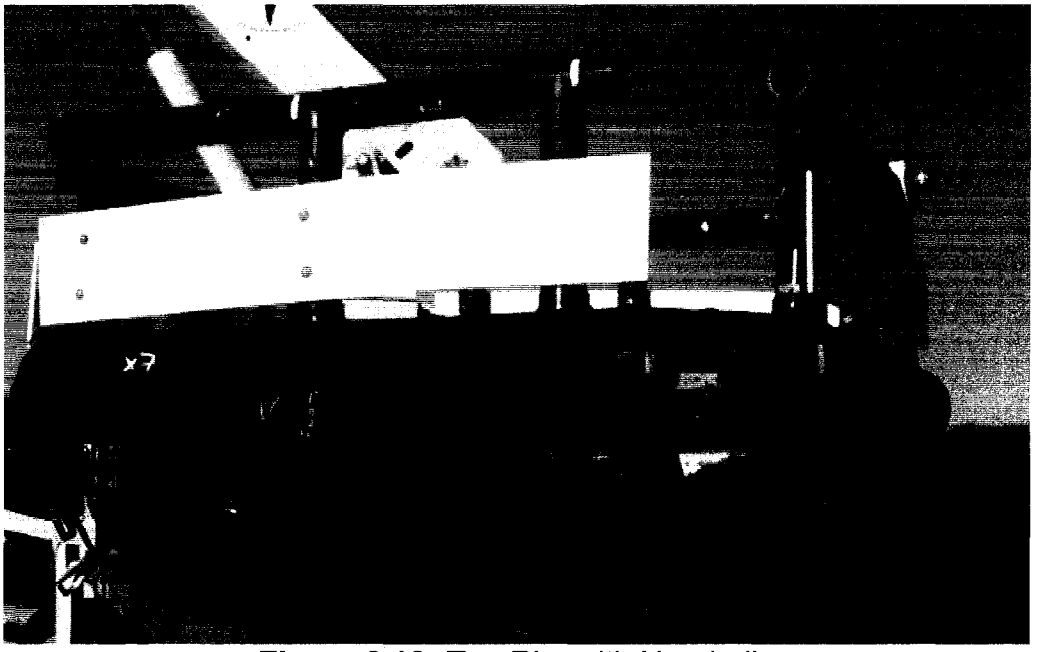

Figure 2.12: Top Rim with Handrails
The handrails were connected using an HDPE weld gun. This gun heated strings of HDPE "rope" and welded the handrails to the top rim.

II.4.2. Phase Two

The cage components were assembled during phase two of the construction process which two took place December 6th and 7th at the New Hampshire Port Authority in Portsmouth New Hampshire.

The first step in constructing the OCAT cage was to assemble the lower rim. The four lower rim segments and corners were laid out as shown in Figure 2.13. Then the rim segments were bolted to the corners with the appropriate hardware, forming the lower rim.

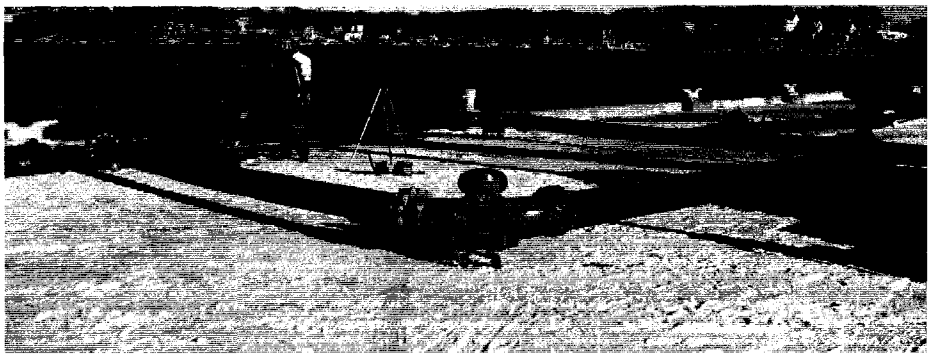

Figure 2.13: Bottom Rim Assembly

While the bottom rim was being secured, the upper section of the cage was being assembled. A small crane first suspended the top rim. Then, a boom-truck picked up each diagonal rim as shown in Figure 2.14. With the help of a scissor lift, workers could manually align the flanges from the top portion of the diagonal rim and the top rim. All four diagonal rims were installed in this manner. The completed upper section assembly can be seen in Figure 2.15.

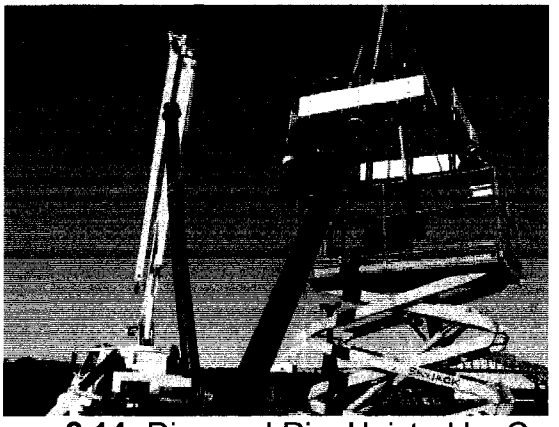

Figure 2.14: Diagonal Rim Hoisted by Crane
Two cranes and a scissor lift were used to attach the diagonal rims to the upper rim.

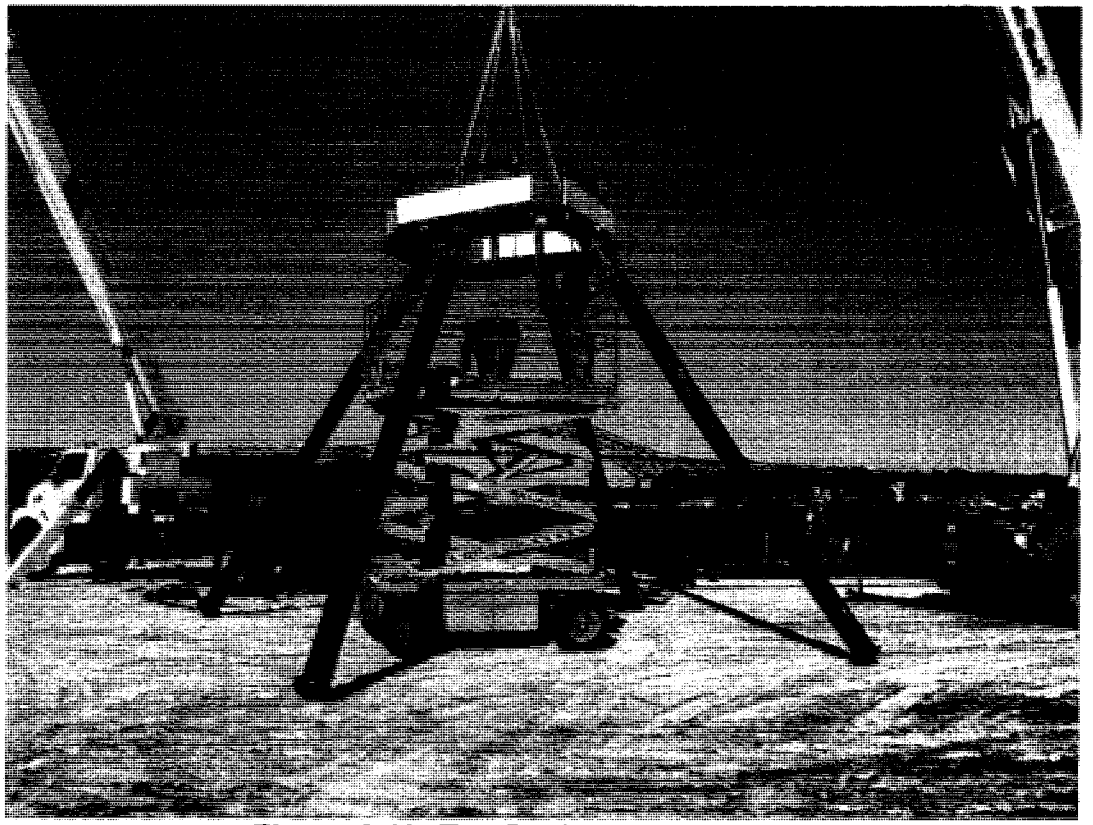

Figure 2.15: Top Portion of ASAIM Cage

Once the diagonal rims were secured to the top rim assembly, it was lifted and placed over the bottom rim framework. The diagonal rims were then bolted into place. Figure 2.16 below shows the finished cage frame.

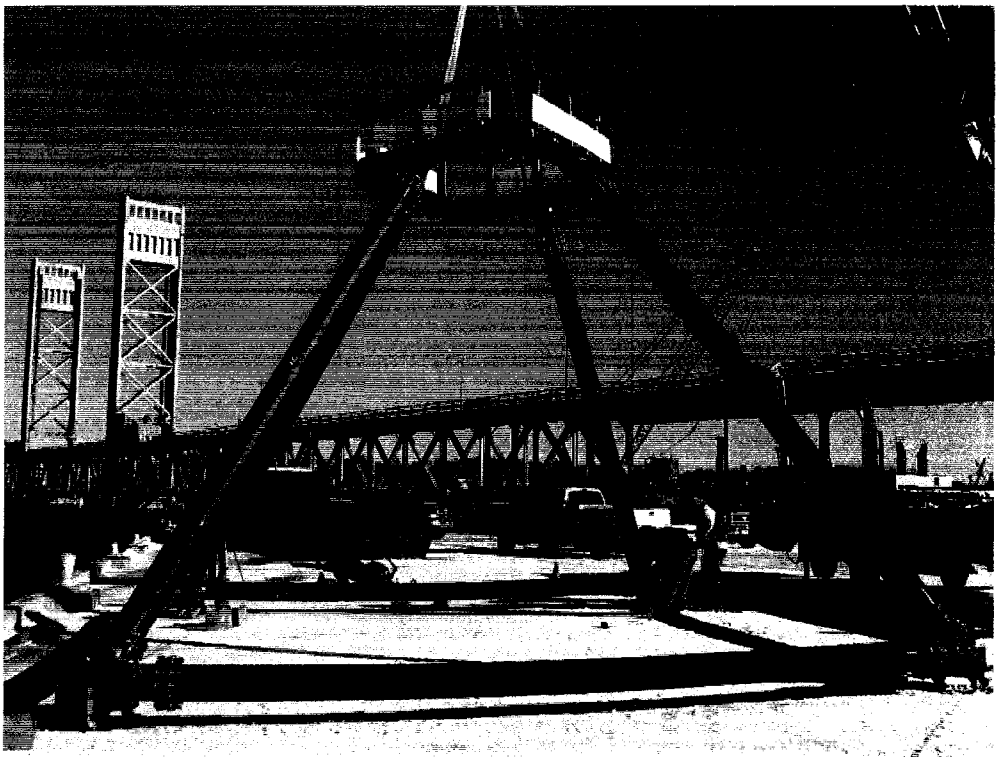

Figure 2.16: Cage Frame
Using a crane and a fork lift, the top section of the cage was lowered into place over the bottom rim. The diagonal rims were bolted and the structure was finished.

The air system which was used to raise and lower the cage out of the water was installed to complete construction of the cage. Note that the air system was a temporary measure installed for testing purposes. Ball valves were threaded into the HDPE rims. Hosing connected the valves of the lower and angled pipes, allowing for a single, centered location for filling. The loose rubber hosing was then secured to the rims via zip ties. The figure below shows a ball valve tapped into a cage rim.

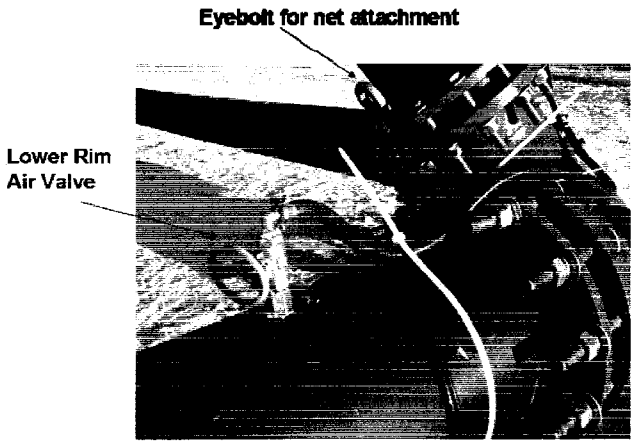

Figure 2.17: Air System Attachment

The net chamber and testing equipment were the final additions to the system. The net chamber was attached to the eight cage frame corners via a pad-eye secured through the two part flanges. Testing instruments were installed for a submergence test. More information on the testing equipment can be found in Celikkol (2008). Figure 2.18 below shows the completed ASAIM cage along with locations of the pressure sensors and current meters.

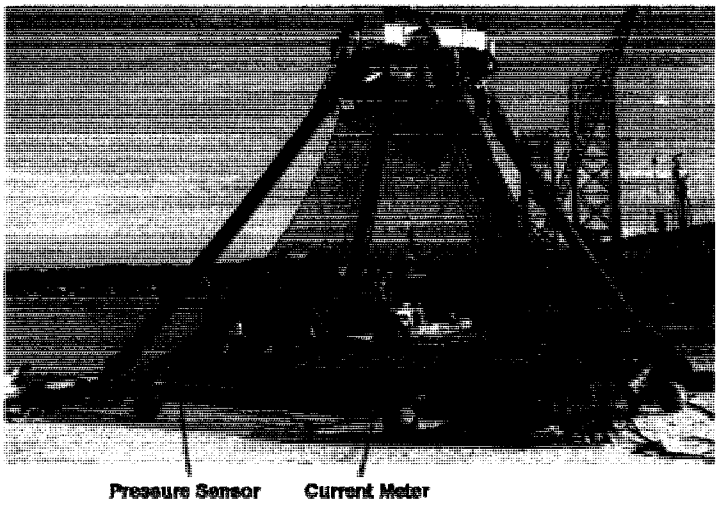

Figure 2.18: Completed ASAIM Cage System
The locations of the current meters and pressure sensors are also shown along with extra floatation which was used for deployment.

CHAPTER III

MOORING FEASIBILITY STUDY

III.1.UNH OCAT Cage Model

The second objection of this study was to develop alternative moorings for the OCAT cage system. Since the purpose of the alternate moorings was to provide a means to secure the cage in extreme environments, the cage mooring configurations designed and analyzed in this study were submerged. This removed the cage from the high energy environment at the surface. To determine the feasibility of using submerged moorings, five configurations were initially analyzed in Aqua-FE. The UNH OCAT cage was used as the blue print for all cages in each mooring. The results from this analysis were used in the design of the final configuration.

III.1.1 Aqua-FE

Aqua-FE is a program based on the Finite Element Analysis Program (FEAP) originally programmed by Professor R.L. Taylor from the Department of Civil Engineering at the University of California, Berkeley. Wave and current loadings on truss elements were incorporated into the model using a Morison

Equation formulation (Morison et al., 1950) for use with aquaculture net pen systems by Gosz et al. (1996). This computer model was successfully used in support of the UNH OOA demonstration project for the design and evaluation of fish cage and mooring systems currently deployed (Ozbay, 1999 and Tsukrov et al., 2000)

Aqua-FE incorporates truss, buoy, and massless elements to model the various parts of a net pen and mooring system. The model uses Lagrangian formulation to accommodate for large displacements of structural elements. Using linear waves, the hydrodynamic forces on the structural elements are calculated using the Morison equation modified to include relative motion between the structural elements and the surrounding fluid. The program is described in detail in Tsukrov et al. (2003).

III.1.2. The Model

The UNH OCAT used as the standard net pen for the feasibility study was first generated in Aqua-FE. The cage was constructed using 68 nodes and 144 elements as shown in Figure 3.1.

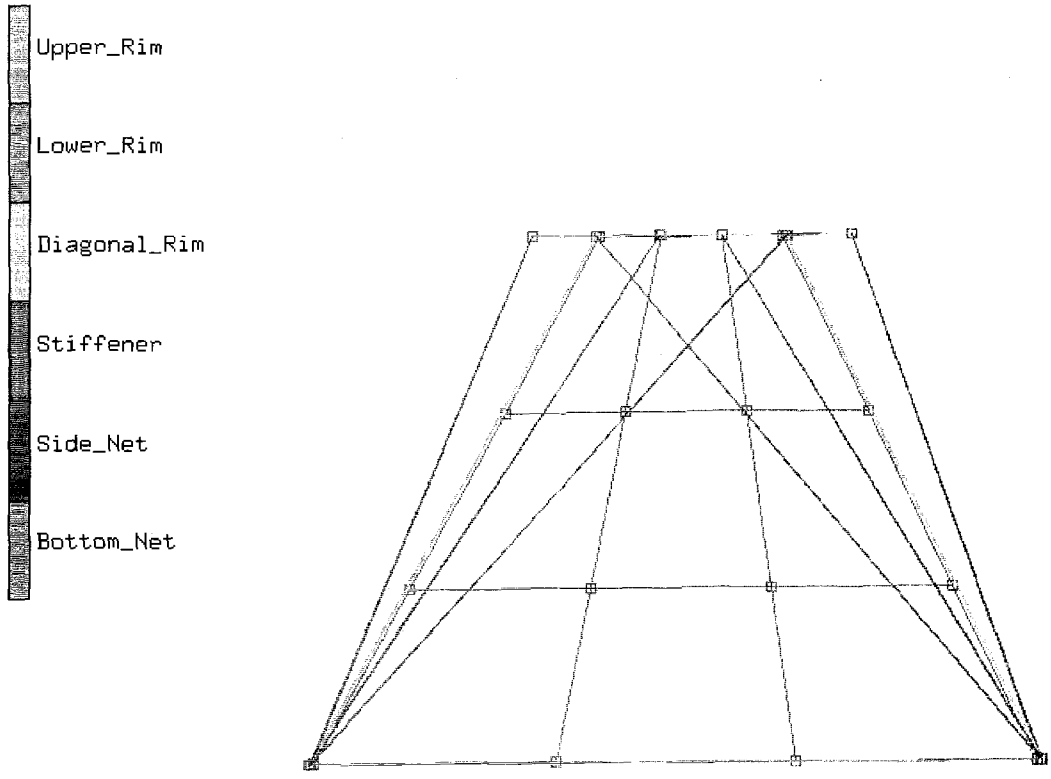

Figure 3.1: UNH OCAT Cage

The finite element analysis (FEA) model of the UNH OCAT system was built to the specifications discussed in section II.4. Aqua-FE requires three material properties of each component: density of the materials, modulus of elasticity, and cross sectional area. The values for these parameters are listed in Table 3.1.

Table 3.1: UNH OCAT System Properties

Material	Density (kg/m^3)	Modulus of Elasticity (GPa)	Cross Sectional Area (m^2)
Upper Rim	316.4	1.172	0.059
Lower Rim	1225	1.172	0.059
Diagonal Rim	800	1.172	0.059
Stiffener	1025	250	$4*10^{-6}$
Side Net (21)*	1025	190	$7.85*10^{-7}$
Bottom Net (63)*	1025	190	$7.85*10^{-7}$

Note: *Denotes number of repetitions for netting elements

As stated previously, the mooring feasibility study analyzed fully submerged cages (10 meters below the surface). Therefore, the buoyancy of the cage and pendent weight were critical.

In order to best size the anchor weight that hung below the cage the anchor in the model was "fixed" from movement and the stresses were recorded in the pendent line for each simulation. It is important to know the needed anchor weight to restrict motion and to assure that it could be deployed and serviced with the UNH research vessel R/V Meriel B. The anchor mooring lines were specified to be 3.8 cm diameter poly-steel while bridle lines directly below the cage were 1.8 cm poly-steel line.

The buoyancy of the UNH OCAT system was set to be 367 kg or 3600 N. This is a result of the original OCAT system buoyancy less the pendent weight which was removed as seen in Figure 3.2. The water depth for all models was 52 meters, with the top of the cages 10 meters below the surface.

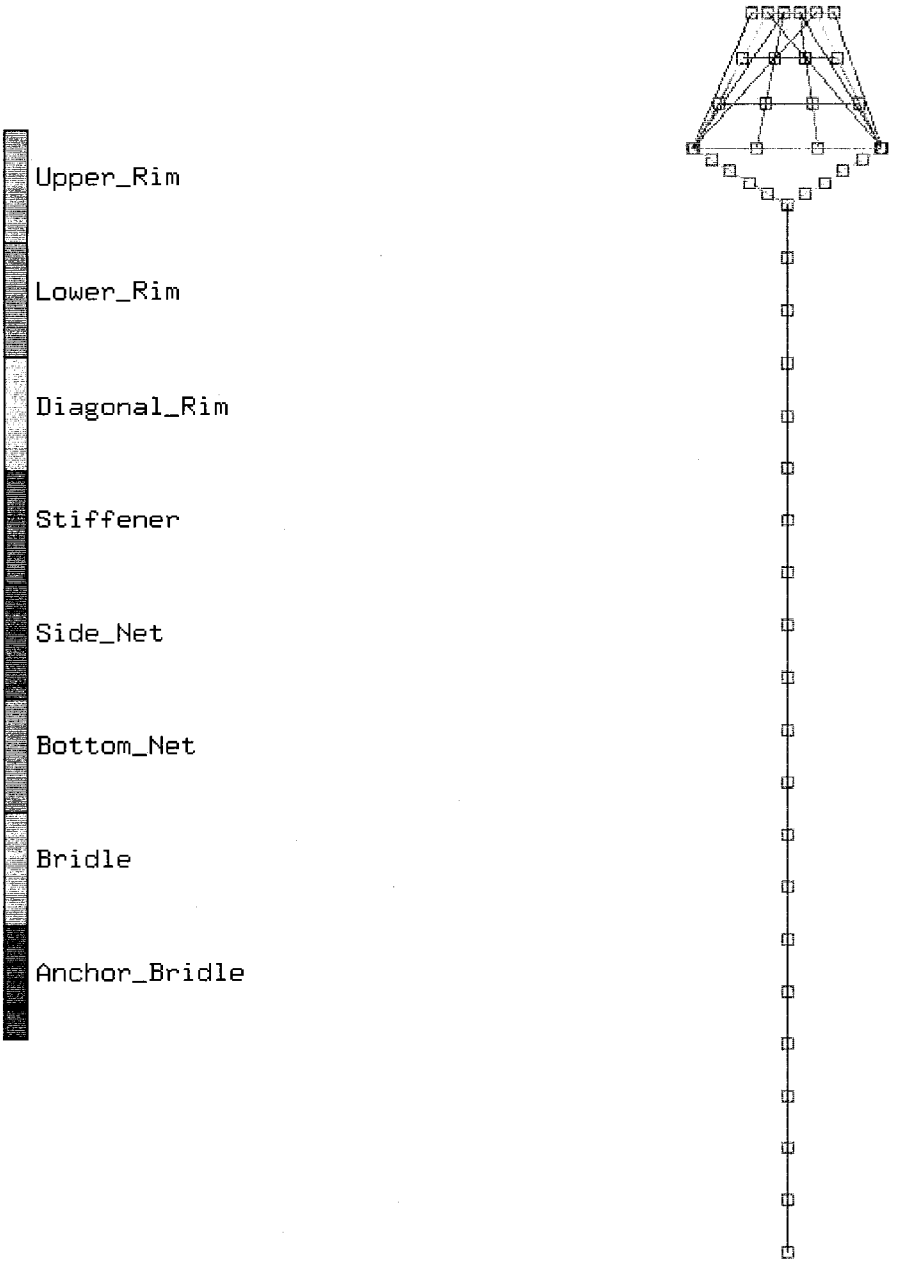

Figure 3.2: UNH OCAT Model Utilized in Aqua-FE
The model was created based on the as built University of New Hampshire ASA cage.

Table 3.2: Nodes, Elements, and Material Types for Aqua-FE Models

Material Label	Effective Density (kg/m^3)	Young's Modulus (Gpa)	Cross Sectional Area (m^2)
Upper Rim	316.4	1.172	$5.9*10^{-2}$
Lower Rim	1,225	1.172	$5.9*10^{-2}$
Diagonal Rim	837.8	1.172	$5.9*10^{-2}$
Stiffener	1,025	250.0	$4*10^{-6}$
Side Net (21)*	1,025	190.0	$7.854*10^{-7}$
Bottom Net (63)*	1,025	190.0	$7.854*10^{-7}$
Bridle	1,250	3.235	$2.545*10^{-4}$
Anchor Line	1,250	3.235	$1.14*10^{-3}$

Notes: * Denotes repetitions for netting elements.

III.2. Load Cases

Each of the models in the feasibility study was subjected to the UNH storm wave loading scenario. A current profile, constant with depth, of 1.0 m/s and an 8.8 second period, 9.0 meter wave height storm wave were applied. The load was applied in-line and transverse to the mooring, as shown in Figure 3.3. In this study, load cases in which the current and waves were applied in direction "A" were designated as "in-line" while direction "B" was labeled as "transverse".

Figure 3.3: Aqua-FE Simulation Directions
Simulations were performed utilizing a 1 m/s current and an 8.8 second period 9.0 meter height wave. Simulations in the "A" direction were run for all models, however, if the model was not symmetric, than simulations in the "B" direction were also performed.

Each mooring configuration was subjected to the current and wave regime in Aqua-FE for 80,000 time steps of 0.005 seconds, or 400 seconds. This was performed to ensure that all models would reach steady state. Once simulations were complete, the results were processed using MATLAB.

III.3. Mooring Design Descriptions

Five mooring configurations were analyzed, three with a single OCAT system and two with multiple. In each test, the pendent line of each cage was modeled as a line with a fixed point to determine the required anchor weight. Any additional mooring line tensions were also recorded. The following sections describe the configurations in more detail.

III.3.1. Single Point Mooring

The single point mooring design utilized only a single anchor below the cage. No additional mooring lines were used. The 3.8 cm diameter anchor line had a length of 35.5 meters placing the top of the cage at a depth of 10 meters. The model was constructed of 105 nodes and 184 elements. The buoyancy of the system was similar to that described in section III.1. Due to the symmetry only one simulation was necessary.

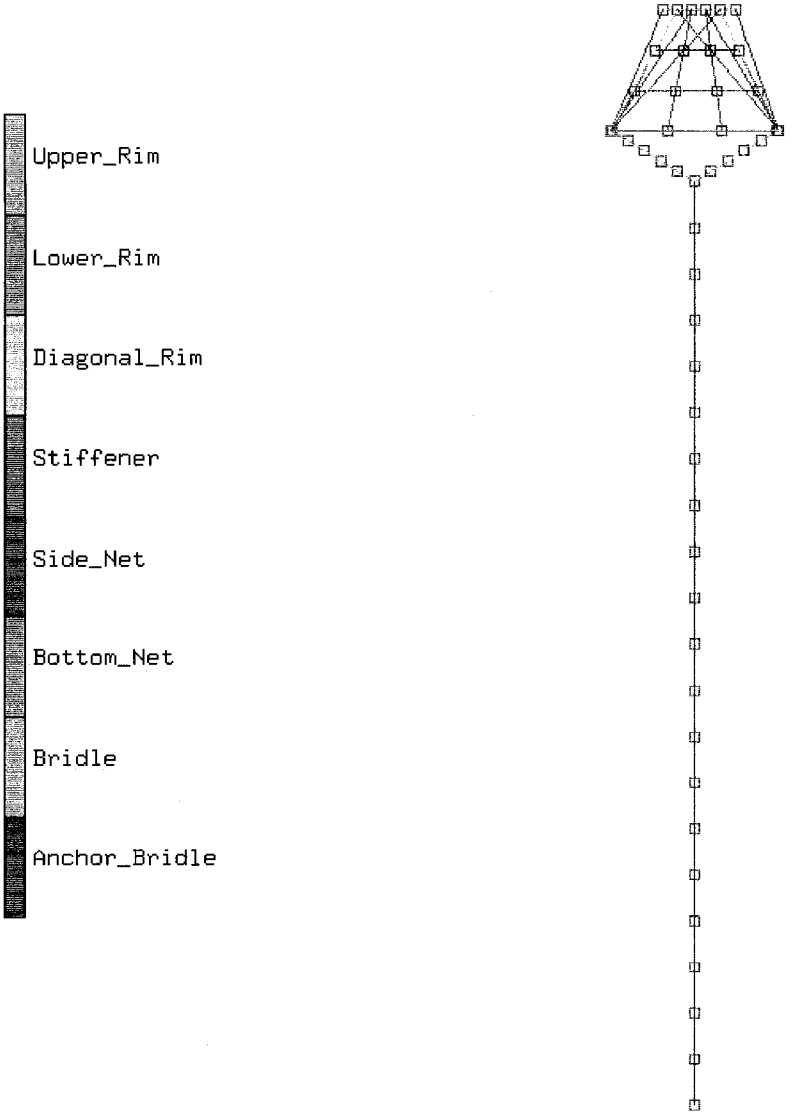

Figure 3.4: Single Point Mooring
The first of five mooring designs utilized for the feasibility study. The model was built according to the "as-built" UNH cage.

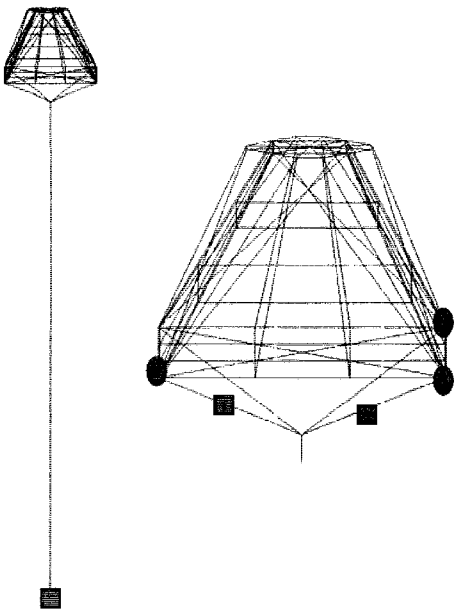

Figure 3.5: Single Point Mooring Areas of Interest
The red squares denote elements recorded for stress results while the blue dots denote nodes recorded for cage motions.

III.3.2. Three Point Mooring

The second single cage mooring design, was similar to the single point mooring, however two additional anchors were added for extra stability. The additional anchors were located 43 meters to each side of the cage. The mooring lines had a scope of 1:1.5 and were made of 3.8 cm diameter poly-steel line. Each side mooring line had a length of 55 meters and connected the cage directly to each of the side anchors. This model utilized 163 nodes and 244 elements. A schematic of the three point mooring design can be seen below in figure 3.6.

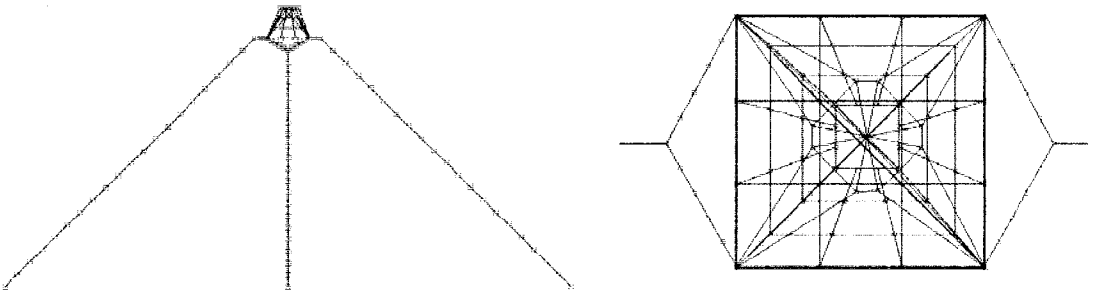

Figure 3.6: Three Point Mooring
The second of the three single cage mooring designs, the three point mooring utilizes three anchors for extra stability.

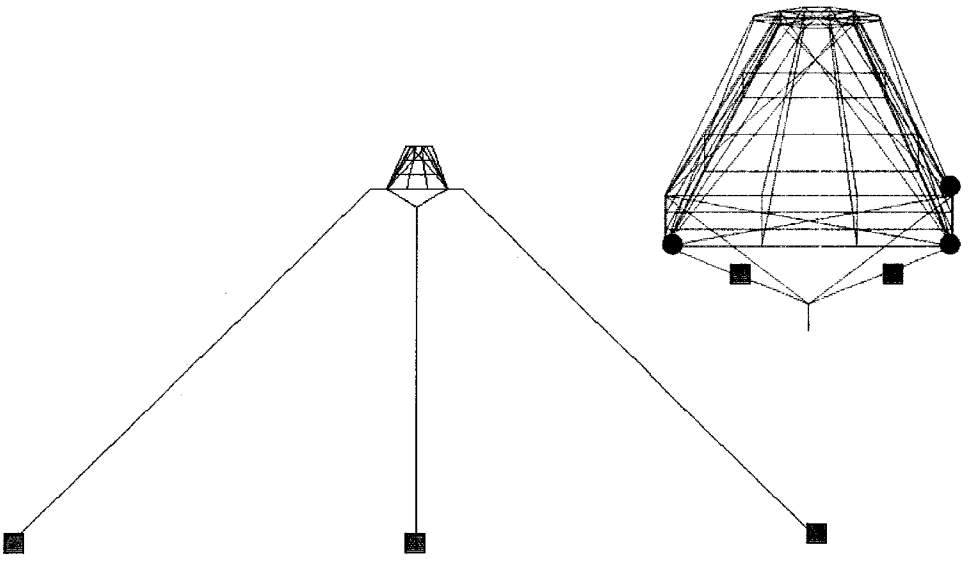

Figure 3.7: Three Point Mooring Areas of Interest
Red squares denote elements recorded for stress values while blue circles denote nodes recorded for motion values.

III.3.3. Grid Mooring

The constructed OCAT cage was eventually deployed into the University of New Hampshire Open Ocean Aquaculture (OAA) grid located off the Isle of Shoals. In an effort to understand and verify the grid capability in handing the deployed systems, a single OCAT cage was modeled in the submerged grid in Aqua-FE (Figure 3.8), Two other systems currently deployed in the site (3000 m^3 Seastation and 600 m^3 Seastation) were also modeled. The OCAT cage was placed in the northwest bay of the grid and secured with four 3.8 cm diameter bridles. Since this model included the UNH grid model, 510 nodes were used in conjunction with 696 elements. This model can be seen below in Figure 3.9.

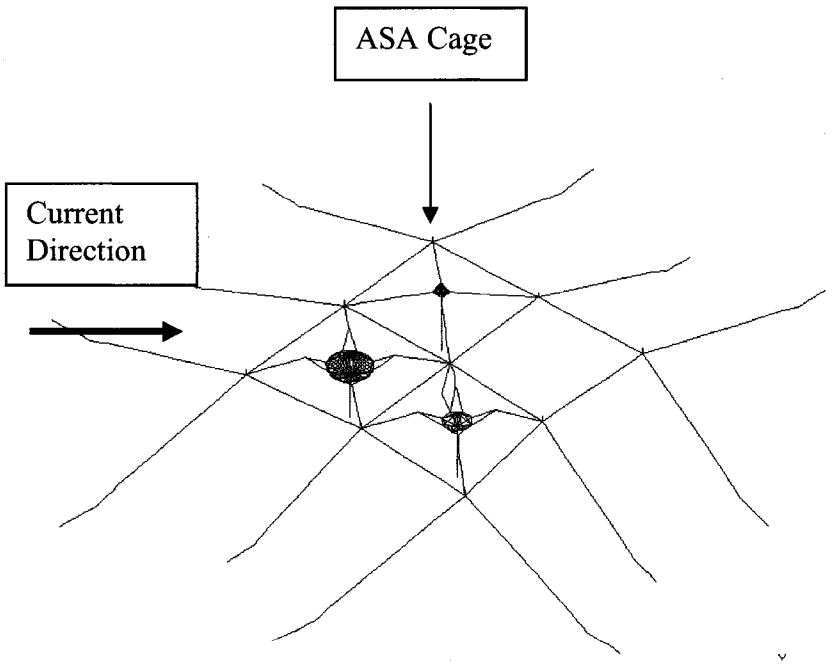

Figure 3.8: UNH Grid Mooring
The third of the three single cage mooring designs, the grid mooring utilizes a model of the UNH OAA grid system in place near the Isle of Shoals.

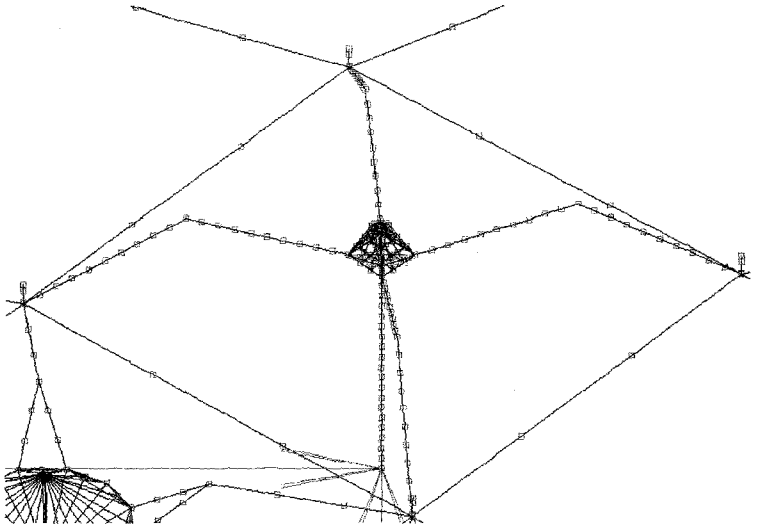

Figure 3.9: UNH OCAT System Deployed in the UNH Grid

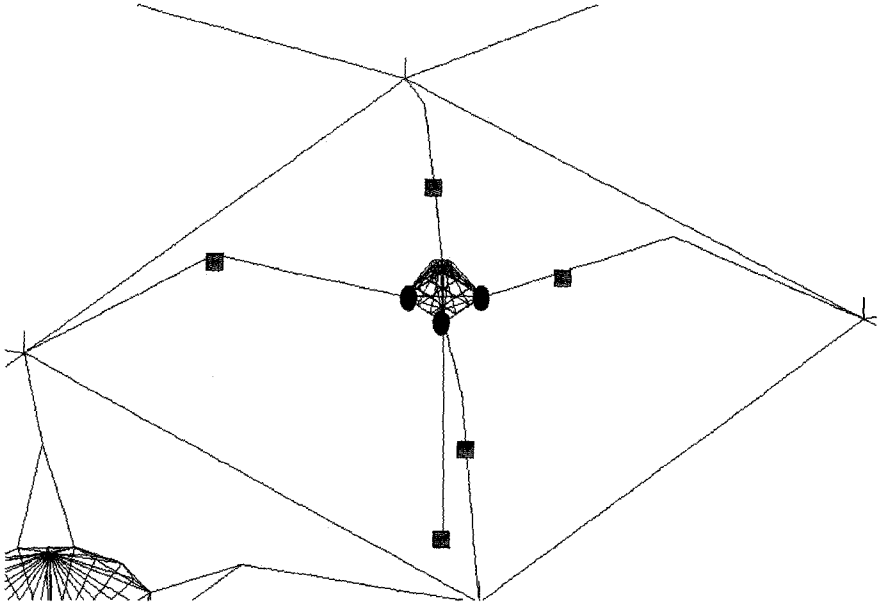

Figure3.10: Areas of Interest for the Grid Mooring
Red squares denote elements recorded for stress values while blue circles denote nodes recorded for motion values.

III.3.4. Rigid String Mooring

In addition to single OCAT cage simulations, two multi-cage moorings were analyzed. The configurations were both "string type" in which all cages were tethered in-line together. The first mooring utilized a rigid connection made of HDPE piping. Two HDPE pipes formed rigid rails on two sides of the cages. The cages were placed between the rails and attached by lashing line on the bottom rims and rails. The rigidity of the HDPE rails assured that the cages would not move toward one another and thus prevented tangling of mooring lines and damage to the cage which may be caused by severe weather. The rails were filled with water to keep the density as close to neutrally buoyant as possible. To assure that the HDPE side rails would not break, stresses in the piping were recorded and compared to the breaking strength of HDPE.

Like the three point mooring, the system was anchored using anchor weights below each cage as well as two additional side anchors. The mooring lines to the side anchors were 3.8 cm poly-steel line. They had a length of 147 meters giving them a scope of 4:1. Figure 3.11 shows the areas of interest on the rigid string model.

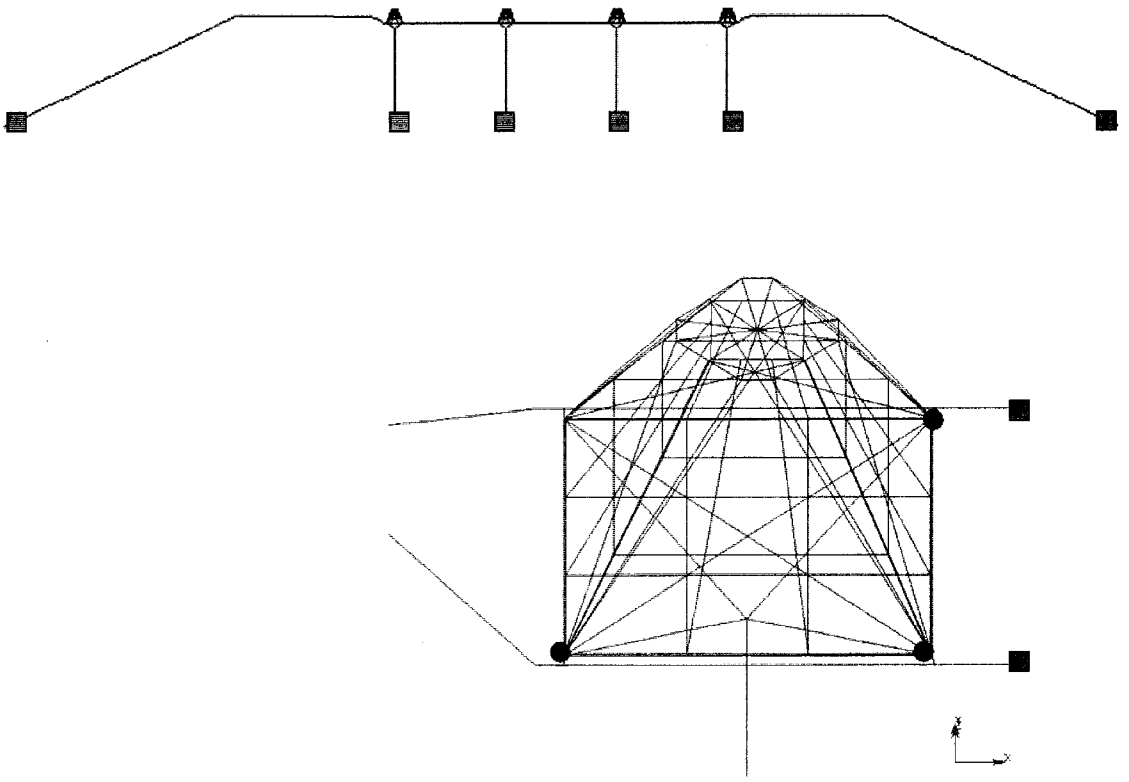

Figure 3.11: Rigid String Model Areas of Interest
Red squares denote elements recorded for stress values while blue circles denote nodes recorded for motion values. Also note that all cages had three nodes record for motion values

The rigid string mooring utilized 1050 nodes and 1382 elements. Figure 3.12 shows the model, while figure 3.13 shows a close up of two cages.

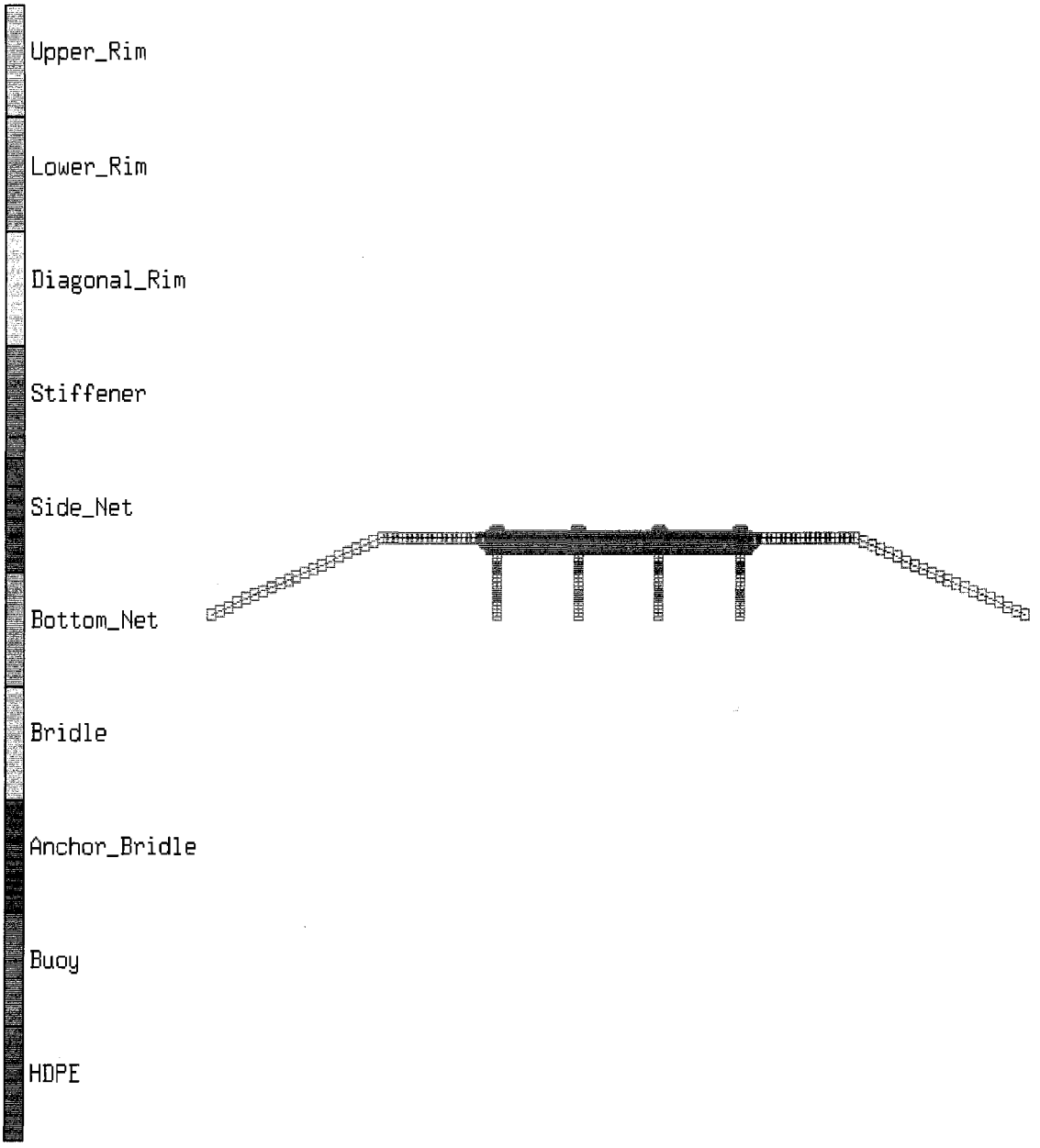

Figure 3.12: Rigid String Mooring
This multi-cage mooring utilizes HDPE piping to act as side rails holding the line of cages in place. The cages are attached to these side rails at the bottom rim using rope.

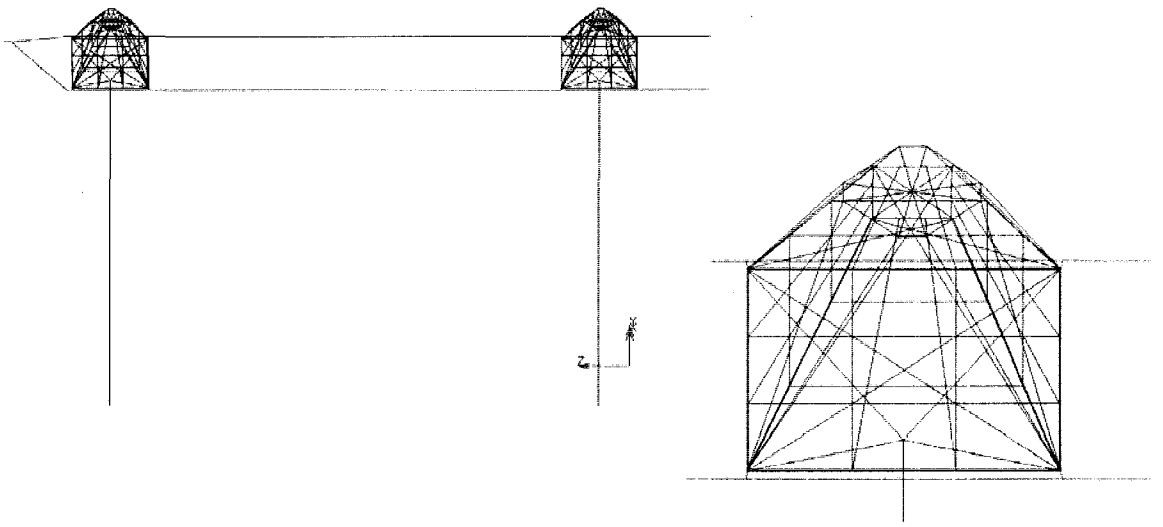

Figure 3.13: Rigid String Mooring Close-up
The cages are attached to the side rails at the bottom rim using rope which can be seen in the figure to the right.

III.3.5. String Mooring

In addition to the rigid mooring, a second multi-cage mooring was designed. The string mooring, similar to the rigid string mooring, replaced the HDPE pipe and instead had the cages attached to one another via a rope bridle. This allowed for more cage motion and allowed one cage to be removed without disrupting the others. Like the three point mooring and rigid string mooring, the string mooring was anchored using anchor weights below each cage as well as two additional side anchors. The mooring lines to the side anchors were 3.8 cm poly-steel line. They had a length of 147 meters giving them a scope of 4:1. Figure 3.14 shows the areas of interest on the string model for tensions. Each cage had three corner nodes recorded for system motion though they are not shown.

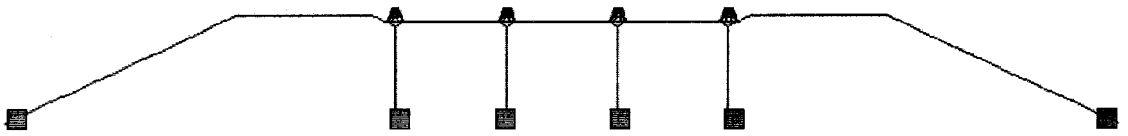

Figure 3.14: String Mooring Areas of Interest
Red squares denote elements recorded for stress values. Also note that all cages had three nodes record for motion values

The string mooring contained 711 nodes and 1038 elements. Figure 3.15 shows the model, while figure 3.16 shows a close up of two cages.

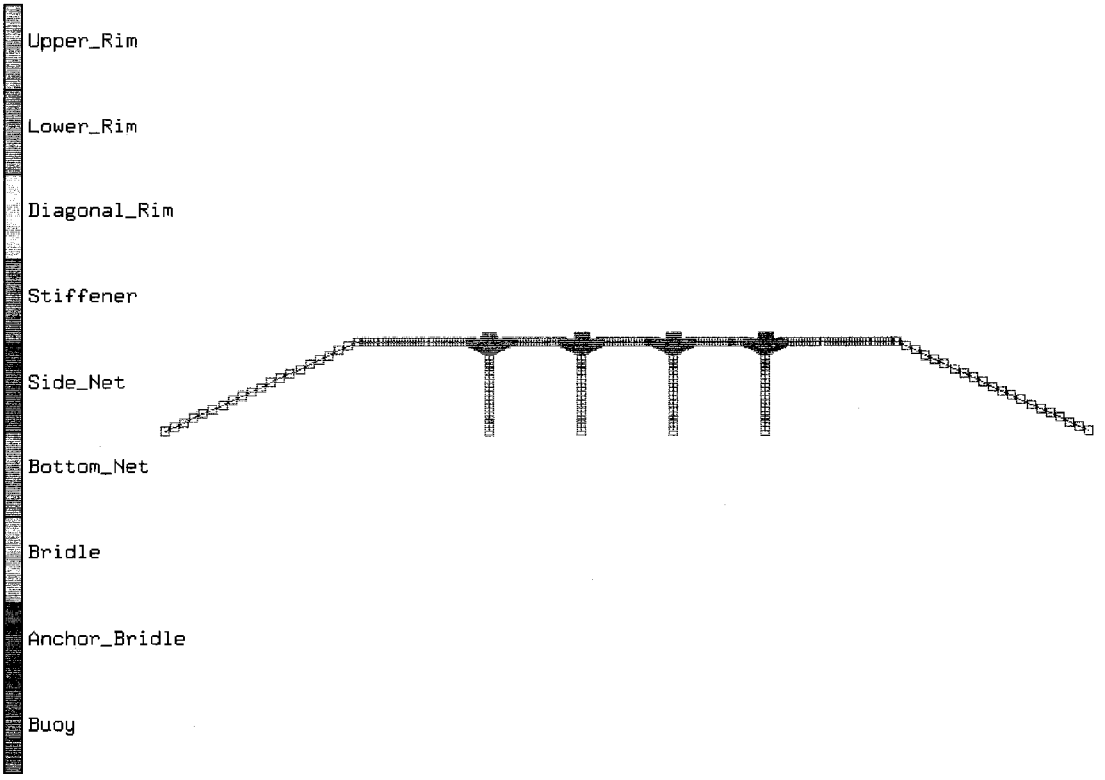

Figure 3.15: String Mooring
The second of the two multi-cage moorings removes the rigid side rails utilized in the rigid string model. This allows for one of the cages to be removed without disrupting other cages.

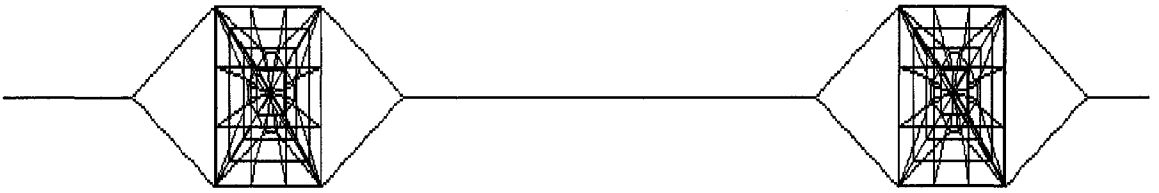

Figure 3.16: String Mooring Close-up
Instead of rigid HDPE pipes connecting cages, rope bridles are used. This design allows for a cage to be removed without disrupting the rest of the system.

III.4. Results

III.4.1. Single Point Mooring

The single point mooring was the first of five mooring designs to be tested using a "worst scenario" load case. The single point mooring model was built according to the UNH OCAT system and teetered to an anchor weight at the seafloor. It was found that the average cage heave was 21 meters, the average surge was 36 meters, and the average anchor bridle line tension was 23.5 kN. All values were found once the cage had reached steady state as shown below in Figure 3.16.

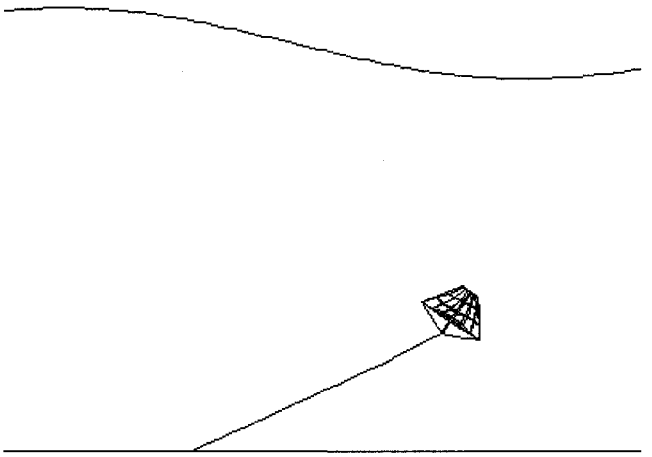

Figure 3.17: Single Point Mooring Subjected to Worst Scenario Load Case

III.4.2. Three Point Mooring

The second of the three single cage moorings tested was the three point mooring. This model was similar to the single point mooring; however, it utilized two additional anchors to the side of the cage. Unlike the single point mooring, the three point mooring design was not symmetrical, thus loadings from two directions had to be applied to get full range of testing. The first simulation loads were applied to the cage in the in-line direction while the second simulation applied loads in the transverse direction. In-line loading results found the cage heaved 20 meters while it surged 12.5 meters. The cage surged less then the single point mooring due to the additional side anchors. The anchor tension was 8 kN, also less than the single point mooring.

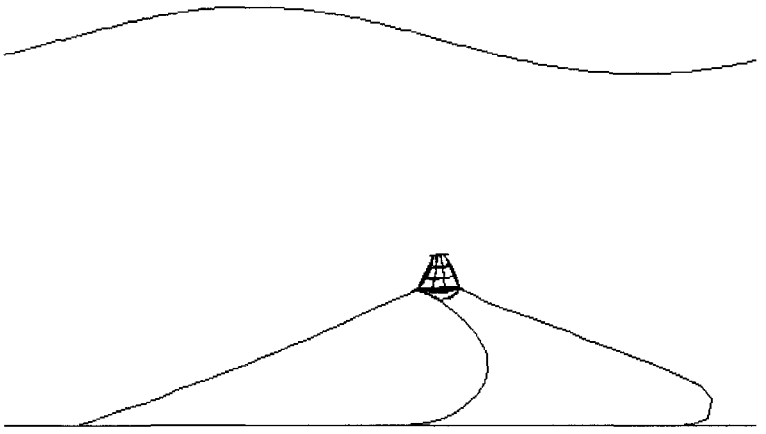

Figure 3.18: Three Point Mooring Subjected to Worst Scenario Load Case In-line with the Cage

Transverse loading results found the cage heaved 22 meters while it surged 35 meters. This loading caused the cage to surge much more then the in-line loading because when the cage receives loading from the in-line direction, it has an anchor behind to prevent it from diving. This is not the case with the transverse loading. The anchor tension was 17 kN, also greater than the in-line loading.

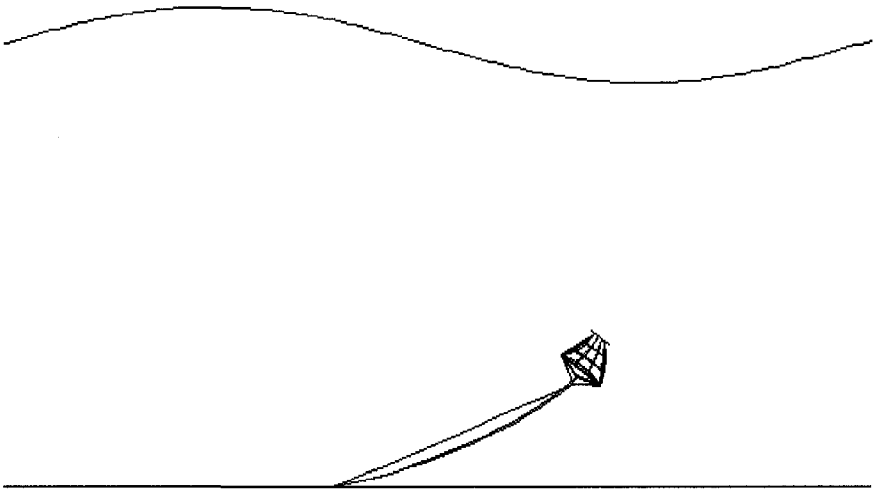

Figure 3.19: Three Point Mooring Subjected to Worst Scenario Load Case Transverse with the Cage

III.4.3. Grid Mooring

The final of the three single cage moorings tested was the grid mooring. This test was performed to determine the grids capability to house the UNH OCAT system for future deployment. This model utilized the single point mooring along with four bridle lines running from the bottom corners of the cage to the grid system which secured the model. The grid mooring like the single point mooring was symmetric allowing for loads to be applied in only one direction.

A majority of the load was taken by the mooring lines attached to the grid system. Initially, the anchor load was over 20 kN, however, after the initial few waves, the anchor load became approximately 3 kN, much less than any of the other single cage moorings. The deformed cage can be seen below.

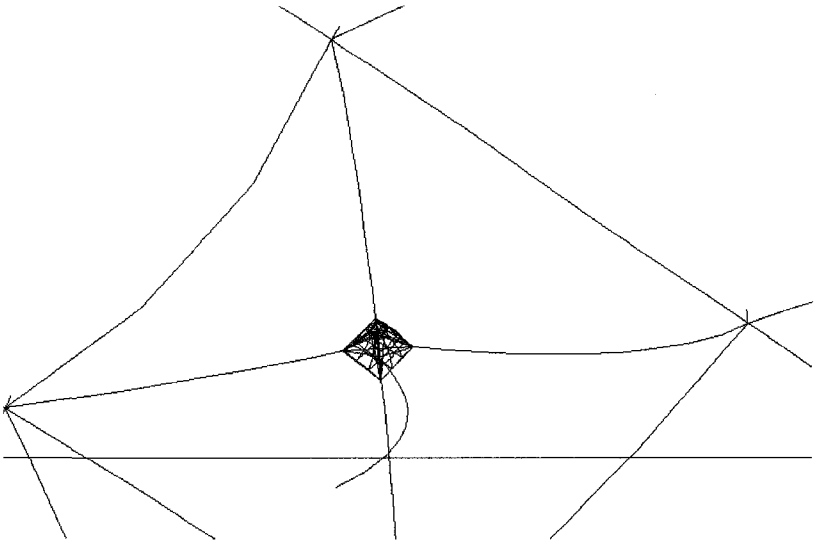

Figure 3.20: Grid Mooring Subjected to Worst Scenario Load Case

III.4.4. Rigid String Mooring

In addition to the three single cage moorings, two multi-cage mooring systems were tested. The first, the rigid string mooring, utilized HDPE pipes as side rails to hold the cages in line. Since this system was not symmetric, loadings were applied in-line to the cage system as well as transverse. To assure that the side rails would not fail, the pipe bending radius was calculated for both loading scenarios. This was more critical for the transverse loading as the load applied in-line would not cause bending forces.

For the in-line loading, the anchor loads reached 27 kNs while the HDPE side rails showed no deformation.

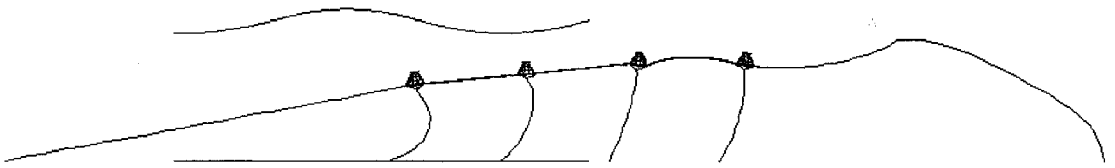

Figure 3.21: Rigid Mooring Subjected to Worst Scenario Load Case in the In-line Direction

The transverse loading showed higher anchor line tensions with the maximum being 29 kNs. This was consistent with the three point mooring system which showed lower tensions when loadings were applied in the in-line direction then the transverse direction. The pipe side rails showed little bending due to the loading.

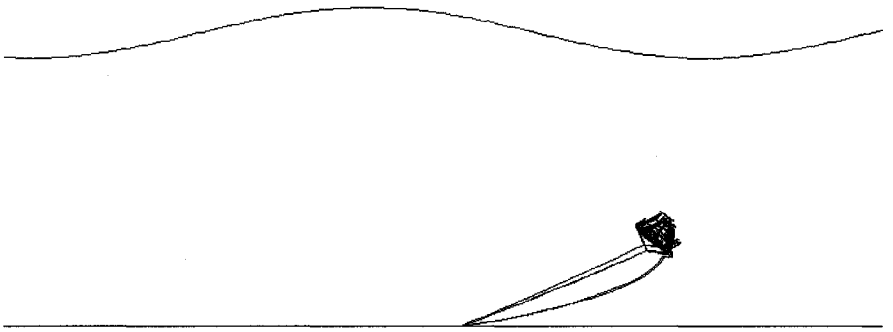

Figure 3.22: Rigid Mooring Subjected to Worst Scenario Load Case in the Transverse Direction

III.4.5. String Mooring

The second of the two multi-cage mooring systems tested was the string mooring. The only difference between the string and the rigid string mooring was how the cages were connected to one another. The string mooring system acted

similar to the rigid mooring system, however, the anchor tensions were slightly lower than the rigid mooring with in-line loading causing a 26 kN tension and the transverse causing a 24 kN load.

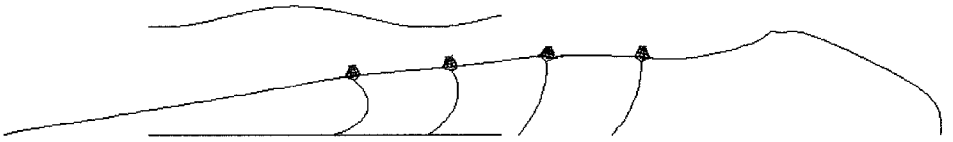

Figure 3.23: String Mooring Subjected to Worst Scenario Load Case in the In-line Direction

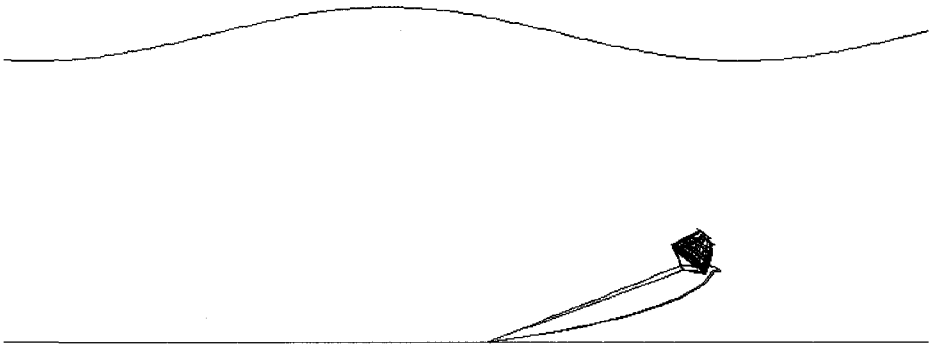

Figure 3.24: String Mooring Subjected to Worst Scenario Load Case in the Transverse Direction

III.5. Feasibility Results

After the simulation data for all five mooring designs had been processed using MATLAB, the tensions in the anchor line below the cages and fore anchor line and cage displacements from all models were compared. If the system had more than one cage, the maximum anchor line tension from below the cages was recorded. The fore anchor was considered to be the anchor which receives the

load on in-line currents for non-symmetric moorings. Below in Table 3.3 are the tensions and cage displacements.

Table 3.3: Aqua-FE Model Results

	Anchor Line Tension Below Cage (kN)	Fore Anchor Line Tension (kN)	System Heave (m)	System Surge (m)
Single Point	23.57	----------	-20.81	36.32
Three Point (in-line)	8.06	31.44	-19.90	12.63
Three Point (transverse)	16.91	5.50	-21.97	35.30
Grid	20.44*	25.58	----------	----------
Rigid (in-line)	27.23	59.46	----------	----------
Rigid (transverse)	29.30	6.40	----------	----------
String (in-line)	25.79	58.21	-13.08	9.69
String (transverse)	24.03	5.52	-21.93	35.72

Notes: *After the first few waves, the tension in the anchor line for the grid mooring went to approximately 3 kN.

III.6. Recommended Design

Utilizing the information from Table 3.3 and other present information, a single configuration, the string mooring was chosen to be further tested. This was based on numerous factors. One major benefit which influenced the choice of the string mooring was its ability to moor any number of cages. If only one cage was desired, the mooring would be similar to the three point mooring already tested. However, if a string of six was desired, this mooring configuration could also be used. A second reason the string design was chosen was based on the low anchor line tensions. For one cage (three point mooring), both directions yielded smaller anchor line tensions then the single point mooring. The grid mooring was

somewhat different since once the cage reached steady state all the cage tensions were transposed to the outer anchors of the actual grid. For the multi-cage system, the maximum anchor line tension was below that of the rigid system. The final reason that the string mooring configuration was chosen over the rigid string mooring was because it allowed for one cage to be taken out of the system without disrupting the others. To remove a cage in the rigid string mooring, the entire system must be floated to the surface, the cage detached, and the entire system re-submerged. To remove a cage in the string mooring, the cage to be removed is floated to the surface, detached from the lines and hauled away. The other cages can stay at depth and should not be affected.

CHAPTER IV

THEORY

IV.1. Response Amplitude Operator (RAO)

One objective of this thesis was to design and analyze a single and multi-cage mooring system. To do this, regular waves were applied to the systems. Linear, small amplitude wave theory was used to approximate the wave characteristics. One useful tool to analyze an objects response is response amplitude operators (RAOs). RAOs are statistical tools which help predict the dynamic behavior of an object when a loading is applied. RAOs were utilized to predict the OCAT cage motion response in three directions, heave (vertical translation of the cage), surge (horizontal translation of the cage in fore and aft directions, and pitch (rotation of the cage about a normal axis). Tension RAOs were also calculated for the anchor, the anchor line, and the lower bridle lines.

RAOs are a ratio of an objects response to the forcing to the objects response or,

$$RAO = \frac{|\text{Response}|}{|\text{Forcing}|} \qquad [4.1]$$

Thus, the RAOs for heave, pitch, surge, and tension are found using the following equations.

$$RAO_{Heave} = \frac{|Heave_{amplitude}|}{|Wave\_Elevation|} \qquad [4.2]$$

$$RAO_{Surge} = \frac{|Surge_{amplitude}|}{|Wave\_Excursion|} \qquad [4.3]$$

$$RAO_{Pitch} = \frac{|Pitch_{amplitude}|}{|Wave\_Slope|} \qquad [4.4]$$

$$RAO_{Load} = \frac{|Load_{amplitude}|}{|Wave\_Elevation|} \qquad [4.5]$$

Where $Heave_{amlitude}$ is the amplitude of the heave response, $Surge_{amplitude}$ is the amplitude of the surge response, $Pitch_{amplitude}$ is the amplitude of the pitch response, and $Load_{amplitude}$ is the amplitude of the load response. To find the forcing amplitudes, small wave amplitude theory was applied. Small wave amplitude theory states that the surface elevation, η, is equal to,

$$\eta = \frac{H}{2}\cos(kx - \sigma t) \qquad [4.6]$$

where H is the wave height, k is the wave number, x is the horizontal position, σ is wave period, and t is time. Since surface elevation is desired, the oscillating term (cosine) can be neglected. This result yields $\eta_{surface}$ equal to,

$$\eta_{surface} = \frac{H}{2} \qquad [4.7]$$

Thus, the denominator of the heave RAO equation, equation 4.2, was found to be equal to half the wave height.

The forcing term for the surge RAO is related to wave excursion. To find the wave excursion small amplitude wave theory was used starting with the velocity potential, Φ. The velocity potential for a wave is described as,

$$\Phi = -\frac{H\sigma}{2k}\frac{\cosh[k(h+z)]}{\sinh(kh)}\sin(kx-\sigma t) \qquad [4.8]$$

where h is water depth, z is vertical distance from the mean sea level to the elevation on the wave with upwards being positive. The derivative of this equation with respect to horizontal position x, results in an equation for horizontal water particle velocity u,

$$u = \frac{Hgk}{2\sigma}\frac{\cosh[k(h+z)]}{\cosh(kh)}\cos(kx-\sigma t) \qquad [4.9]$$

where g is the gravitational constant. If this equation is integrated with respect to time, t, then the wave excursion ζ is found to be,

$$\zeta = -\frac{H}{2}\frac{\cosh[k(h+z)]}{\sinh(kh)}\sin(kx-\sigma t) \qquad [4.10]$$

Like wave slope, the oscillating term was dropped since only the maximum was needed. Similar to the surface elevation, the wave excursion at the surface is desired, the z term was neglected. Thus $\zeta_{surface}$ was found to be equal to,

$$\zeta_{surface} = \frac{H}{2}\frac{\cosh(kh)}{\sinh(kh)} \qquad [4.11]$$

To calculate the RAO for pitch, wave slope was used as the forcing. Wave slope was calculated by taking the derivative of the surface elevation, equation 4.6, with respect to position x. This derivative is equal to,

$$\varphi = \frac{Hk}{2}\sin(kx - \sigma t) \qquad [4.12]$$

Where φ is wave slope. Only the amplitude of the slope was of importance as it would provide the greatest forcing. This allowed for the oscillation term to be neglected resulting in a wave slope equation for $\varphi_{amplitude}$,

$$\varphi_{amplitude} = \frac{Hk}{2} \qquad [4.13]$$

Table 4.1 below shows the resulting values used for the wave slope, wave excursion, and surface elevation for each of the wave regimes RAOS. For the six cage systems, RAOs were originally calculated for each cage in the mooring configuration separately. However, all cages utilized the same forcing parameter.

Table 4.1: RAO Forcings Used for RAO Calculations

Regime Number	Surface Elevation (m)	Wave Excursion (m)	Wave Slope (rad)
1	0.8	0.8	0.572
2	1.4	1.4	0.564
3	1.63	1.63	0.292
4	1.3	1.3	0.131
5	2	2.005	0.129
6	1.2	1.221	0.055
7	1.1	1.137	0.043

IV.2. Catenary Equations

To determine pre-tensions in anchor chain and bridle lines, the catenary equations were used. The loads which were calculated should eventually become the equilibrium tensions if zero loading was to occur. Figure 4.1 below shows the parameters which were used in the catenary equations.

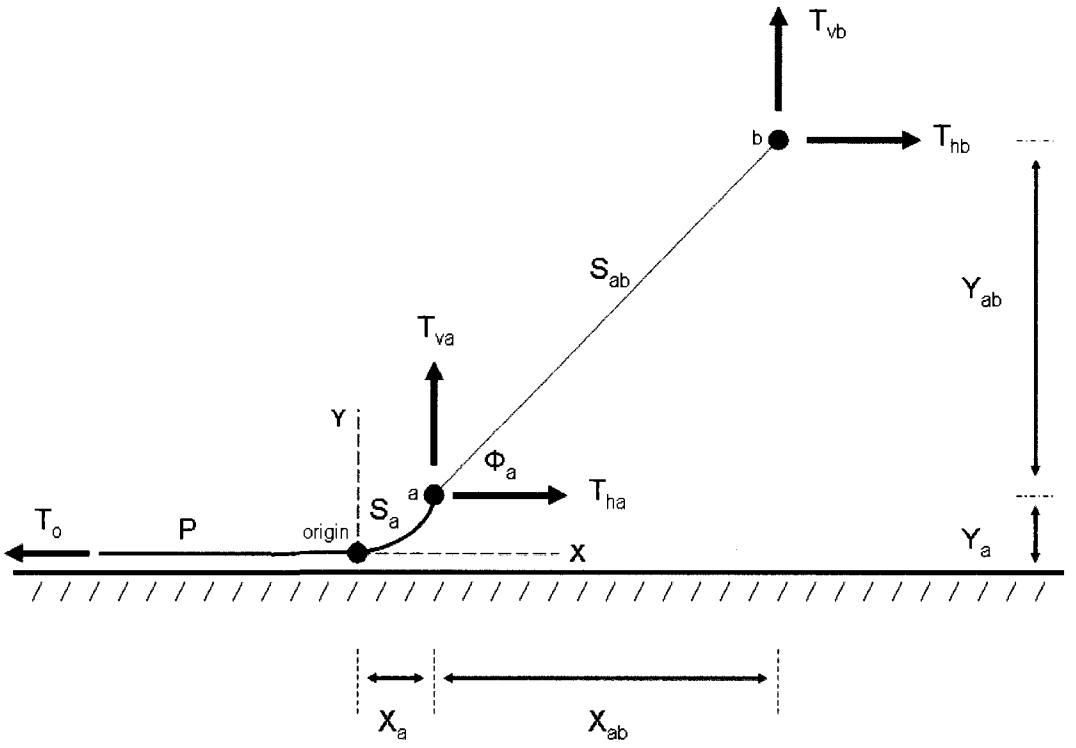

Figure 4.1: Catenary Equation Parameters
Point "a" is the location where the bottom chain attaches to a section of rope and point "b" is where the rope attaches to the buoy.

The variables above are defined as follows:
T_o = tension at the origin
X_a = horizontal distance from the origin to point a
Y_a = vertical distance from the origin to point a
S_a = length from the origin to point a
X_{ab} = horizontal distance from point a to point b
Y_{ab} = vertical distance from point a to point b
S_{ab} = length from point a to point b
Φ_a = angle of vector T and T_{va}
T_{va} = vertical tension at point a
T_{ha} = horizontal tension at point a
T_{vb} = vertical tension at point b
T_{hb} = horizontal tension at point b
P = net weight per unit length in water

Some of the parameters listed above were set by design including T_o, which was equal to the tension in the anchor line; T_{vb}, which was equal to the buoyancy of the buoy; P, the weight of chain per unit length in water; the length of the anchor line, S_{ab}; and the length of chain S_a. Utilizing static mechanics analysis it was found that for the OCAT anchor system, T_{ha} and T_{hb} were both equal to T_o and that T_{va} was equal to T_{vb}. To solve for the remaining parameters, the catenary equations, equations 4.14, 4.15, and 4.16, were used along with geometry.

$$S_a = \frac{T_o}{P} * \sinh\left(\frac{PX_a}{T_o}\right) \qquad [4.14]$$

$$Y_a = \frac{T_o}{P}\left[\cosh\left(\frac{PX_a}{T_o}\right) - 1\right] \qquad [4.15]$$

$$T_{va} = PS_a \qquad [4.16]$$

CHAPTER V

MOORING ANALYSIS

V.1. Design Criteria

The chosen mooring design to be further tested was the string mooring. This mooring was chosen due to its versatility, low anchor tensions, and its ability to easily harvest the cages. The string mooring was modified to allow for both a single and multi-cage system to better understand mooring limitations. Each of these systems had a similar mooring set-up with two side anchors on each side of the system and each cage having an anchor weight below it. Since neither mooring configuration was symmetrical, both had to be tested with loads in in-line and transverse directions.

In an attempt to assure accurate results, system parameters were set to realistic field values. These parameters included cage buoyancy and anchor weights below the cages. Other design criteria such as ease of harvest and mooring tensions had to be tested to assure the chosen design would meet requirements.

V.1.1. Mooring Lines Parameters

The design criteria for the system mooring lines included tensions and scope. The scope of a mooring system is defined as the ratio of the length of mooring line to the depth of water. It is ideal to have a scope between 5:1 and 7:1. To assure that the scope would be in this acceptable range, the lengths of the mooring lines had to be at least five times as long as the depth of the water or approximately 150 meters.

A second mooring constraint was to assure that a cage could be floated to the surface without disrupting other cages in the system. For this to occur, distances between cages had to be set apart such that one cage could be floated at least 10 meters vertically without disrupting other cages in the system.

To allow the cage to be disconnected from the mooring system by divers, the tensions in these mooring lines could not exceed a set tension of 150 lbs. This pre-tension also restricts the system movement.

V.1.2. Cage Parameters

The major design criteria for the cage included cage buoyancy and the ability to harvest the cage. The buoyancy of the cages in the feasibility study was designed to be higher than the actual value to account for the lack of an anchor below the cage. This was changed and the cages were given a buoyancy of 125 kilograms, 1,225 newtons. This was based on the UNH OCAT system. This change in cage buoyancy also helped to size the deadweight below the cage. Since the cage would be floated to the surface by increasing cage buoyancy to overcome the deadweight below, the weight was chosen to be 225 kilograms.

This was chosen because a UNH research vessel could deploy a deadweight of that size and the 100 kilogram difference between the buoyancy and the weight could be overcome by displacement of water.

V.2. Final Design Modifications

V.2.1. Single Cage System

The string mooring design used for the feasibility study was slightly modified for the single cage mooring analysis. The cage was modeled after the cage discussed in section III.1.2. Some modifications were made to assure system criteria set in section V.1 could be met. One of these modifications was changing the density of the diagonal rims to be positively buoyant. This caused the cage to have a positive buoyancy of 125 kilograms. This change also made the system more realistic since in the field the cage would be submerged or raised to the surface by pumping air or water into the diagonal rim.

Since the cage was now positively buoyant, to prevent it from floating to the surface, a deadweight was modeled under the cage instead of the original fixed point. The chosen anchor weight for under the cage was, 225 kg, slightly larger then the buoyancy of the cage. This size would prevent the cage from floating to the surface while having a low enough weight to be deployed and moved using the UNH R/V Meriel B.

A shot (90 ft) of 3/4" grade 3 stud-link anchor chain was also added to the model on each side connecting each side anchor to the poly-steel mooring lines. This chain weighed 480 lbs per shot and had a breaking strength of 64,000 lbs.

The chain was added to add compliance to the system as well as prevent the anchor from being lifted vertically when pulled by a vessel. Figure 5.1 shows the single cage system used in the mooring study while Figure 5.2 shows the materials used.

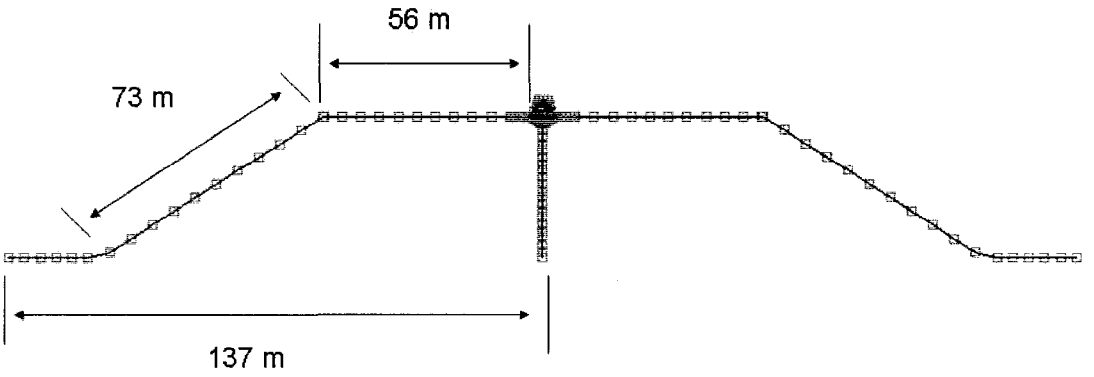

Figure 5.1: Single Cage Mooring Study Model

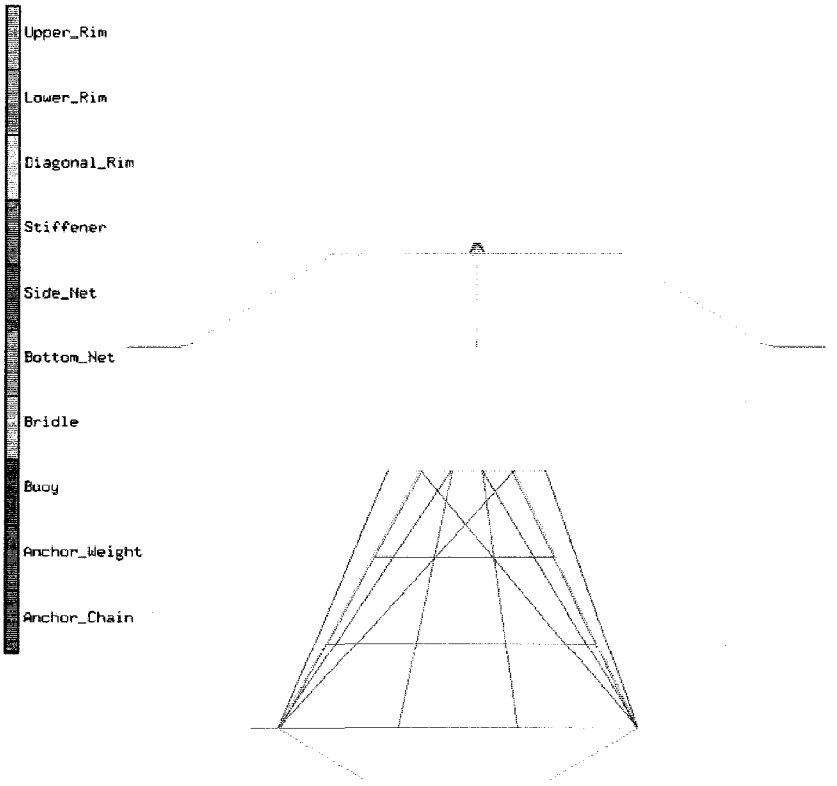

Figure 5.2: Single Cage Material Properties

To ensure that a cage could be harvested at the surface while not disrupting other cages in the system the distance between cages was changed to 46 meters. This distance made certain that a cage could be raised to the surface while causing minimal impact to the other cages. This distance between the cages also guaranteed that the cages would not be able to surge into one another during extreme weather conditions.

The last change to the model was adding pre-tensioned lines with values determined from the catenary equations seen in Table 5.1. The parameters for these equations can be found in section IV.2.

Table 5.1: Catenary Equation Solutions

T_o (lbf)	175
S_a (m)	6.302
S_{ab} (m)	67
Φ_a (rad)	0.562
T_{va} (N)	490.5
T_{ha} (lbf)	175
T_{vb} (N)	490.5
T_{hb} (lbf)	175
P (lbf/ft)	5.33

These changes made the scope of the mooring lines slightly larger than 5:1. The designed scope was right in the range of the ideal scope values making this an acceptable design.

Like the original study, the two outside anchors remained as fixed points to determine loads in the anchor lines so an anchor could be sized for the mooring.

V.2.2. Six Cage Modifications

In addition to the single cage string model, a multi-cage model was created. The six cage mooring design was changed to be exactly like the single cage as described in section V.2.1, including all pre-tensioned lines, bridle line lengths, and anchors.

Increasing the number of cages in the system was done because it was assumed that six cages would be the largest number of cages in this type of mooring. Thus testing would help bracket potential mooring situations. Simulations using four cages were also performed to determine if there was any linear correlation in anchor forces when the number of cages was increased.

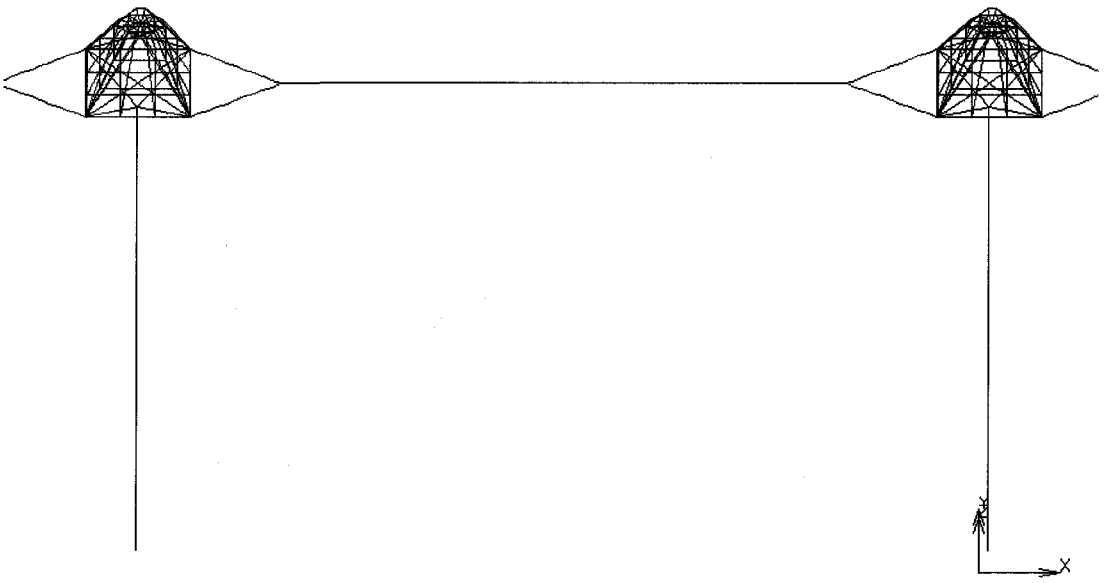

Figure 5.3: Multi-cage Bridle Connection
The duel line bridle between cages used in the feasibility model was modified to a more realistic and easily deployed single line bridle.

V.2. Finite Element Model Creation

The models were modified using the changes discussed in sections V.1.1 and V.1.2. The number of nodes, elements, and material properties for each of the models are listed in Table 5.2.

Table 5.2: Nodal, Element, and Material Property Counts for the Original Cage and Modified Single and Six Cage Models

	Total Nodes	Total Elements	Total Material Properties
Single Cage System	197	278	10
Six Cage System	1006	1497	10

The material properties used for each of the moorings were based upon values taken from Risso (2007). Changes were made to cross sectional areas where applicable as well as buoy size and chain types. Below in Table 5.3 are the material properties for the models.

Table 5.3: Finite Element Model Material Properties

Material Properties	Density (kg/m^3)	Young's Modulus (GPa)	Cross Sectional Area (m^2)
Upper Rim	316.4	1.172	0.059
Lower Rim	1225	1.172	0.059
Diagonal Rim	975	1.172	0.059
Stiffener	1025	250	4.0×10^{-6}
Side Net	1025	190	7.854×10^{-7}
Bottom Net	1025	190	7.854×10^{-7}
Bridle	963.5	3.235	1.14×10^{-3}
Buoy	275	2.3	0.1333
Anchor Weight	7850	200	0.01613
Anchor Chain	7850	200	1.011×10^{-3}

V.3. Load Cases

V.3.1. Pre-loading Tests

Before the mooring systems could be tested with current and wave loadings, three tests were performed on both models to assure that the models were built to acceptable standards. The first test, a free release test, was performed to determine natural frequency and damping coefficient of the cage. This test utilized only the cage without the mooring or bridle lines. For the first free release test, the cage was placed 0.5 meters above the water surface and allowed to free fall and reach steady state. Once this was completed, a second free release test was run. To perform this test, the cage was placed back into the water and rotated about the axis running vertically through it by 5°. It was released and allowed to reach steady state. The results from these two tests were plotted and the natural frequency and damping coefficients were calculated by taking values directly from the plots.

Once the results from the free release test were found to be acceptable, a static simulation to assure that the tension values in the bridle and anchor lines were close to the values found using the catenary equations was performed. This test was executed by applying zero loading to the systems and allowing them to reach steady state. Once at steady state, the tensions in the lines were analyzed and compared to the values from the catenary equations.

The last check which was performed on each of the two models before simulations began was to assure that cages in each model could be floated to the surface without causing tensions in bridle lines to become too high. In the

case of the multi-cage system, this test also assured that floating one cage to the surface would not cause other cages in the mooring to be affected. The design tension was set at 150 lbs to allow for a diver to disconnect the cage.

V.3.2. Current Loadings

Both current and wave loading were used for in-depth testing. The current loadings were the same as used by Risso (2007), starting at 0.25 m/s or ½ a knot, and increasing by 0.25 m/s to 2.0 m/s or 4 knots. These currents were applied in-line as well as transverse to the cage.

V.3.3. Wave Loadings

Wave regimes were also taken from original work performed by Risso (2007). The one difference was doubling the wave heights. This was done since the original work modeled the cage at the surface while this testing occurred at a depth of 10 meters. These heights could be doubled without causing any issues with comparability between the two systems since the wave RAOs, were compared. The table below shows the seven wave regimes utilized for testing. Like the current loadings, the wave loadings were applied both in-line and transverse to the cage.

Table 5.4: Wave Regimes Applied to the Cage Systems

Wave Regime	Wave Height (m)	Wave Length (m)	Wave Period (s)	Slope (L/H)
1	1.6	8.782	2.372	5.489
2	2.8	15.606	3.162	5.574
3	3.26	35.112	4.743	10.771
4	2.6	62.437	6.325	24.014
5	4.0	97.32	7.906	24.33
6	2.4	138.028	9.487	57.517
7	2.2	159.459	10.277	72.481

V.3.4. Wave and Current Loadings

The last loadings that were applied used both wave and current loadings. These loads were chosen to apply conditions which would be similar to storms at the UNH OAA site as well as normal operational conditions. For the operational loading, the current was based on a value published in Marine Technology Society Journal in an article about the UNH OAA site (Tsukrov et al., 2000). This article stated "The input current value used for the typical loading condition consists primarily of the tidal component of the coastal current near the demonstrations site, which is estimated to be 0.25 m/s." The wave loading was based on wave periods published by Fredriksson (2001). Similar to the current and wave simulations, both duel loading scenarios were applied in-line and transverse to the cage systems. The table below shows the wave and current loadings.

Table 5.5: Wave and Current Loadings

	Current Velocity (m/s)	Wave Height (m)	Wave Length (m)	Wave Period (s)
Storm	1.0	9.0	119.836	8.8
Operational	0.25	2.0	44.507	5.34

V.4. Areas of Investigation

The major areas of investigation include cage movements in the heave, surge, and pitch directions as well as the stresses in bridle lines and anchor lines. All cage motions were assumed to be oriented with respect to the propagation direction of the incoming current or waves. The cage movements were tracked by recording motion data from three corner nodes on each cage.

Stress values were recorded for the anchor line and bridle line elements. For the multi-cage model, stresses in bridle lines between the cages were also recorded. These stresses were then multiplied by the cross sectional area of the element to get a tension value. These tensions helped to assure lines would not fail as well as characterize anchor forces to check holding strengths.

The figures below show the single cage and the six cage moorings with locations of recorded values. The blue dots are nodes which have been recorded for motion while the red squares denote elements which have been recorded for stress data. All simulations, whether forcing was applied in the transverse or in-line direction, utilized the same nodes and elements for data acquisition.

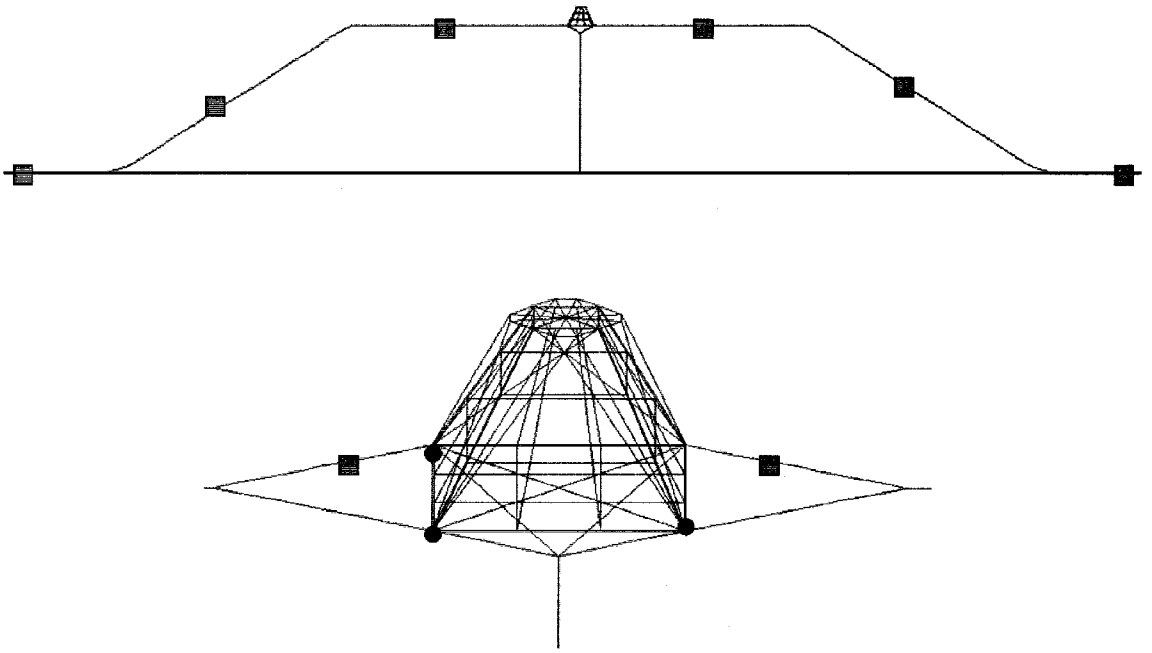

Figure 5.4: Single Cage Mooring with Nodes and Elements for Data Acquisition Marked

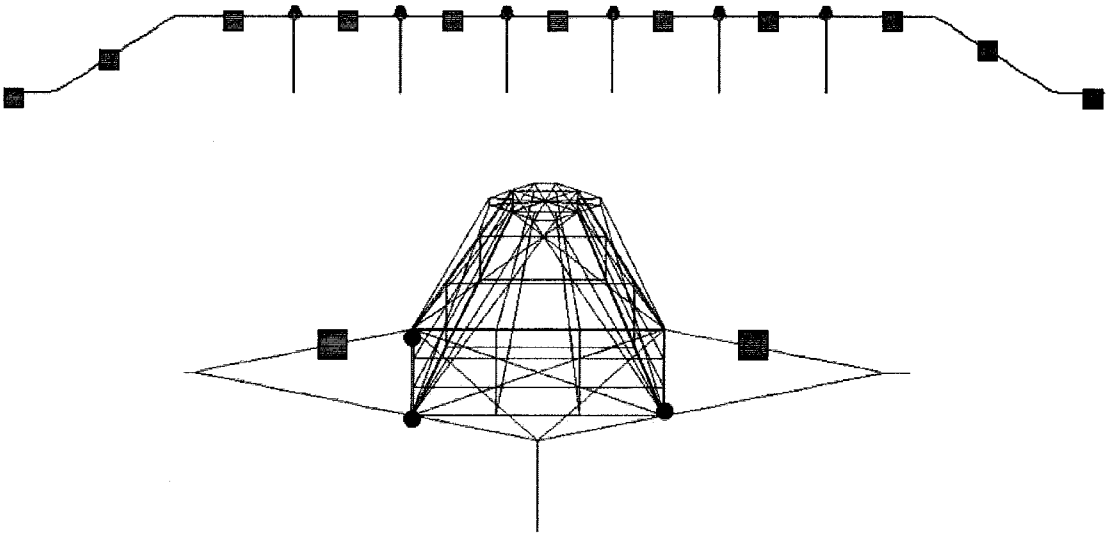

Figure 5.5: Six Cage Mooring with Nodes and Elements for Data Acquisition Marked

CHAPTER VI

MOORING ANALYSIS RESULTS

VI.1. Pre-loading Simulation Results

To further test the string mooring limitations, two models were created, one for a single cage and one for a multi-cage system. These models were tested under a variety of current and wave loadings to determine cage motion responses and mooring line tensions. However, before motion simulations were run, three tests were performed to assure the models were created with the correct parameters and to determine system characteristics.

The first step was to obtain the OCAT cage natural frequency and damping coefficient. The cage system, discussed in section III.1.2, underwent a free release test in heave and pitch. The results from these two tests can be found in Table 6.1. The low natural period is desirable as it shows that the cage will be excited by short period waves which tend to have less energy than higher period waves. Figure 6.1 shows the cage motion from the heave experiment.

Table 6.1: Free Release Results

	Heave	Pitch
Damped Natural Period (s)	2.85	5.35
Damping Coefficient	-0.015	-0.021

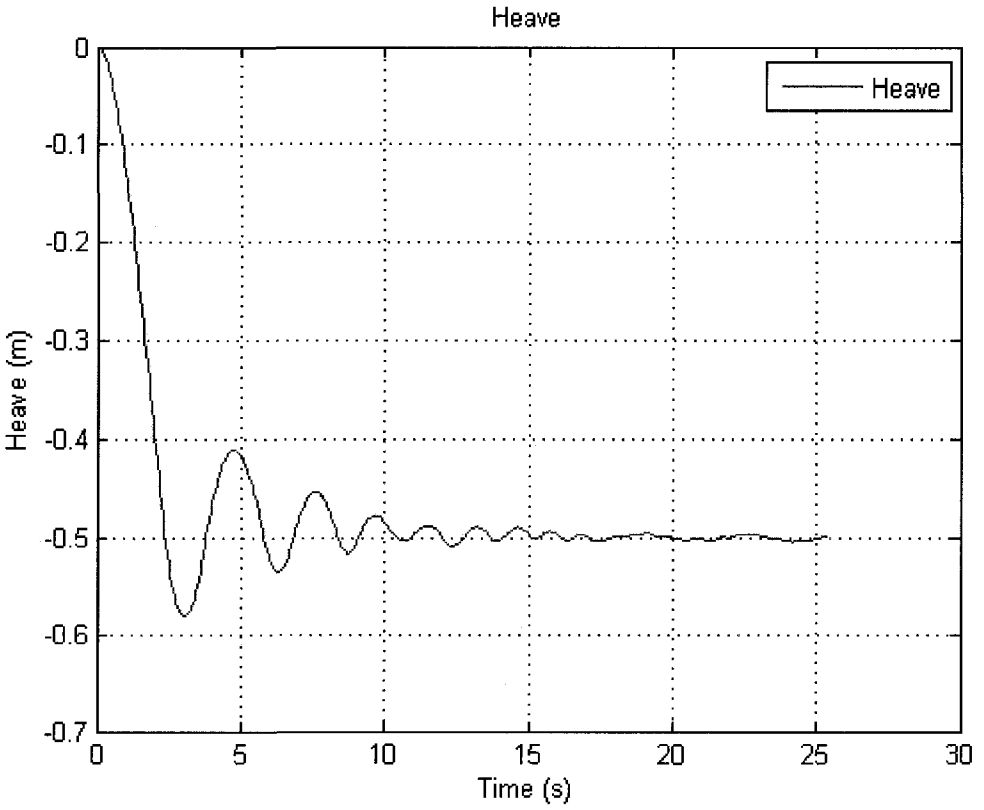

Figure 6.1: OCAT Cage Heave Response

The second test was performed to ensure that the mooring line tensions would be pre-tensioned to the design values determined using the catenary equations. The single and multi-cage moorings, discussed in section V.2, were tested in Aqua-FE with no applied waves or currents. The mean calculated and predicted mooring line tensions are listed in Table 6.2.

Table 6.2: Static Test Resulting Tensions

	Calculated Tension (kN)	Aqua-FE Tension (kN)	Percent Difference
Anchor	0.78	0.84	7.7%
Anchor Line	0.92	0.98	6.1%
Lower Bridle Line	0.78	0.83	6.4%

After completing the static test, the tension values in the mooring lines were slightly larger than the design values. This was deemed acceptable.

The final pre-loading test which was performed was used to verify that a cage could be floated to the surface without disrupting other cages or creating mooring line tensions over the 150 lb design criteria. This "harvest test" was executed by floating a single cage from the six cage mooring to the surface. The tensions in mooring lines were monitored to ensure they did not greatly exceed the design tension. Figure 6.2 shows the cage at the surface for harvest. Table 6.3 shows the resulting tensions found for the six cage mooring.

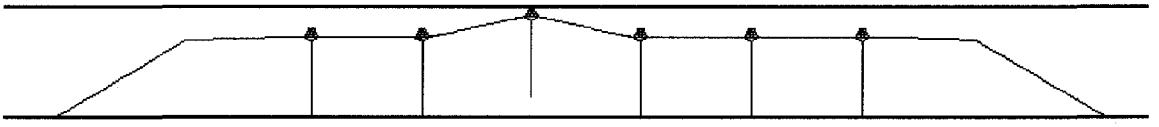

Figure 6.2: Six Cage System with Floating Cage
As seen, the original cages are not affected by floating a cage to the surface.

Table 6.3: Harvest Test Results

	Designed Tension (kN)	Aqua-FE Tension (kN)	Percent Difference
Cage Bridle Line	0.67	0.96	30.2%

The harvest test proved a cage could be floated to the surface without disrupting other cages in the system. This paired with the resulting tensions in mooring lines of 210 lbs, close to the design tension, proved the mooring to be acceptable in pre-loading simulations.

VI.2. Loading Results

The single and multi-cage mooring systems were then analyzed under currents and waves in the numerical model program Aqua-FE. Once the simulations were complete, the results were processed using MATLAB. For the current load cases, mean system displacements and mooring line tensions were recorded. For wave loadings, RAOs were calculated for heave, surge, pitch, and tensions. For loadings with both current and waves, time series system motions were plotted. The organization of the following sections is as follows. First a current or wave regime will be highlighted, and then if presentable, all the results will be presented. Due to the large quantity of data, only select plots will be shown in each section. Results for each simulation can be found in Appendices C-M.

VI.2.1. Single Cage Current Loading Results

To help ensure that the designed system could survive in the field, current loadings were applied in the in-line and transverse directions. The current velocity ranged from 0.25-2 m/s, in 0.25 m/s increments. These correspond to the current ranges which were tested by Risso (2007). Time series motion and tension results were obtained. The steady state motion values were averaged to

determine the cage's heave, surge, and pitch. Figure 6.3 shows the average motion response for the single cage mooring subjected to a current loading of 1.0 m/s (1 knot) directed in the in-line direction. As seen, the cage heave was 13 meters while the cage surge was 8.5 meters. The initial response seen in the first 25 seconds is an artifact of the system starting in an undeformed, equilibrium state. This would not occur in field observations.

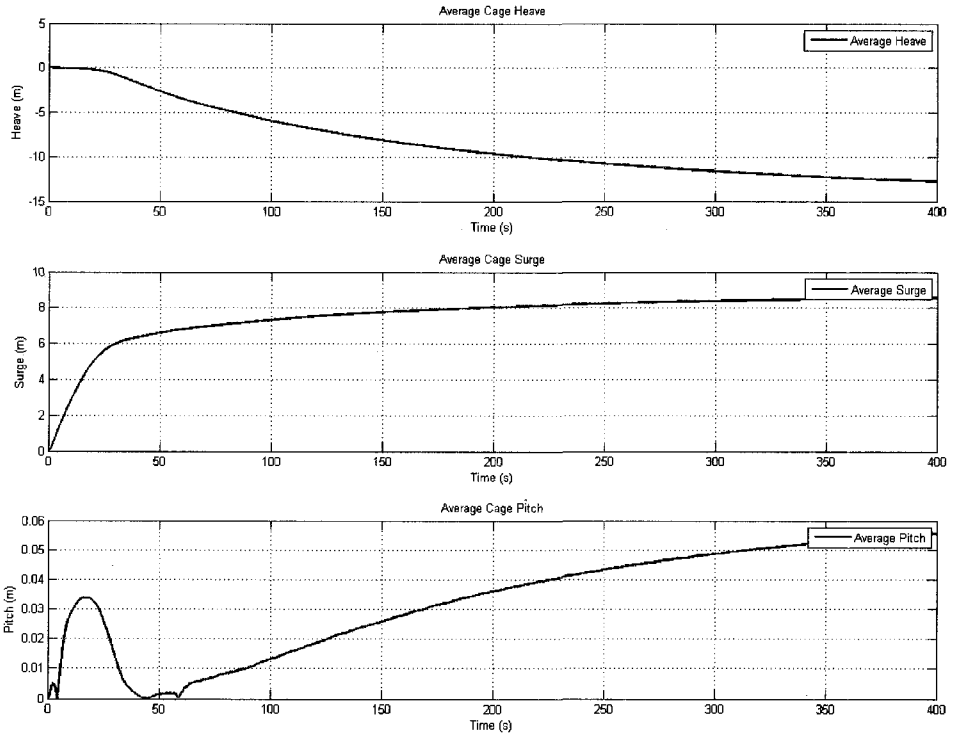

Figure 6.3: Motion Results for a Single Cage Mooring Subjected to 1.0 m/s Current in the In-line Direction

Time series mooring line tensions were also obtained. Figure 6.4 shows the average tension plots from the single cage mooring subjected to a 1.0 m/s current in the in-line direction. "Fore" denotes the area which is first subjected to

the incoming current, while "aft" refers to the area which is subjected second as labeled in Figure 5.4. The maximum anchor tension was found to be 8.5 kN.

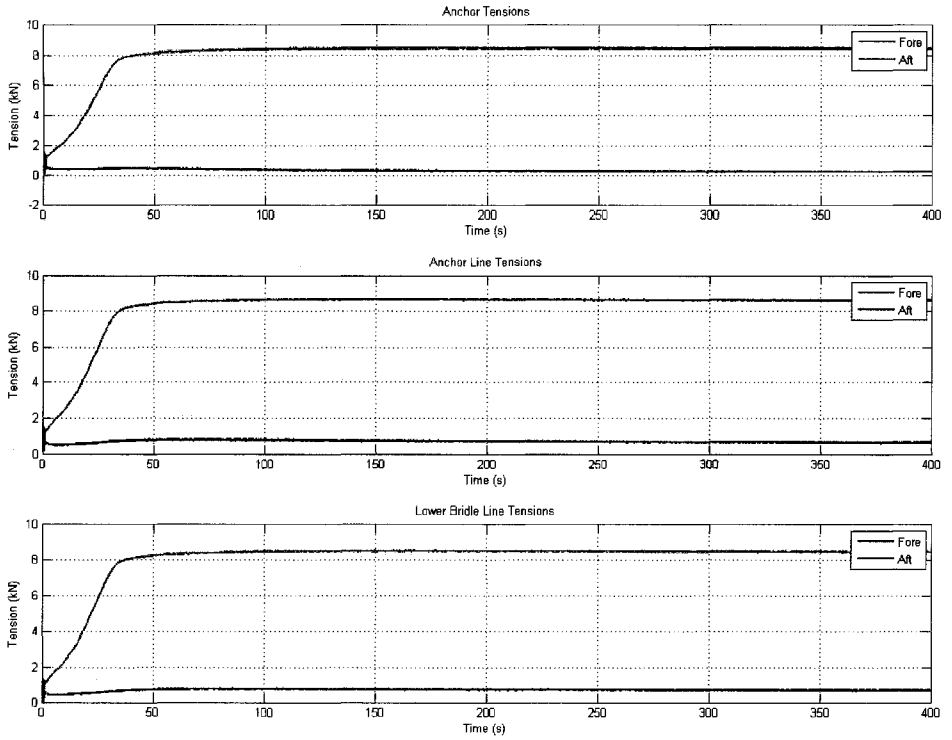

Figure 6.4: Tension Results for a Single Cage Mooring Subjected to 1.0 m/s Current Applied in the In-line Direction

The method outlined above to determine average cage motions and tensions was used on all current loadings both in-line and transverse to the cage. Figures 6.5 and 6.6 show the cage motion and mooring line tensions, respectively, subjected to a 1.0 m/s current in the transverse direction. It can be noted that unlike the in-line directions, tension values for transverse show that the "fore" lines and "aft" lines share the same loading values due to symmetry. Motion results show that the cage heave was 24 meters while the cage surge was 55 meters, both much higher then the in-line loading. Anchor tensions were found to be 15 kN, also higher than the in-line loading. Table 6.4 shows the

results for average motions in both in-line and transverse directions while Table 6.5 shows the results for tensions in the in-line and transverse directions.

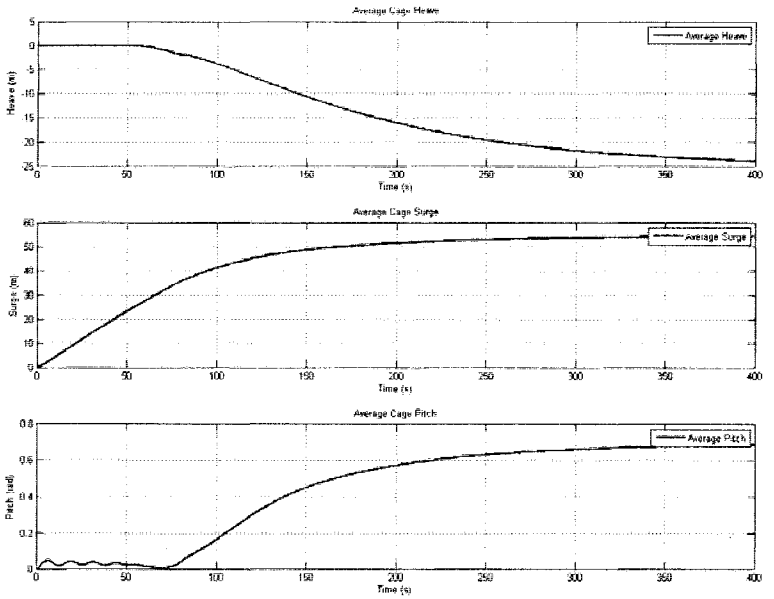

Figure 6.5: Motion Results for a Single Cage Mooring Subjected to 1.0 m/s Current Applied in the Transverse Direction

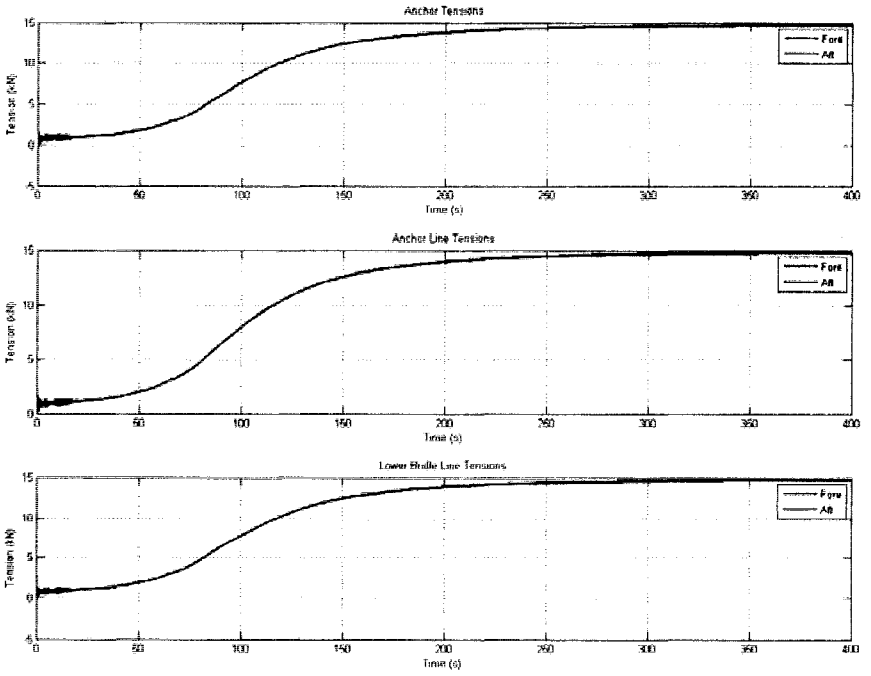

Figure 6.6: Tension Results for a Single Cage Mooring Subjected to 1.0 m/s Current Applied in the Transverse Direction

Table 6.4: Single Cage System Average Motion Response for the In-line and Transverse Loading Directions

Current Velocity (m/s)	Average Cage Heave (m)		Average Cage Surge (m)		Average Cage Pitch (rad)	
	In-line	Transverse	In-line	Transverse	In-line	Transverse
0.25	0.00	0.02	2.78	25.77	0.03	0.01
0.5	-2.01	-6.44	5.46	43.38	0.03	0.15
0.75	-5.17	-18.52	6.83	51.31	0.01	0.39
1.0	-12.67	-23.94	8.56	54.24	0.06	0.69
1.25	-19.51	-26.67	9.72	56.11	0.12	0.93
1.5	-24.61	-28.75	10.42	57.69	0.16	1.10
1.75	-28.04	-30.34	10.87	59.12	0.20	1.22
2.0	-31.98	-31.32	11.26	60.55	0.23	1.29

Table 6.5: Single Cage Average Mooring Tensions

Current Velocity (m/s)	Average Anchor Tension (kN)		Average Anchor Line Tension (kN)		Average Lower Bridle Tension (kN)	
	In-line	Transverse	In-line	Transverse	In-line	Transverse
0.25	1.24	1.21	1.38	1.36	1.23	1.21
0.5	2.76	4.07	2.92	4.24	2.77	4.11
0.75	5.25	8.22	5.45	8.31	5.33	8.24
1.0	8.43	14.71	8.59	14.77	8.49	14.71
1.25	12.43	23.54	12.56	23.58	12.48	23.53
1.5	17.39	34.24	17.48	34.27	17.40	34.21
1.75	23.39	46.48	23.45	46.49	23.39	46.43
2.0	30.12	60.80	30.15	60.79	30.09	60.71

Note: Only the fore mooring lines were listed since fore lines received the dominant loading for in-line simulations and transverse simulations yielded symmetric results.

All single system motion and tension results for the in-line load cases can be found in Appendix C. Motion results and tension plots for transverse loadings can be found in Appendix D.

VI.2.2. Six Cage Current Loading Results

Similar to the single cage mooring system, current loadings were run both in-line as well as in transverse directions to the six cage mooring at velocities ranging from 0.25 m/s to 2.0 m/s. Time series motion and tension results were also obtained. Cage motions for all net pens (total of six) were found using the same method as described for the single cage. Figure 6.7 shows the average motion response for the six cage mooring subjected to a current loading of 1.0 m/s directed in the in-line direction. All cages had different heave values, while the maximum heave was 20 meters by the first cage. Like the heave, the surge values for each cage were different, with the maximum at 12 meters by the sixth cage.

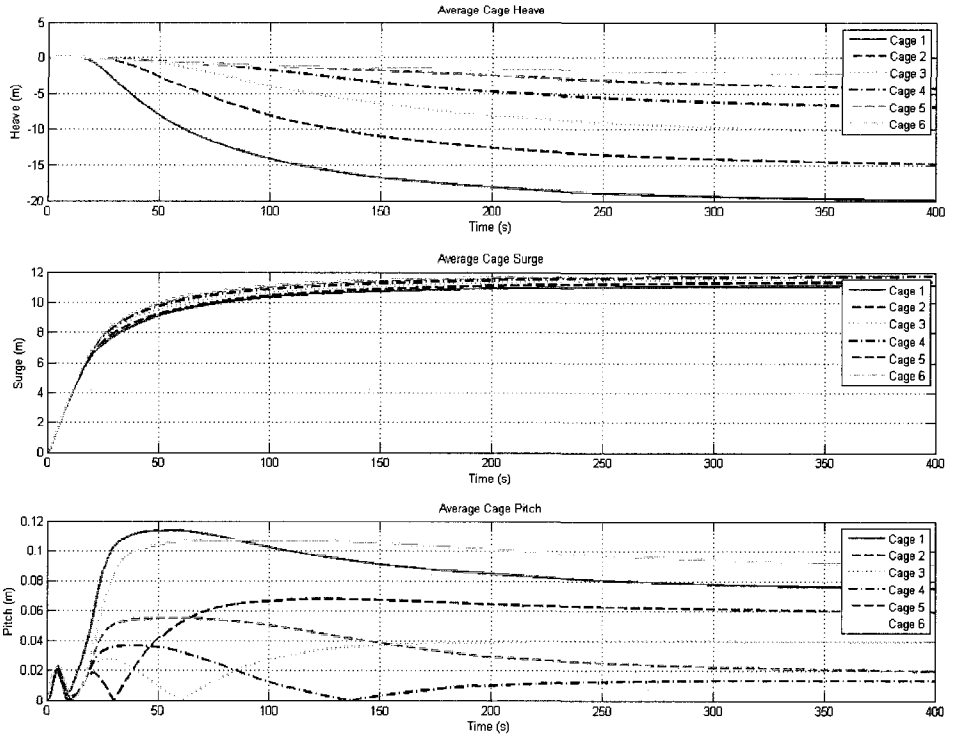

Figure 6.7: Motion Results for the Six Cage Mooring Subjected to 1.0 m/s Current Applied in the In-line Direction

Table 6.6: Average Motion Response Values for the Single Cage Mooring Subjected to a 1.0 m/s Current in the In-line Direction

Cage Number (from fore to aft)	Average Cage Heave (m)	Average Cage Surge (m)	Average Cage Pitch (rad)
Cage 1	-19.87	11.14	0.075
Cage 2	-14.77	11.37	0.059
Cage 3	-10.38	11.57	0.039
Cage 4	-6.85	11.74	0.014
Cage 5	-4.29	11.86	0.020
Cage 6	2.34	11.88	0.091

Due to the large quantity of data, a table of average motion results for the six cage in-line simulations can be found in Appendix E, while time series motion and tension plots for in-line loadings can be found in Appendix F.

Line tension values were calculated using a similar method as discussed previously. Figure 6.8 shows a tension plot for the six cage mooring.

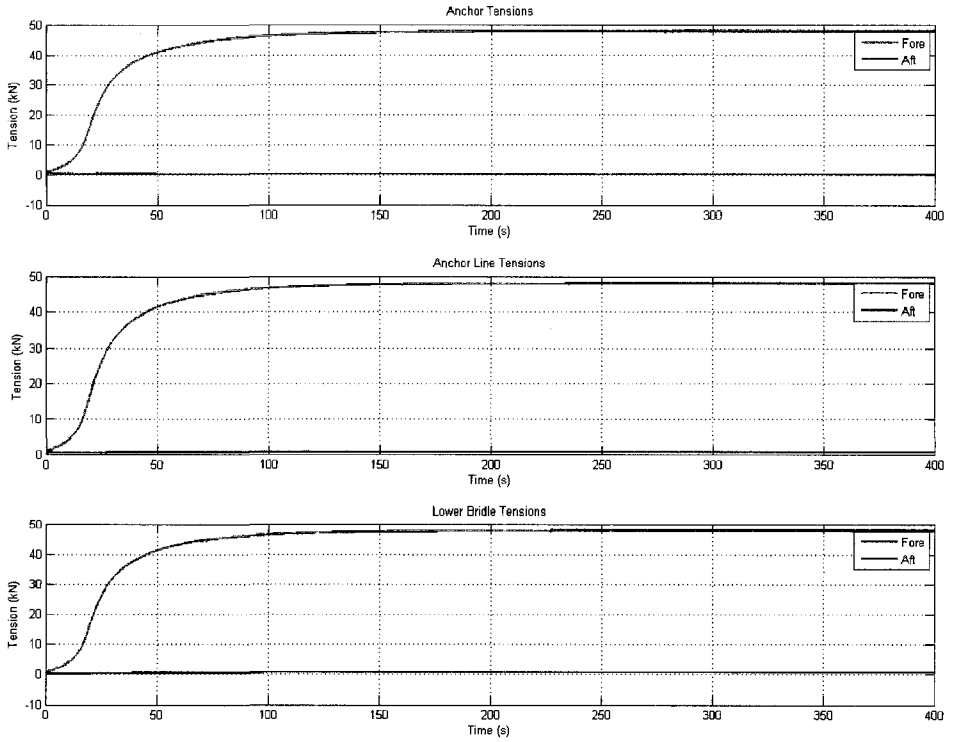

Figure 6.8: Tension Results for the Six Cage Mooring Subjected to 1.0 m/s Current in the In-line Direction

It can be seen that when subjected to in-line loading, the fore moorings absorbed the majority of the load. The maximum anchor tension was 50kN. Table 6.6 displays the resulting tension values for the 1.0 m/s current for fore lines.

The method outlined above to determine average cage motions and tensions was used on all current loadings both in-line and transverse to the cage moorings. Figures 6.9 and 6.10 show time series motion results and tension results respectively, for the six cage mooring subjected to a 1.0 m/s current in the transverse direction. Motion results for the 1.0 m/s current can be found in Table 6.7, while tension results can be found in Table 6.8 which compares anchor, anchor line, and lower bridle line tensions for in-line loadings and transverse loadings. It can be noted in figure 6.9, that there appears to be a delay before

heave takes place. This event is also seen in all the tension plots from Figure 6.10. Similarly to the in-line loading, the first cage had the most heave, 23 meters, however as seen the sixth cage had almost the same heave. It should be noted that unlike the in-line tension, the cage which had the highest surge is the fourth cage.

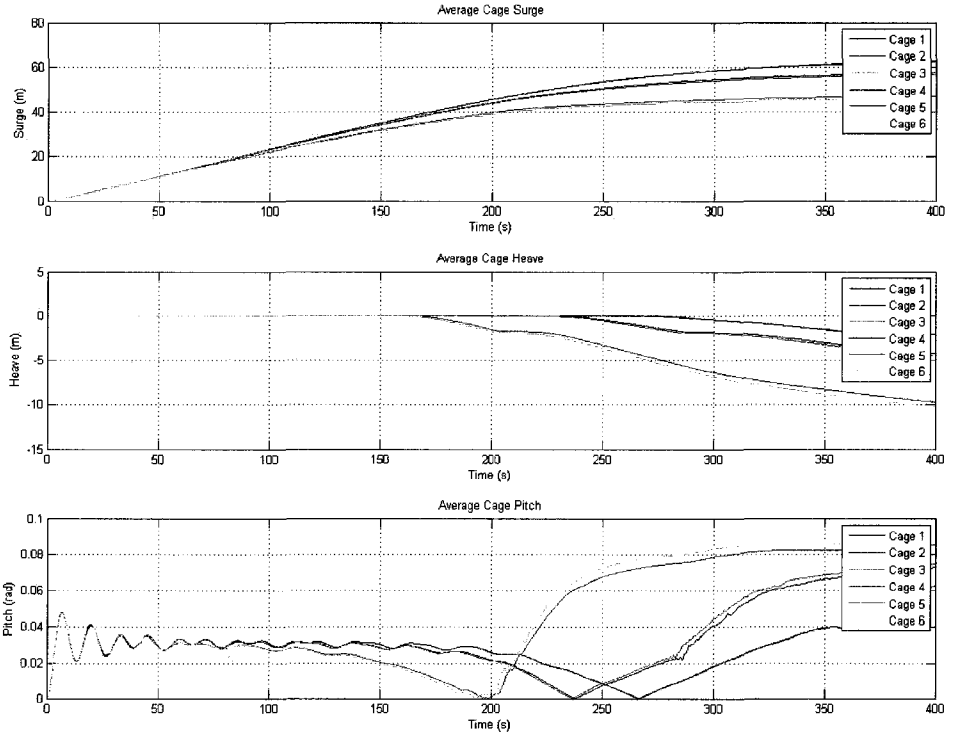

Figure 6.9: Motion Results for a Six Cage Mooring Subjected to 0.5 m/s (1 knot) Current in the Transverse Direction

Table 6.7: Average Motion Response Values for the Single Cage Mooring Subjected to a 1.0 m/s Current in the In-line Direction

Cage Number (from fore to aft)	Average Cage Heave (m)	Average Cage Surge (m)	Average Cage Pitch (rad)
Cage 1	-23.18	59.24	0.422
Cage 2	-20.03	72.55	0.431
Cage 3	-18.43	79.21	0.436
Cage 4	-18.49	78.86	0.437
Cage 5	-20.21	71.52	0.434
Cage 6	-23.48	57.57	0.427

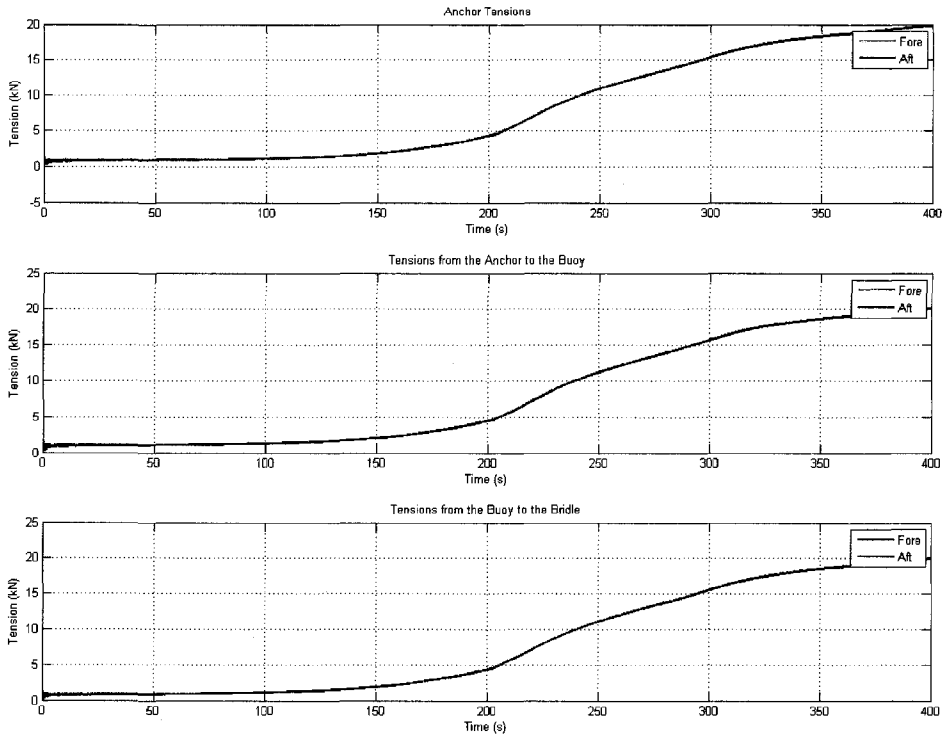

Figure 6.10: Tension Results for a Six Cage Mooring Subjected to 0.5 m/s (1 knot) Current in the Transverse Direction

Table 6.8: Average Tension Values for the Six Cage Mooring

Current Velocity (m/s)	Average Anchor Tension (kN)		Average Anchor Line Tension (kN)		Average Lower Bridle Tension (kN)	
	In-line	Transverse	In-line	Transverse	In-line	Transverse
0.25	3.76	2.04	3.97	2.21	3.83	2.06
0.5	13.03	19.80	13.28	20.06	13.17	19.96
0.75	27.90	39.87	28.11	39.91	28.02	39.97
1.0	47.92	66.89	48.08	67.01	48.00	66.95
1.25	72.92	100.95	73.05	101.04	72.99	100.98
1.5	102.92	141.61	103.02	141.69	102.97	141.62
1.75	140.22	187.79	140.30	187.85	140.25	187.77
2.0	181.32	238.69	181.38	238.73	181.35	238.64

Due to the large quantity of data, motion results for the six cage simulations can be found in Appendix E, while time series motion and tension plots for transverse loadings can be found in Appendix G.

VI.2.3. Wave Loading Results

In addition to the current loadings, seven wave regimes were applied to the mooring configurations. These wave regimes were taken directly from previous work performed by Risso (2007) with the exception of wave heights. Risso investigated a surface system, whereas this study utilized submerged cages. Thus to increase the response to wave loadings, the wave heights used by Risso (2007) were doubled. This change was acceptable since linear small amplitude wave theory is used and the calculated RAOs are normalized by the wave height, excursion, or slope. Like the current loadings, wave loadings were applied in both in-line and transverse directions.

VI.2.4. Single Cage Mooring Wave Results

RAO values were found for the single cage mooring in heave, surge, and pitch. These values were obtained from the steady state response of the system. Figure 6.11 shows the time series motion response plot to wave regime 5.

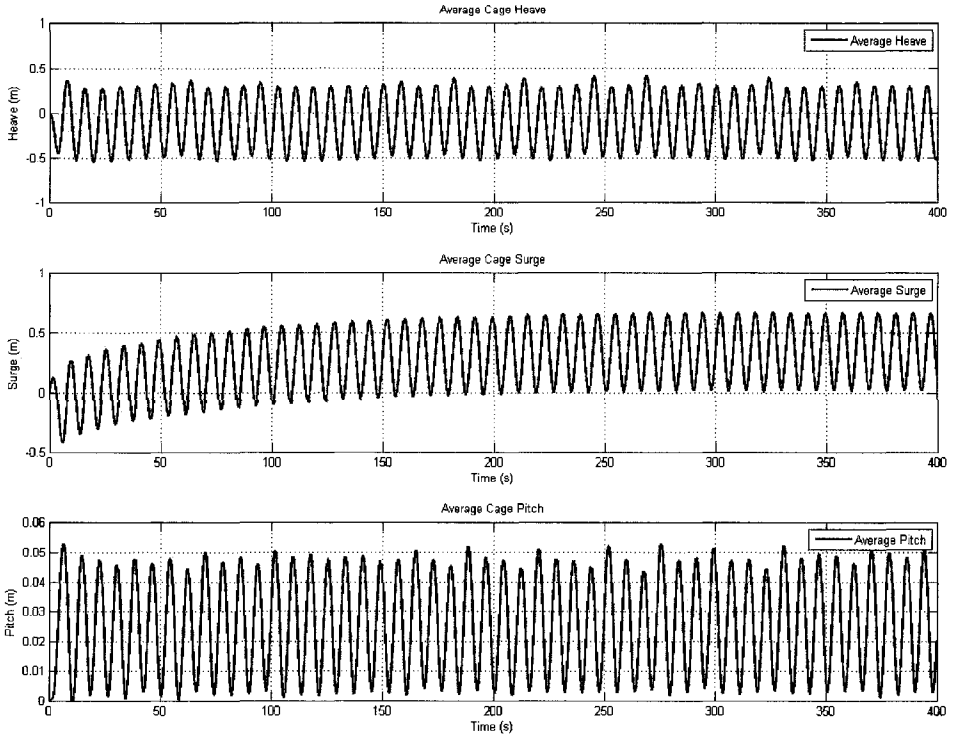

Figure 6.11: Motion Response to Wave Regime 5 in the In-line Loading Direction

Tension RAOS were also calculated for tensions at the anchor, anchor line, and lower bridle line. Unlike the current loading results, both the fore and aft anchor lines absorb some tension in each wave regime. A phase shift can sometimes be seen. As the crest moves past the cage, the fore lines are loaded while the aft lines become partly slack. As the wave trough moves past the cage, the loading is transferred to the aft lines as the fore lines begin to slacken. This can be seen in Figure 6.12 which shows a portion of the tension loads resulting from wave regime 5.

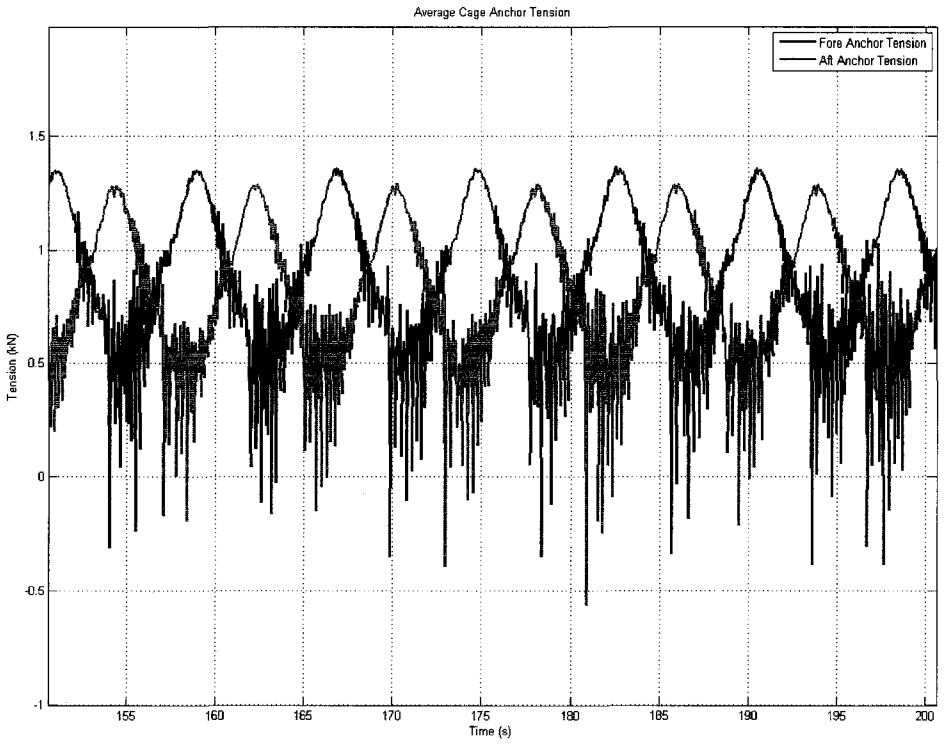

Figure 6.12: Tension Response to Wave Regime 5 in the In-line Loading Direction
As the crest moves past the cage, the fore lines are loaded while the back lines become partly slack. As the wave trough moves past the cage, the loading is transferred to the back lines as the fore lines begin to slacken.

Table 6.9 contains the RAO results for heave, surge, and pitch for in-line and transverse loadings. Table 6.10 contains RAO results for the tension RAOs for both in-line and transverse loadings.

Table 6.9: Motion RAO Results for Both In-line and Transverse Loading

Wave Regime	Surge RAO (m/m)		Heave RAO (m/m)		Pitch RAO (rad/rad)	
	In-line	Transverse	In-line	Transverse	In-line	Transverse
1	0.0049	0.0034	0.0012	0.0014	5.7 e-5	0.0024
2	0.0017	0.0026	9.1 e-4	0.0023	1.4 e-4	0.0010
3	0.0379	0.0427	0.0494	0.0489	0.0081	7.5 e -4
4	0.1102	0.1151	0.1406	0.1357	0.0264	0.0012
5	0.1606	0.1822	0.2086	0.2025	0.1793	0.0019
6	0.2182	0.2320	0.2879	0.2899	0.2871	0.0023
7	0.2603	0.2558	0.3128	0.3162	0.2356	0.0063

Table 6.10: Tension RAO Results for Both In-line and Transverse Loading

Wave Regime	Anchor Tension RAO (kN/m)		Anchor Line Tension RAO (kN/m)		Lower Bridle Line Tension RAO (kN/m)	
	In-line	Transverse	In-line	Transverse	In-line	Transverse
1	0.0195	0.0143	0.0189	0.0118	0.0192	0.0130
2	0.0017	0.0088	0.0067	0.0075	0.0072	0.0081
3	0.0590	0.0410	0.0559	0.0402	0.0868	0.0457
4	0.0479	0.0640	0.0401	0.0587	0.0397	0.0722
5	0.1333	0.0714	0.1238	0.0602	0.1350	0.0747
6	0.1628	0.0570	0.1390	0.0602	0.1447	0.0732
7	0.1653	0.0638	0.1391	0.0672	0.1457	0.0677

The RAOs were plotted as functions of wave frequency to determine if any trends were present. Figure 6.13 and 6.14 show the heave RAOs vs. frequency for the in-line loading and transverse loadings respectively. Both plots show that

at high frequencies the cage response is negligible. The maximum RAO is found to be in heave for the wave period of 10.28 s, 0.313 for in-line and 0.316 for transverse loading. All other RAO vs. frequency plots for the single cage mooring can be found in Appendix H.

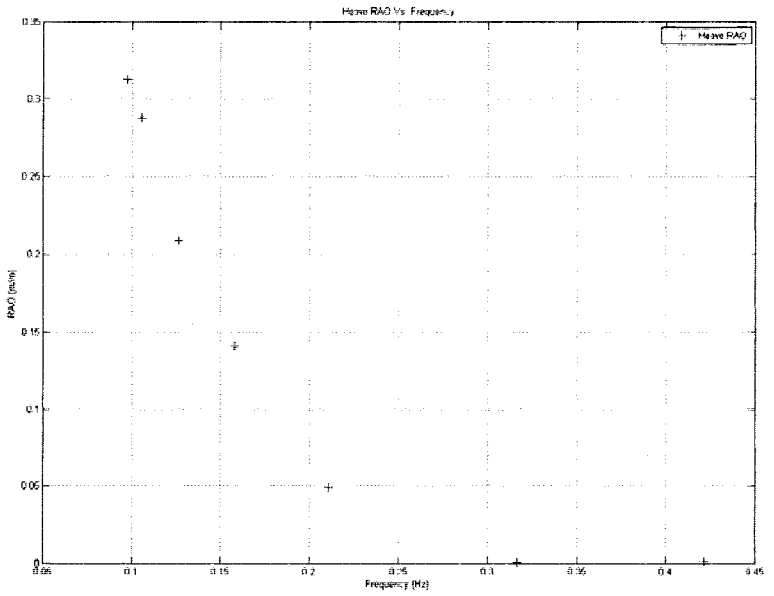

Figure 6.13: Heave RAO vs. Frequency for the Single Cage Mooring with In-line Loading

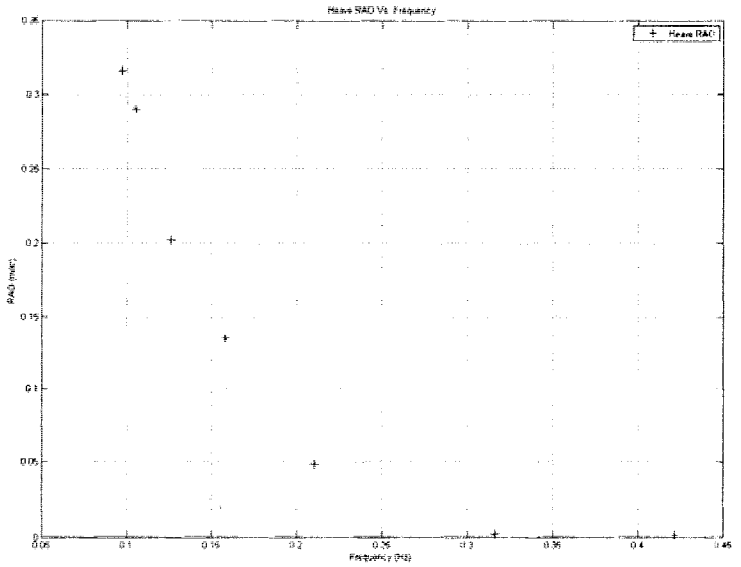

Figure 6.14: Heave RAO vs. Frequency for the Single Cage Mooring with Transverse Loading

Similarly to the motion RAOs, tension RAOs were plotted vs. frequency. As seen in Figure 6.15, as frequency gets larger, the tension RAOs get smaller. The tension RAO plot for transverse loading can be found in Appendix H.

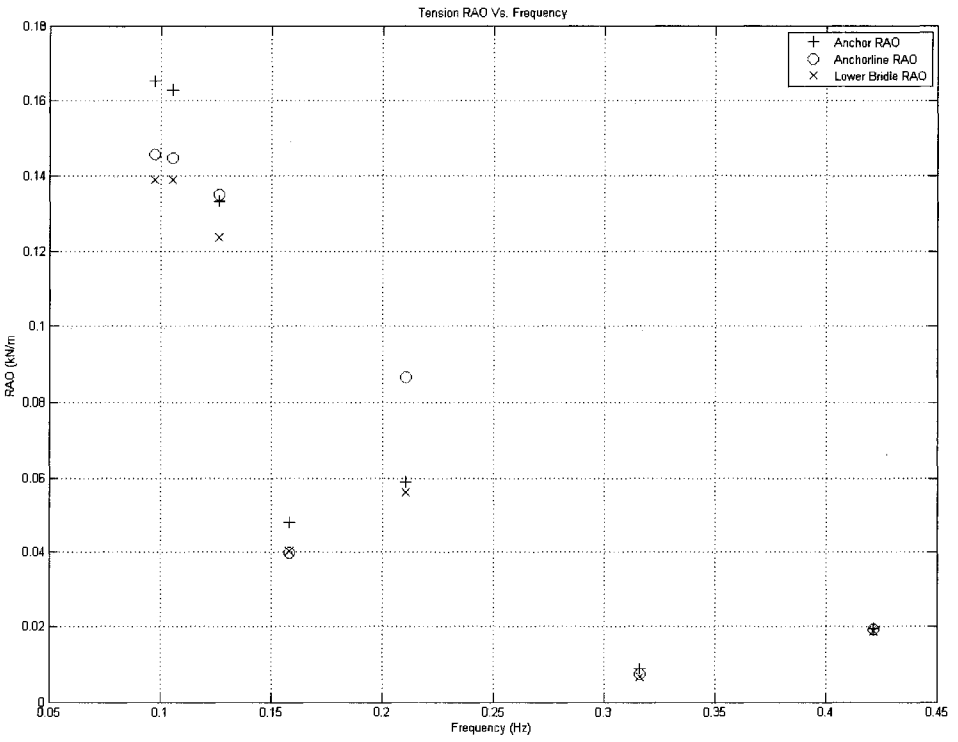

Figure 6.15 Tension RAO vs. Frequency for the Single Cage Mooring with In-line Loading

VI.2.5. Six Cage Mooring Wave Results

RAO values were also found for the six cage mooring in heave, surge, and pitch. These values were taken from the steady state of the time series motion plots. Figure 6.16 shows the time series motion response plot to wave regime 2.

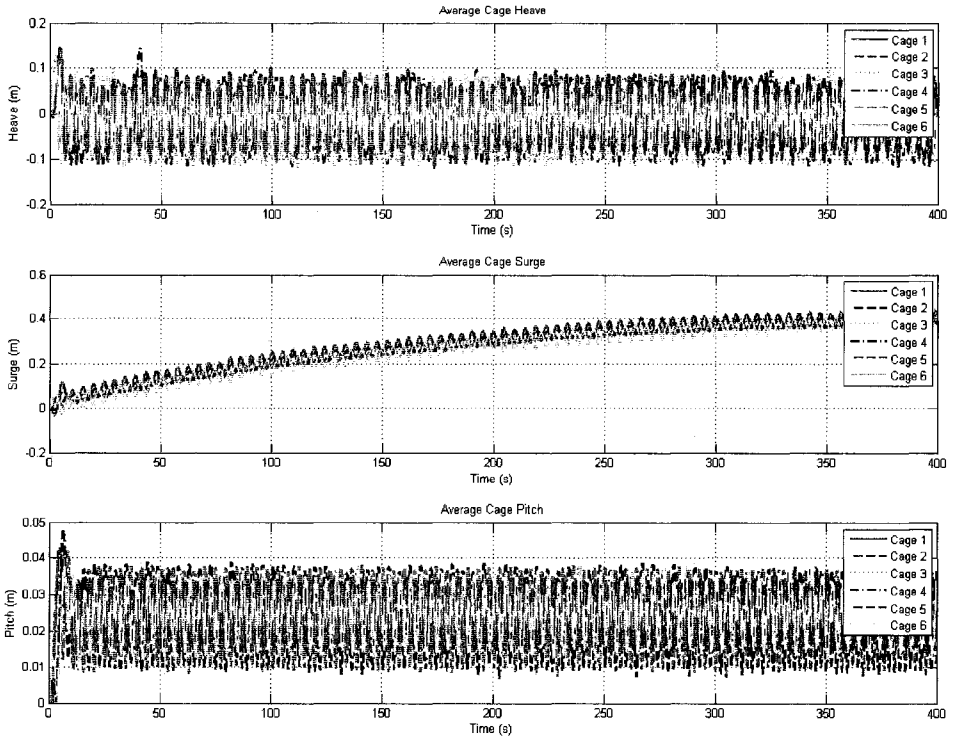

Figure 6.16: Motion Response to Wave Regime 2 in the In-line Loading Direction

Unlike the current loadings, all cages had similar values for heave, surge and pitch. RAOs were calculated for the motion response data for each of the six cages utilizing the theory discussed in section IV.1. The tension RAOs for the anchor, anchor line, and lower bridle lines were also calculated. Due to the large volume of data all calculated RAOs can be found in tables in Appendix I.

Like the RAOs for the single cage mooring, the six cage mooring RAOs were plotted as functions of wave frequency. Figures 6.17 and 6.18 show the plots of heave RAOs vs. frequency for the in-line loading and transverse loading respectively. It should be noted that as frequency approaches zero, the heave RAO gets larger. All other RAO vs. frequency plots for the single cage mooring can be found in Appendix J.

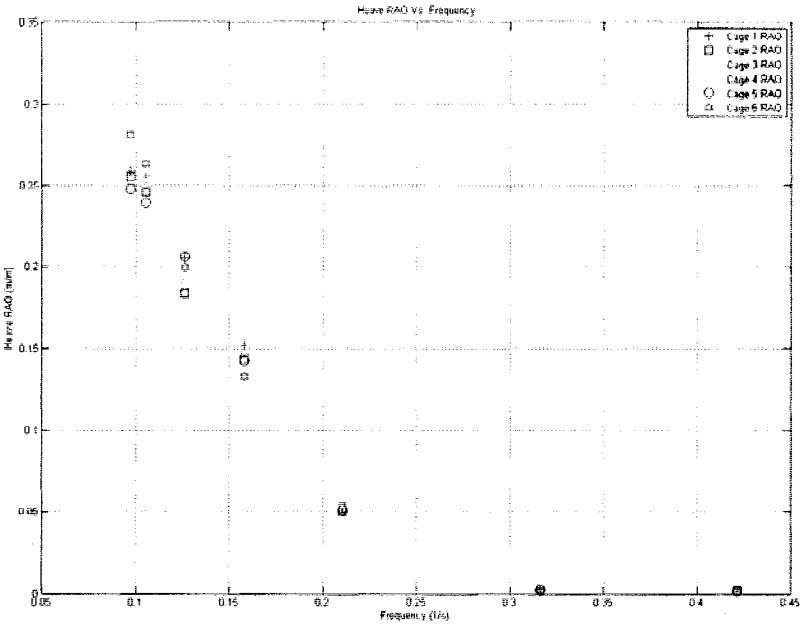

Figure 6.17: Heave RAO vs. Frequency for the Six Cage Mooring with In-line Loading

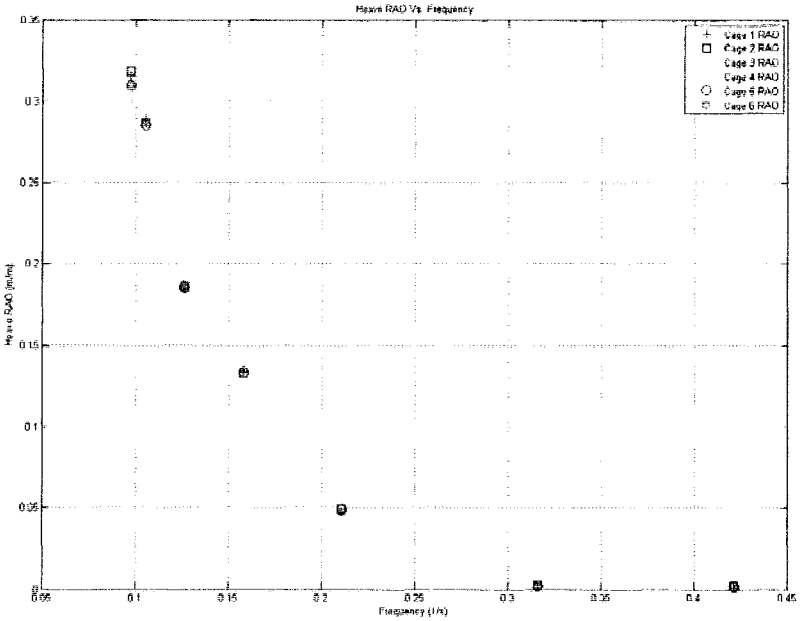

Figure 6.18: Heave RAO vs. Frequency for the Six Cage Mooring with Transverse Loading

VI.2.6. Current and Wave Loading

The final load cases investigated the systems response under a condition of waves and current. The two loadings were designed to simulate storm conditions and normal operational conditions. The load cases were applied in-line and transverse to the moorings for the single and multi-cage systems. The storm condition consisted of a 1.0 m/s current and a wave with a height of 9.0 m and period of 8.8 seconds. The operational condition consisted of a 0.25 m/s current and a wave with a height of 2.0 m and period of 5.34 seconds. Results from these simulations include time series motion and tension. Figures 6.19 and 6.20 show the motion results for the single and six cage moorings when the "storm" loading was applied in the in-line direction.

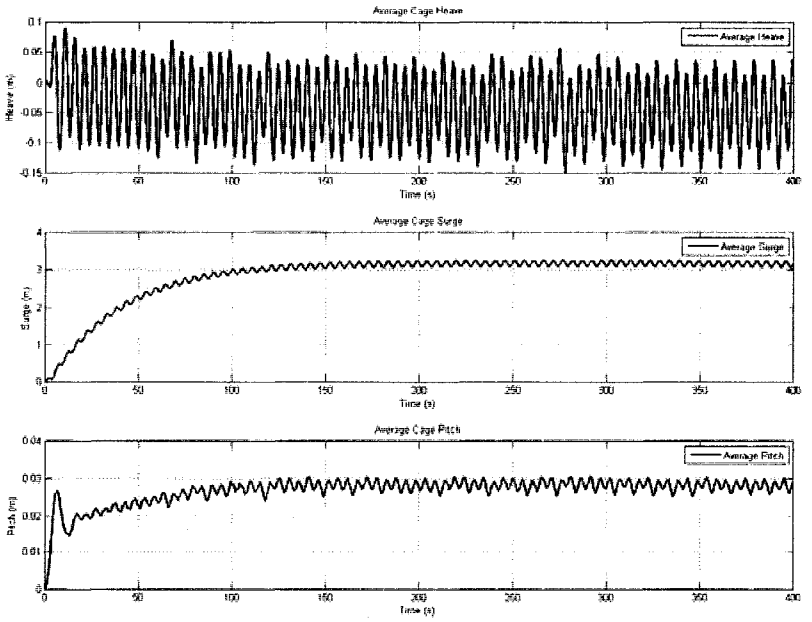

Figure 6.19: Single Cage Mooring Subjected to the Operational Loading in the In-line Direction

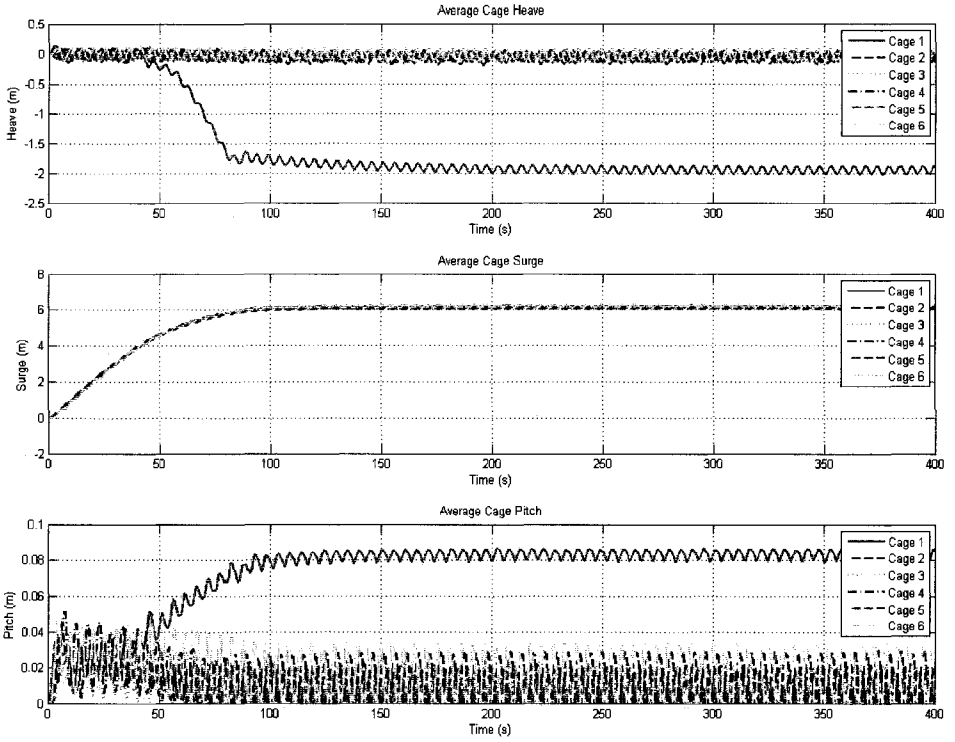

Figure 6.20: Six Cage Mooring Subjected to the Operational Loading in the In-line Direction

As seen in the figures, the current, although only 0.25 m/s, dominates the overall loading. This was expected, as Risso (2007) found the same trend for similar loadings. Since the current dominated, RAOs would be of little use and thus were not calculated. Another interesting note is seen in Figure 6.20 where the first cage has a greater heave and pitch compared to the other cages in the system. Plots for the other duel loading salutations for the single cage mooring can be found in Appendix K while the six cage mooring plots can be found in Appendix L.

VI.2.7. Tension Correlation

Since the mooring configurations for the single and six cage moorings were similar, one final study was performed to determine if there was any anchor or mooring line tension correlations based on the number of cages in the mooring. To do this, a four cage mooring model was constructed using the same parameters as the single and six cage moorings (Figure 6.21).

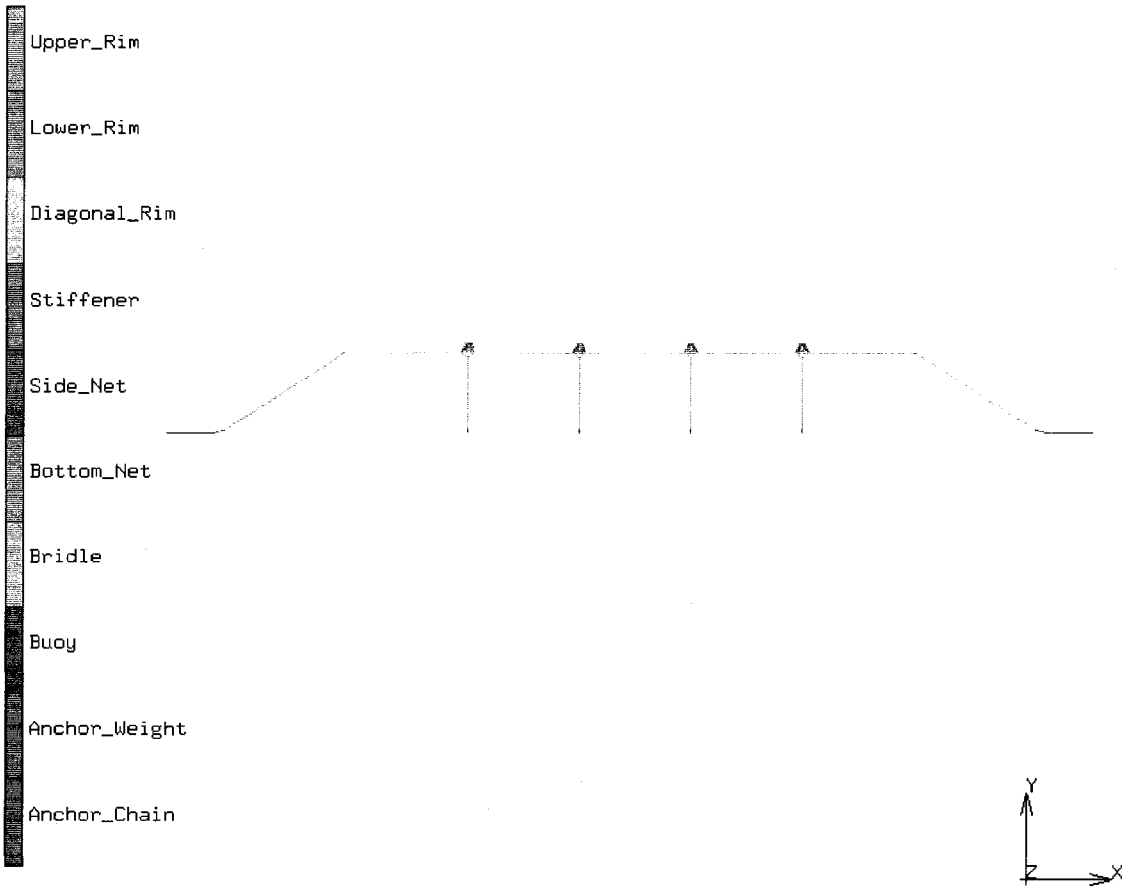

Figure 6.21: Four Cage String Model

Simulations were run for only two current loads, 0.5 m/s and 1.25 m/s. System motion was not investigated since only tension correlation was of interest. From these simulations, tension results were found using the same procedure as

outlined for the single and six cage moorings. These results were plotted as functions of time and steady state values were recorded. Figure 6.22 shows the tension plot for the four cage mooring subjected to 1.25 m/s current loading in the in-line direction.

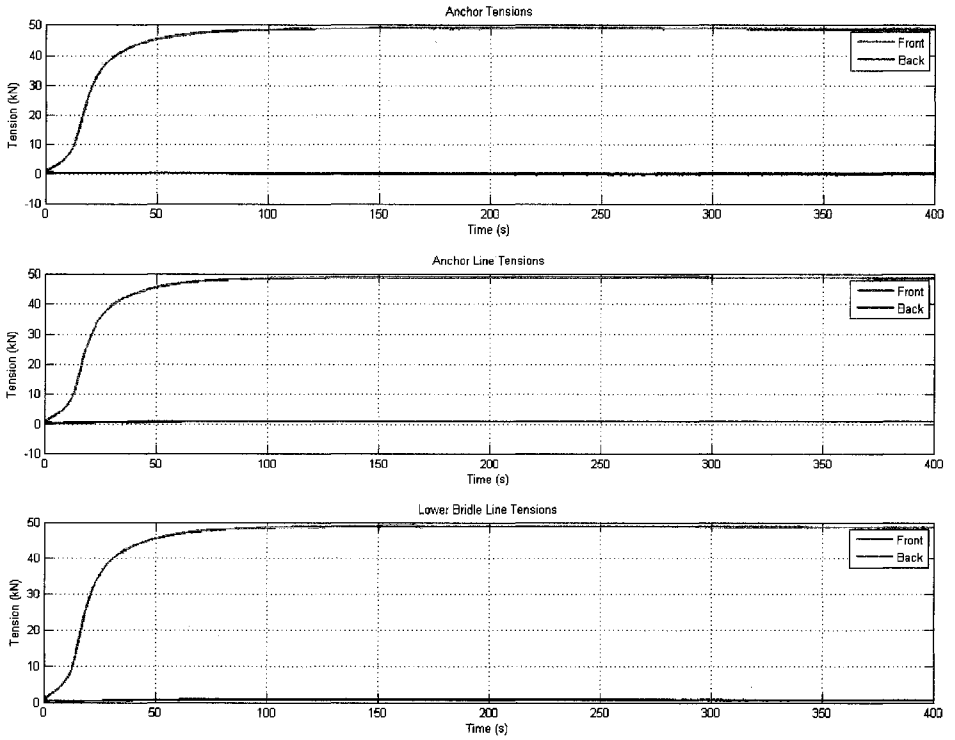

Figure 6.22: Four Cage Mooring Subjected to 1.25 m/s Current Loading in the In-line Direction

Table 6.11displays the results from the two loadings applied in both the in-line as well as transverse directions. Like the tensions results for the single and six cage moorings, only fore mooring line tensions are shown since transverse load yielded equal symmetric tensions while in-line loading yielded full tensions on the fore mooring lines.

Table 6.11: Tension Results for the Four Cage Mooring

	0.5 m/s Current		1.25 m/s Current	
	In-line	Transverse	In-line	Transverse
Fore Anchor (kN)	8.87	13.72	48.54	71.35
Fore Anchor Line (kN)	9.00	13.87	48.60	71.38
Fore Lower Bridle (kN)	9.12	13.98	48.68	71.44

To visually understand if any correlation between number of cages in the mooring and tensions in key mooring lines existed, tensions were plotted as functions of number of cages in the mooring. For both in-line and transverse loading, only the fore mooring line tensions were plotted. Figure 6.21 shows the correlation plot of anchor tensions for both loading cases. In can be noted that there is a strong linear relationship between number of cages in the mooring and expected anchor tensions for both in-line as well as transverse loadings. This was expected because the mooring tensions were directly proportional to the total drag force on the system. Since drag force is a function of surface area, the more cages the more drag force and thus higher mooring line tensions. No current shadowing was utilized for in-line loading in Aqua-FE. Thus each cage in the multi-cage systems was subjected to the full current velocity. This would not be the case for field deployment meaning the in-line tensions found in Aqua-FE are higher than actual field measurements.

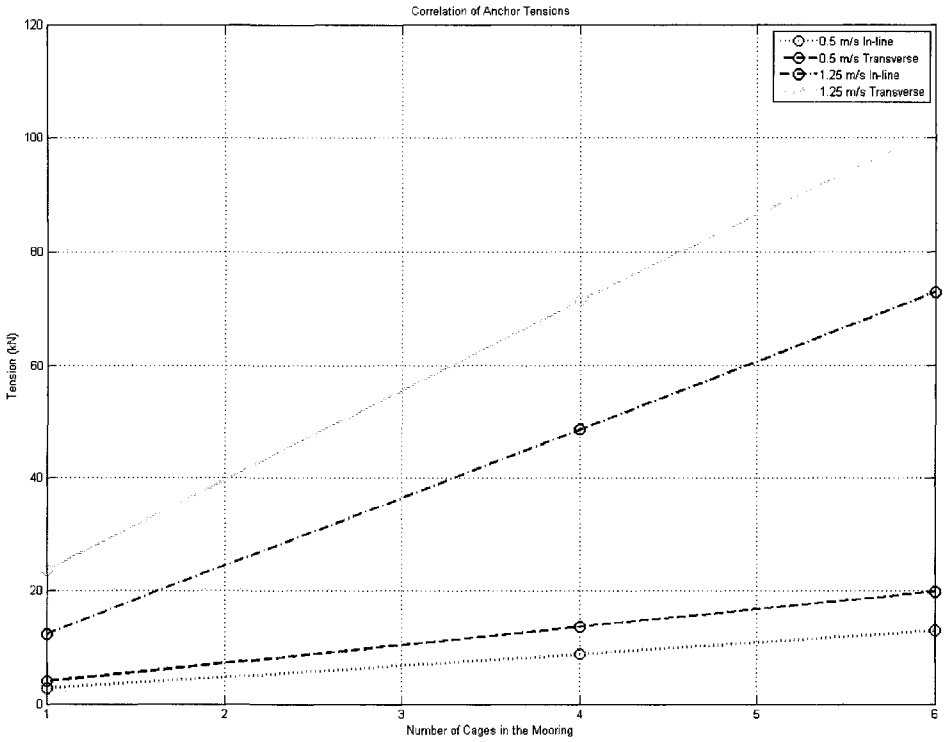

Figure 6.23: Anchor Tension Correlation

It can be noted that there appears to be a strong linear correlation between number of cages in the mooring and the expected anchor tensions.

Plots like figure 6.23 were created for tensions in the anchor line and lower bridle line. All plots showed similar linear relationship between number of cages in the mooring and expected tensions. These other plots can be found in Appendix M.

CHAPTER VII

DISCUSSION OF RESULTS

Before loadings were applied, pre-loading testing was performed on the two mooring configurations. These tests included a free release test, static tension test, and "harvest test". The free release test found the cage system to have a natural period of 2.85 seconds. This means that the cage system would not be excited when waves with longer periods are applied. This is beneficial since it adds system stability.

Upon completion of the analysis, differences in magnitude for tensions found for in-line and transverse loadings proved to be quite large. Transverse loading constantly caused larger loads in mooring lines even though the load was distributed equally between both sides of the mooring. This is a result of the direction of the applied environment conditions. For in-line loadings, the system drag and anchor line tension are approximately equal and opposite. As shown in Figure 7.1.

This is not the case for transverse loading however. When subjected to loads perpendicular to the mooring system, the cages set back in a "U" shape instead of a straight line. This causes the forces applied to mooring lines to lie

along a different vector. Blue solid arrows depict directions of cage drag force due to current while red dashed arrows depict the direction of the resulting loads on the mooring lines. For clarification, black dashed areas are used to show the two components of the resultant force. Direction of the current is also labeled for clarification. Also note that (A) is viewed from the side of the cage system while (B) is looking down at the cage system.

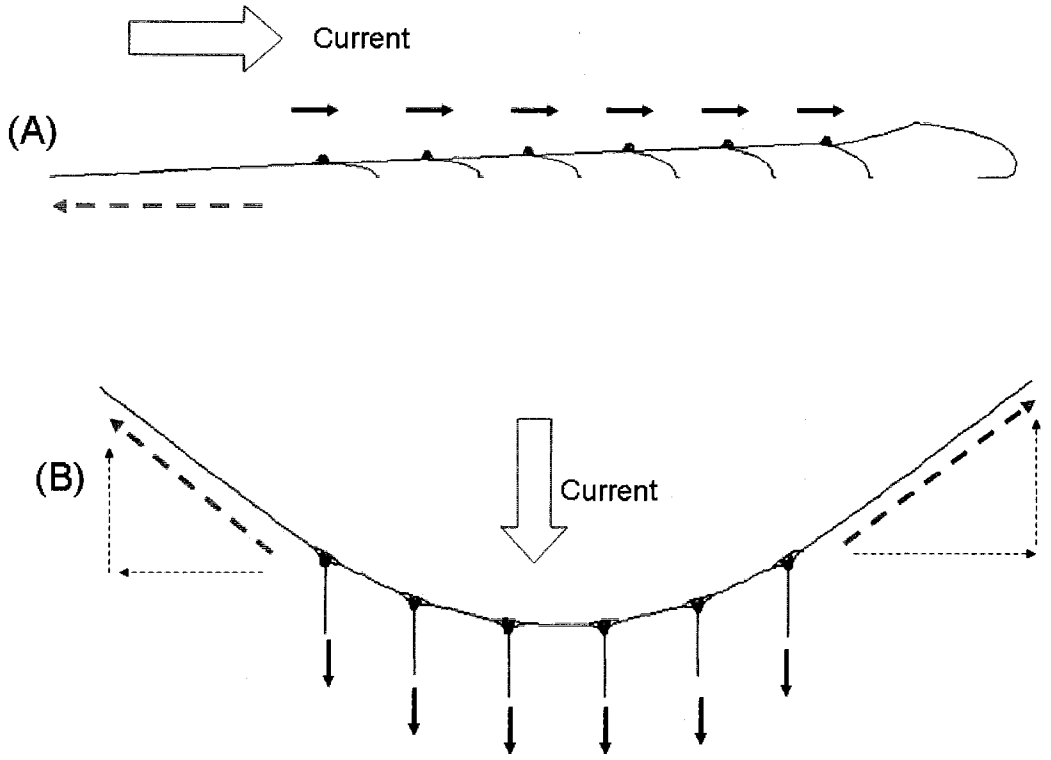

Figure 7.1: Vector Loading on the Six Cage System
(A) In-line response to current loading. (B) Transverse response to current loading. Blue solid arrows depict cage drag force direction while red dashed arrows depict the direction of the resulting loads on the mooring lines.

As seen, for in-line loadings, cage drag forces align with the mooring and thus produce a resultant force parallel with the mooring. Conversely, the transverse loading causes the cage drag to be perpendicular to the mooring.

Using trigonometry, the magnitude of this resultant vector for transverse loadings is greater than the total drag force and is thus larger than the in-line resultant force.

This same reasoning can be used to explain why the multi-cage system consistently surged more when subjected to transverse loadings. For example when subjected to a 1.0 m/s current, in-line loading produced a maximum surge of 11.9 meters, while transverse loading produced a maximum surge of 79.2 meters. This can also be seen in Figure 7.2 which shows system surge vs. current velocity. For the six cage systems the system surge was taken as an average of all six cages surge values.

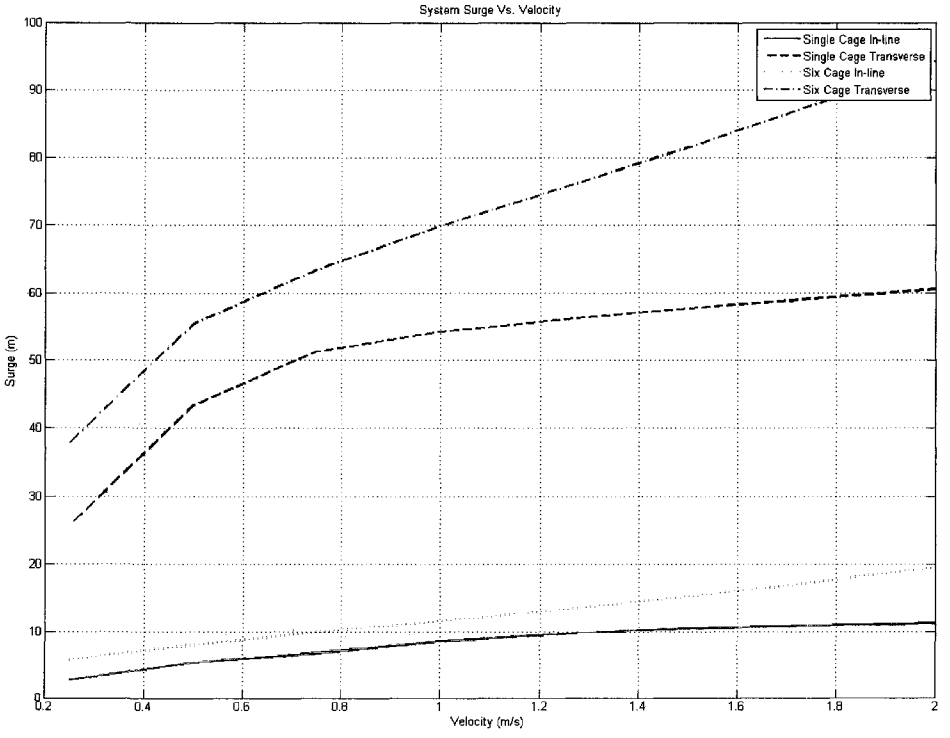

Figure 7.2: System Surge vs. Velocity

Cage motions also were consistently higher when subjected to transverse loading. For example, when subjected to an in-line current loading of 0.5 m/s the single cage model had a heave of 2 meters and a surge of 5.5 meters while the same loading applied transverse to the mooring produced a cage heave of 6.5 meters and a surge of 43.5 meters. One possible reason this occurred was mooring line configuration. When subjected to in-line loadings, all cages surged and pulled on the fore anchor. This anchor restricts the system movement and prevents the cages from surging. This did not occur for transverse loading as seen in Figure 7.2 where the cages were able to set back without restriction by the fore anchor.

Both time series motion and tension plots showed a lag in system response. This is seen in Figure 7.3 where most noticeably heave shows approximately a 150 second delay during transit.

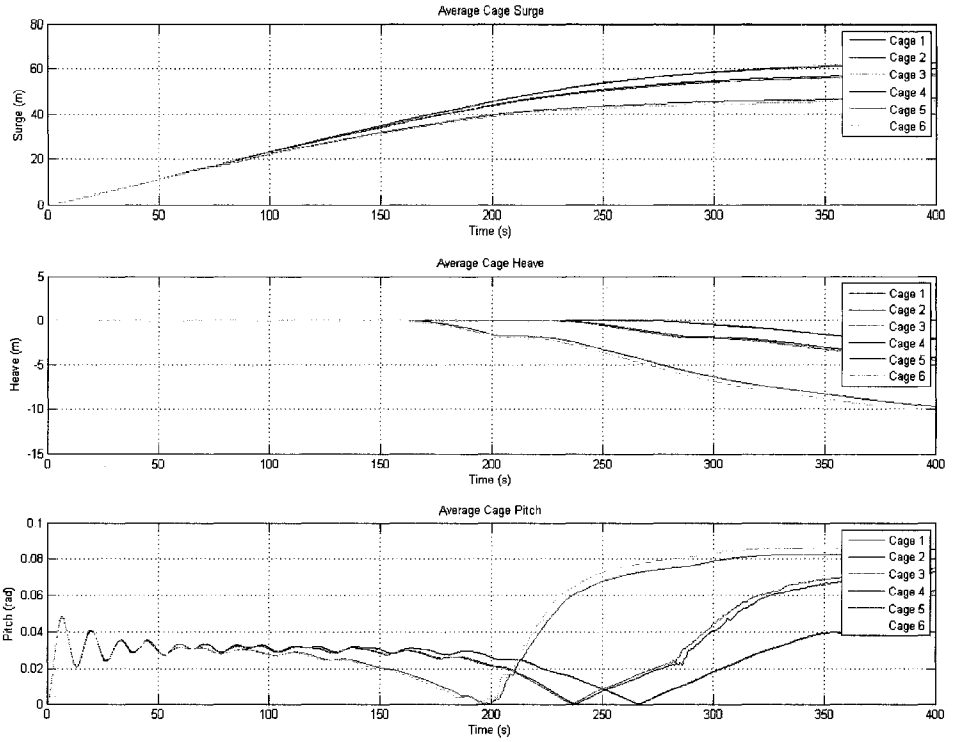

Figure 7.3: Motion Results for a Six Cage Mooring Subjected to 0.5 m/s (1 knot) Current in the Transverse Direction

The length of time in the transit state of the cage was a function of the system set-back. Since Aqua-FE does not apply friction on the seafloor, the weights below the cages slid during simulations. This happened for all simulations including in-line and single cage tests. Once the weights slid so much that the anchor lines began to pull, the cages responded as expected. It is believed that the sliding only caused a delay in reaching steady state and did not cause any faulty results.

The tension results allowed for the anchors to be tentatively sized. The highest anchor tension for the single and multi-cage systems were 61 kN and 241 kN respectively. The anchor type chosen was the LWT® Danforth. This type of anchor is recommended for use on offshore rig moorings and is a fixed

mooring. The holding power of a Danforth anchor is 9:1 meaning that for every pound of weight, it holds nine pounds of force. Since it is desirable for anchors to drag as opposed to having mooring lines fail, the anchors were sized such that the holding strength was lower than the breaking strength of the poly-steel bridle lines, approximately 210 kN. Therefore, for the single cage model, the anchors were set with a holding strength of 120 kN which gave a safety factor of 2. This meant a 3,000 lb anchor. For the six cage system, the holding strength was lower than the 210 kN breaking strength. Therefore an anchor with 190 kN holding strength was used. This holding strength corresponded to a 4,750 lb Danforth anchor. It is important to note that the largest weight a UNH research vessel can deploy is 5,000 lbs, which would correspond to a Danforth anchor with a holding strength of 200 kN. If it is desired to have the anchor hold at a 2.0 m/s current, the bridle line diameter would have to be increased.

In addition to the eight current velocities, seven wave regimes were used to test the models. Motion results from these wave regimes showed that the cages moved out of phase as seen in Figure 7.4. However, the cages never got close enough to hit or tangle with one another.

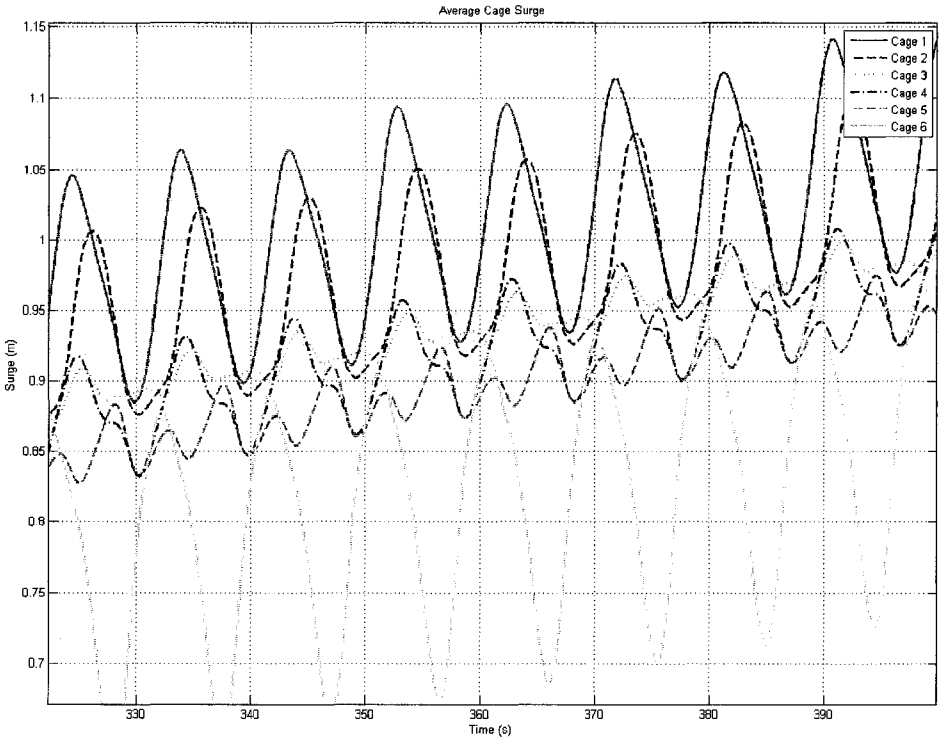

Figure 7.4: Six Cage Mooring Subjected to Wave Regime 4

RAO values were also investigated as part of this study. Heave and surge RAO values were much closer together. Surge RAO results yielded 0.2182 for in-line and 0.232 transverse while heave RAO results yielded 0.2879 for in-line and 0.2899 for transverse. There were large discrepancies between pitch RAO values for inline and transverse loadings. For example, the single cage mooring subjected to wave regime 6, wave height of 2.4 meters and period of 9.52 seconds, yielded pitch RAO values of 0.2871 for in-line loading, and 0.0023 for transverse loading.

One possibly explanation for this inconsistency was orientation of the cage in the mooring in relation to the applied waves direction. As previously stated, heave, surge, and pitch were orientated in the direction of wave propagation. In-

line pitch was therefore rotation about the axis of the mooring lines, while transverse pitch was rotation about the axis perpendicular to the mooring lines. The mooring system thus had a different effect on the pitch response, resulting in the in-line RAOs to be greater than the transverse RAOs.

The RAO vs. frequency plots showed an inverse relationship. This is expected since as the frequency gets shorter the cage becomes a wave follower. Therefore, for long period waves, such as tides, the cage will have close to the same amount of reaction as the forcing. Since the original cage was designed to follow large period waves, this is a desirable trend.

As seen in the transverse loading heave plot, all cages have close to the same heave RAO. This was expected since all the cages dove together. Another interesting note was that like the single cage RAO vs. frequency plots, as the frequency gets shorter, the RAO gets larger. This occurs for the same reason as the single cage mooring.

The correlation between the tensions in mooring lines and the number of cages in the mooring system seemed to show a strong linear correlation. Motion result correlations were not tested; however, testing on the motion may yield similar results. The strong correlation between the tensions and cage numbers suggest that prediction of assumed forces based on the number of cages in the mooring maybe acceptable. Further testing should still be performed to assure predicted values are correct when sizing the mooring.

CHAPTER VIII

CONCLUSION

The construction process of the UNH ASAIM fish cage was documented along with modifications made to the original design. Testing including hydrostatics and solid modeling to assure modifications would cause no major changes to cage parameters. The cage was assembled successfully in December 2007 and later deployed.

Alternative mooring designs were developed to allow the cage to be moored in a variety of environments. In total, five different configurations, three single cage and two multi-cage mooring designs were analyzed. A feasibility study was performed utilizing a worst case scenario loading to determine a final design to be further tested. The string mooring was chosen as the best mooring configuration due to its ease of harvesting and its ability to distribute loads among the mooring lines.

An in-depth analysis was then performed on the string mooring with one and six cage systems. This test utilized eight current and seven wave loadings as well as two loadings which included both current and waves. These loadings were applied in-line and transverse to the mooring systems. Cage motions and mooring line tensions were calculated and compared for all simulations. These

results showed that transverse loadings supplied higher anchor and mooring line tensions and higher system motions. This was because the forces on the cage were applied at a difference orientation causing the mooring lines to react differently.

It was found that the 1.5 inch poly-steel bridle lines were not sufficient for use on the six cage mooring. Tensions reached as high as 240 kN, higher than the 210 kN tensile strength of the lines. This suggested that larger poly-steel lines, or bridle lines of a different, stronger material have to be used to prevent system failure.

A correlation test was also performed to determine if any trends could be found between the number of cages in a system and the tensions experienced by the mooring lines. To do this a four cage mooring was used and tested using two current loadings performed in the in-depth analysis. This test showed there was a strong linear correlation between the number of cages and the anchor tensions. This was expected since the only forces acting on the mooring were due to cage drag. Since drag force is a function of surface area, as more cages are added to the system, the tensions should increase.

This testing concludes that the string mooring design is a good option for the ASAIM cage system. This mooring allowed for easy harvest, addition of many cages with little affect to the overall design, and distributed loads among the mooring lines well.

REFERENCES

Celikkol, B., DeCew, J., Swift, M.R., Tsukrov, I., Baldwin, K., Risso, A., Despins, R., and Irish, J., *"OCAT Cage System Engineering Analysis and Testing,"* report prepared for the American Soybean Association.

Dean, R.G., and R.A. Dalrymple (1991). Water Wave Mechanics for Engineers and Scientists. World Scientific Publishing Company, Sinapore. 353 p.

DeCew, J.C. (2002). *Numerical and Physical Modeling of a Sadco Shelf Submersible Fish Cage.* Master's Degree Thesis submitted in partial requirement for the Degree of Master in Ocean Engineering. University of New Hampshire, Durham, NH. 267 p.

Fredriksson, D.W., (2001). *Open Ocean Fish Cage and Mooring System Dynamics*. Ph.D. Dissertation submitted to the University of New Hampshire in partial fulfillment of the Engineering Systems Design Program. Durham, NH, 296 p.

Fredriksson, D.W., J. DeCew, M.R. Swift, I. Tsukrov, M.D. Chambers, and B. Celikkol. (2004). *The Design and Analysis of a Four-Cage, Grid Mooring for Open Ocean Aquaculture*. Aqua. Eng. Vol 32 (1) pp 77-94.

Gosz, M., Kestler, K., Swift, M.R. and Celikkol, B. (1996). *Finite Element Modeling of Submerged Aquaculture Net-pen Systems.* In: Open Ocean Aquaculture. Proceedings of an International Conference. May 8-10, 1996, Portland, Maine, Marie Polk, Editor. New Hampshire/Maine Sea Grant College Program Rpt #UNHMP-CP-SG-96-9. pp. 523-554.

Goudey, C (2004). *"Cage and Mooring Specifications for the ASA 2 m x 4.5 m x 7 m Prototype Offshore Cage,"* report prepared for the American Soybean Association.

Morison, J.R., Johnson, J.W., O'Brien, M.P. and Schaaf, S.A. (1950). *The forces exerted by surface waves on piles.* Petroleum Transactions. American Institute of Mining Engineers, Vol 189.

Ozbay, M. (1999). *Development of an Offshore Aquaculture Site.* Master's Degree Thesis submitted in partial requirement for the Ocean Engineering program. University of New Hampshire, Durham, NH. 111 p.

Risso, A.M. (2007). *Structural Analysis of a Small Volume Offshore Aquaculture Cage System Utilizing Numerical Modeling and Scaled Physical Testing.* Master's Degree Thesis submitted in partial requirement for the Degree of Master in Ocean Engineering. University of New Hampshire, Durham, NH. 267 p.

Tsukrov, I., Ozbay, M., Fredriksson, D. W., Swift, M.R., Baldwin, K. and Celikkol, B. (2000). *Open Ocean Aquaculture Engineering: Numerical Modeling.* Mar. Tech. Soc. J. Washington D.C. Vol 34, No 1 pp 29-40.

Tsukrov, I., Eroskin, O., Fredriksson, D., Swift, M.R., and Celikkol, B. (2003). *Finite Element Modeling of Net Panels using a Consistent Net Element.* In: Ocean Engineering. Great Britain. Vol 30, Issue 2 pp 251-270.

APPENDICES

APPENDIX A – Corner Fitting Drawings

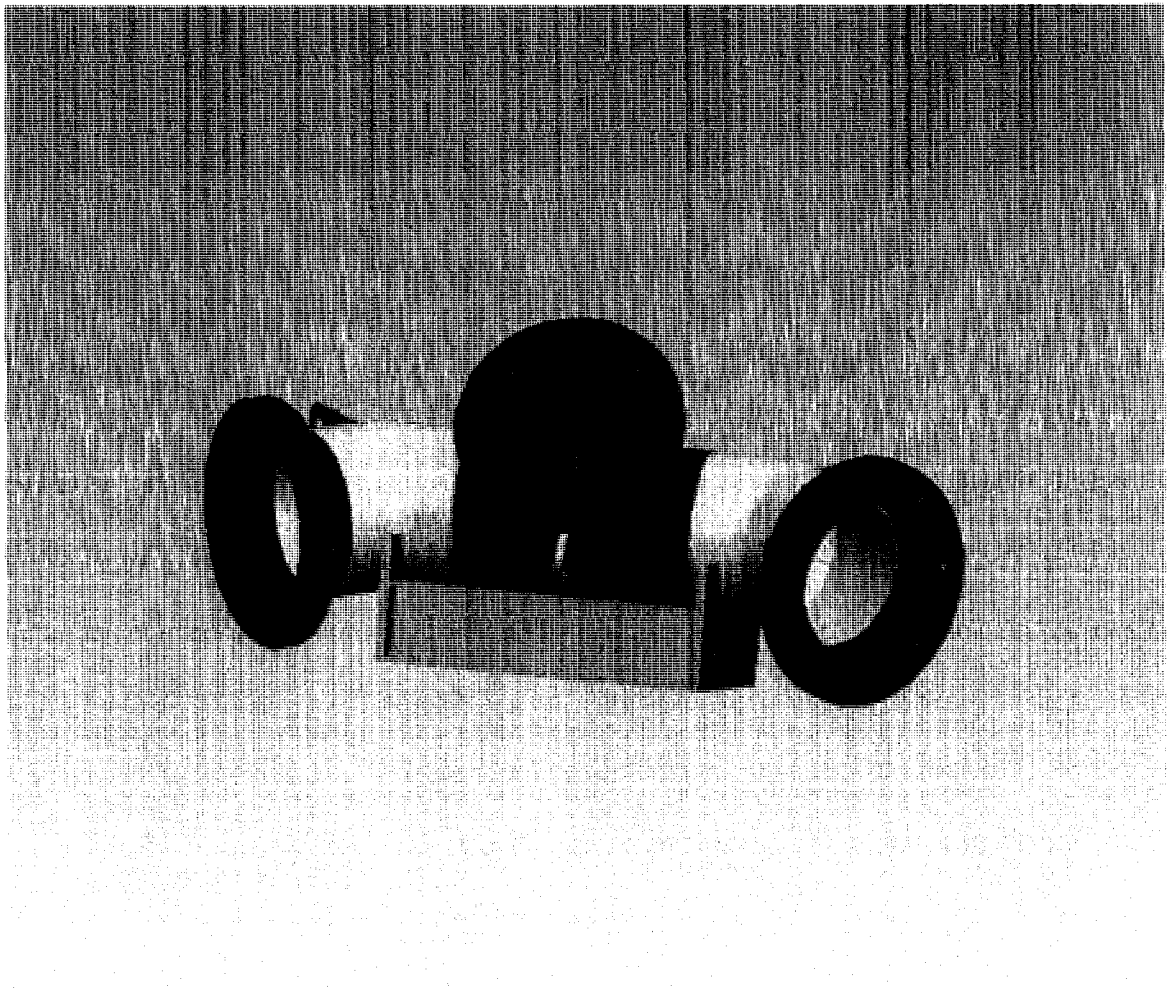

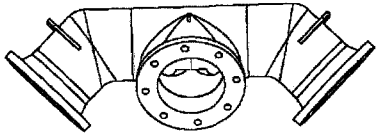

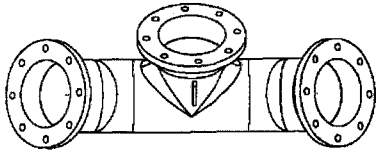

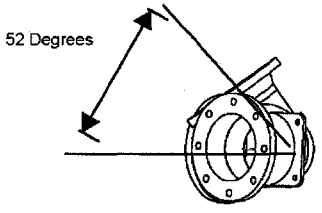

		24 Colovos Rd. Durham, NH 03824
Title: CORNER_NOBOTTOM		
Description:		
Size: A	* All Dimensions in Inches *	
Type: ASSEM	Part Number:	Drawn by: R.R.D
Sheet: 1 of 1	Quantity: 4	Date: 24-Sep-07

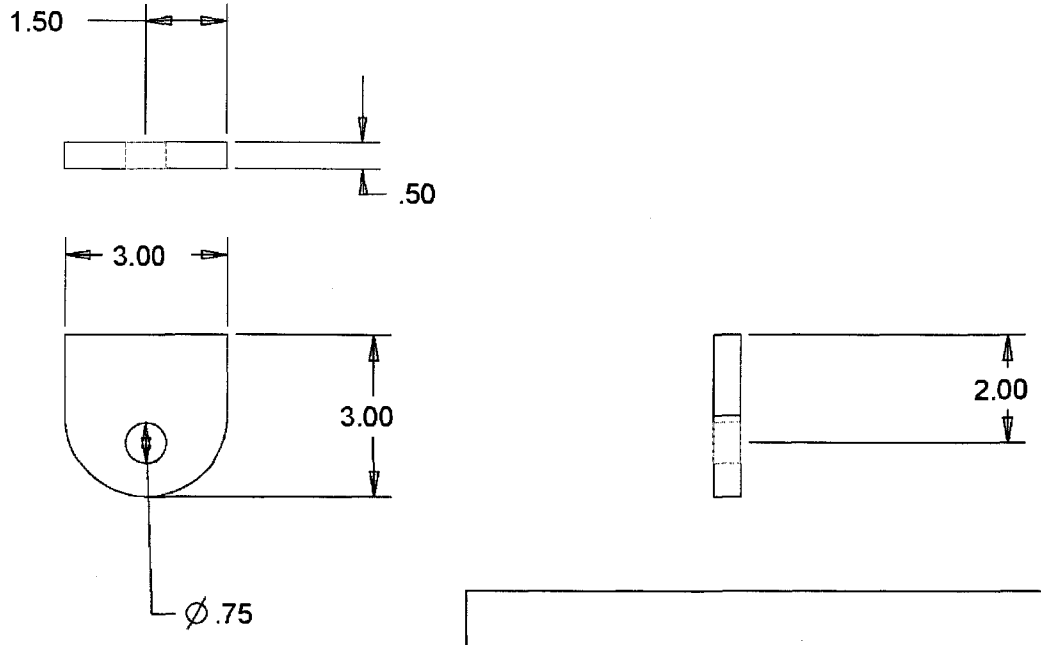

		24 Colovos Rd. Durham, NH 03824
Title: NEW_PADEYE		
Description:		
Size: A	* All Dimensions in Inches *	
Type: PART	Part Number:	Drawn by: R.R.D
Sheet: 1 of 1	Quantity: 4	Date: 24-Sep-07

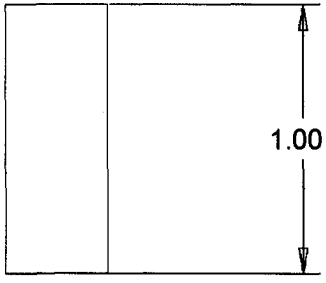

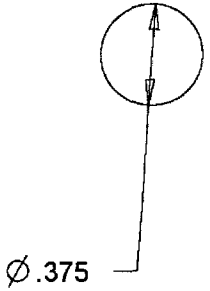

		24 Colovos Rd. Durham, NH 03824
Title: ROD		
Description:		
Size: A	* All Dimensions in Inches *	
Type: PART	Part Number:	Drawn by: R.R.D
Sheet: 1 of 1	Quantity: 4	Date: 24-Sep-07

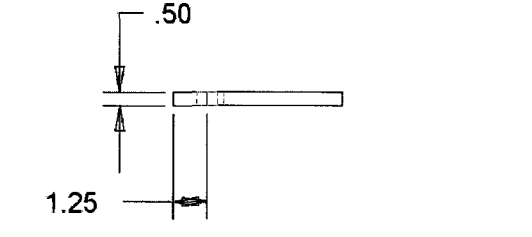

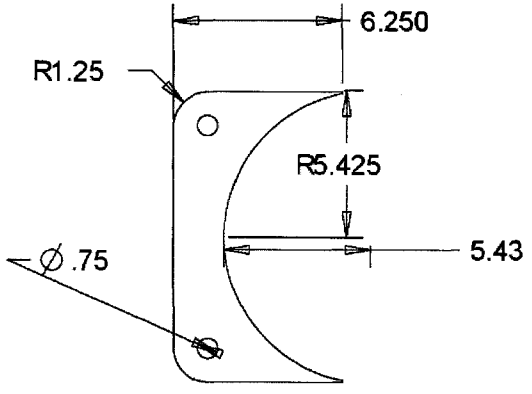

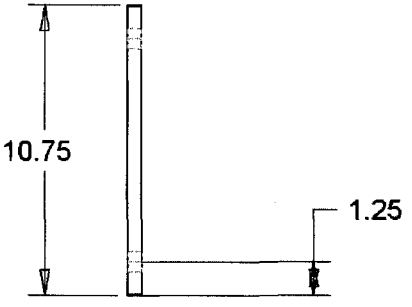

		24 Colovos Rd. Durham, NH 03824
Title: PADEYE		
Description:		
Size: A	* All Dimensions in Inches *	
Type: PART	Part Number:	Drawn by: R.R.D
Sheet: 1 of 1	Quantity: 8	Date: 24-Sep-07

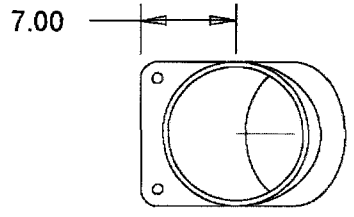

Padeye placement mirrored for other elbow.

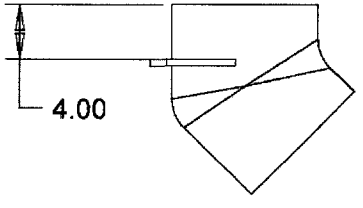

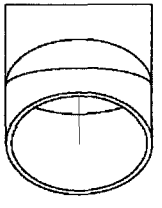

		24 Colovos Rd. Durham, NH 03824
Title: ELBOW		
Description:		
Size: A	* All Dimensions in Inches *	
Type: ASSEM	Part Number:	Drawn by: R.R.D
Sheet: 1 of 1		Date: 24-Sep-07

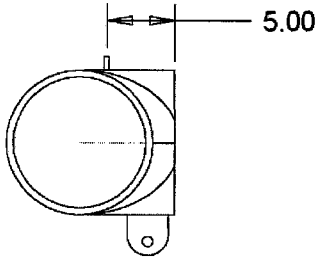

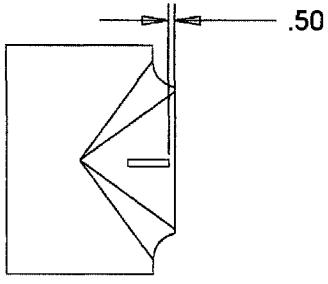

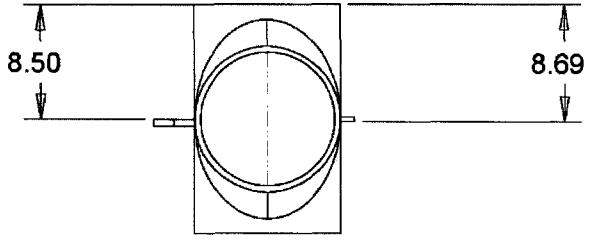

		24 Colovos Rd. Durham, NH 03824
Title: TEE		
Description:		
Size: A	* All Dimensions in Inches *	
Type: ASSEM	Part Number:	Drawn by: R.R.D
Sheet: 1 of 1		Date: 24-Sep-07

APPENDIX B – Corner Support Drawings

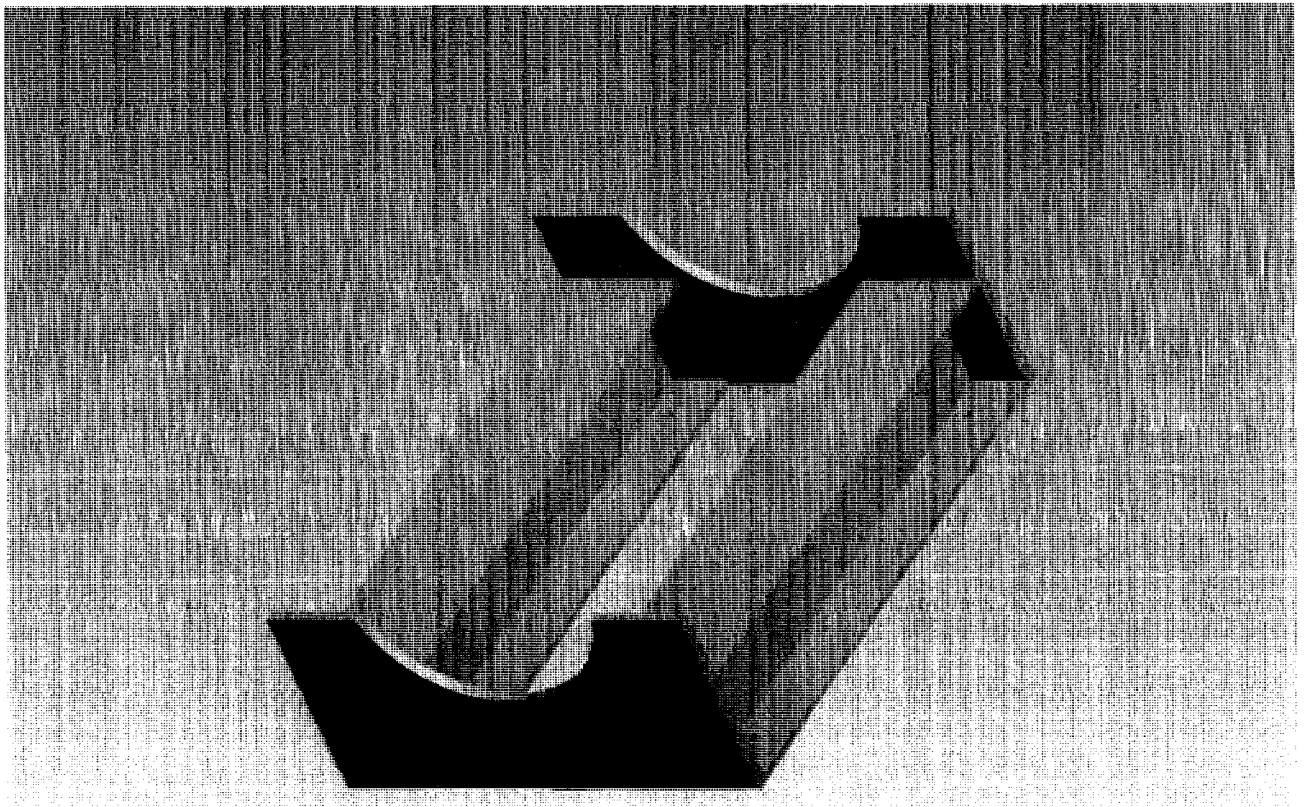

Note: Casters not shown. Casters from McMaster-Carr: part # 19505T31

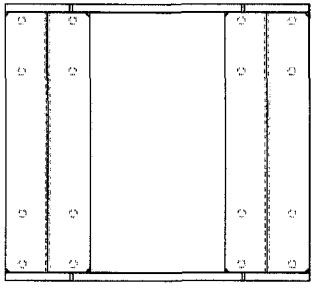

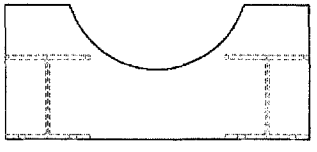

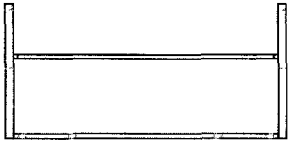

		24 Colovos Rd. Durham, NH 03824
Title: BOTTOM_SUPPORT		
Description:		
Size: A	* All Dimensions in Inches *	
Type: ASSEM	Part Number:	Drawn by: R.R.D
Sheet: 1 of 1	Quantity: 4	Date: 24-Sep-07

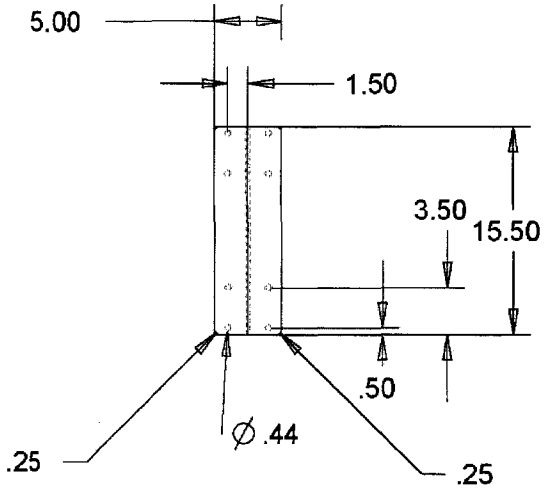

Standard 3/8 Bolt Holes for 500#
Caster (19505T31 McMaster Carr)
(all holes are 7/16")

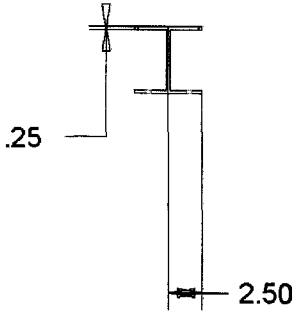

		24 Colovos Rd. Durham, NH 03824
Title: I-BEAM		
Description:		
Size: A	* All Dimensions in Inches *	
Type: ASSEM	Part Number:	Drawn by: R.R.D
Sheet: 1 of 1	Quantity: 8	Date: 24-Sep-07

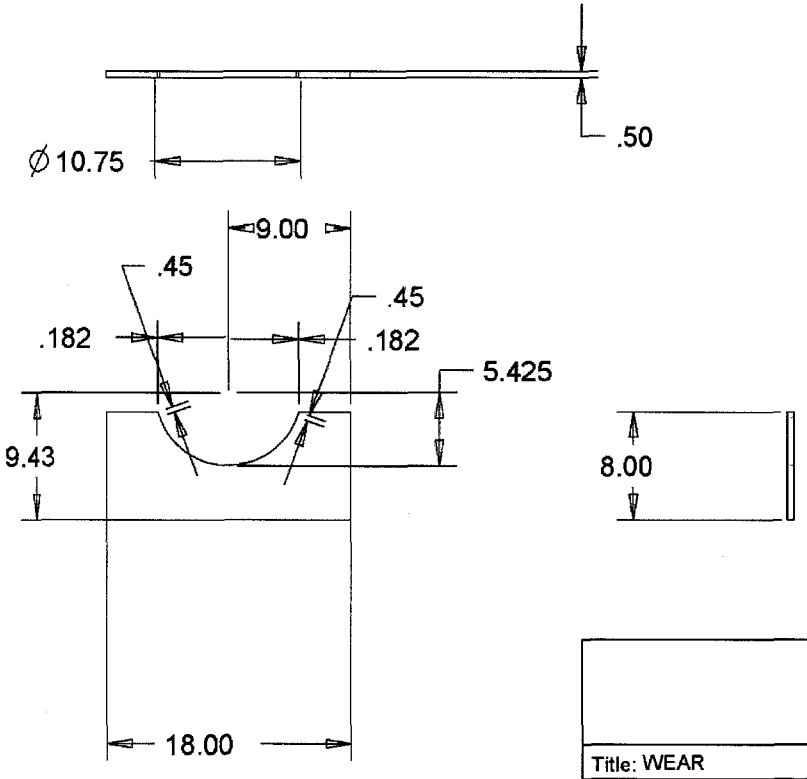

		24 Colovos Rd. Durham, NH 03824
Title: WEAR		
Description:		
Size: A	* All Dimensions in Inches	
Type: PART	Part Number:	Drawn by: R.R.D
Sheet: 1 of 1	Quantity:8	Date: 24-Sep-07

APPENDIX C - Motion Response and Tension Plots for the Single Cage Mooring: In-line Loading

0.25 m/s

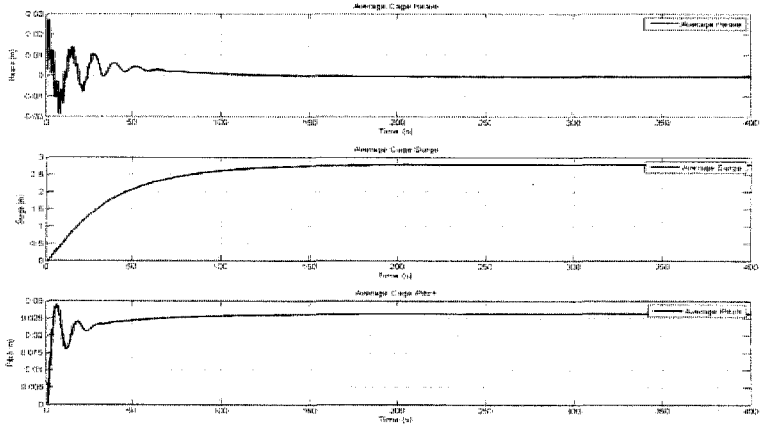

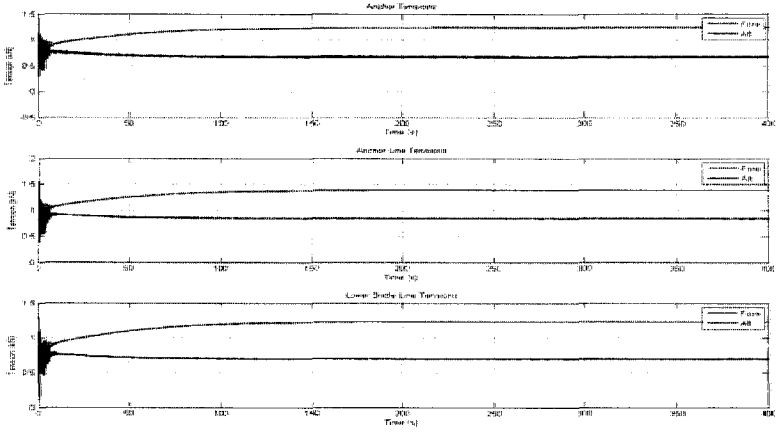

0.5 m/s

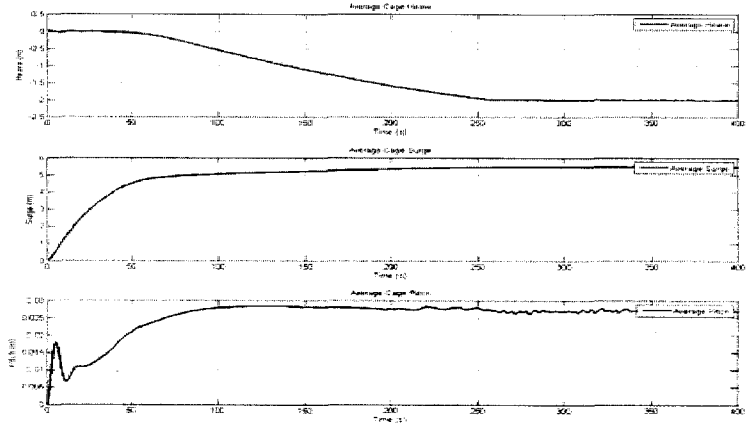

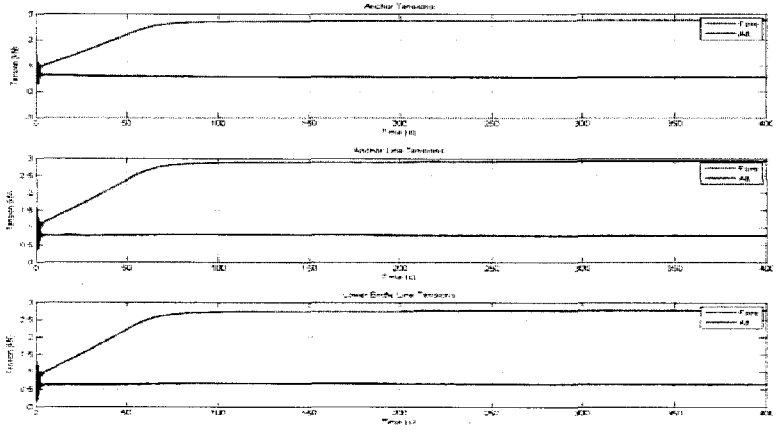

0.75 m/s

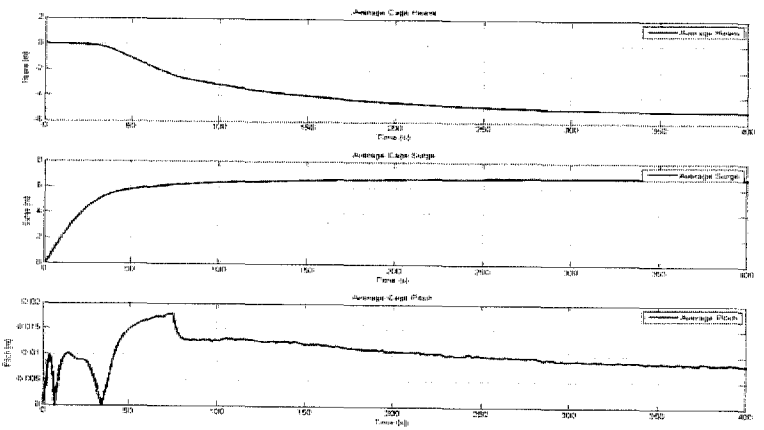

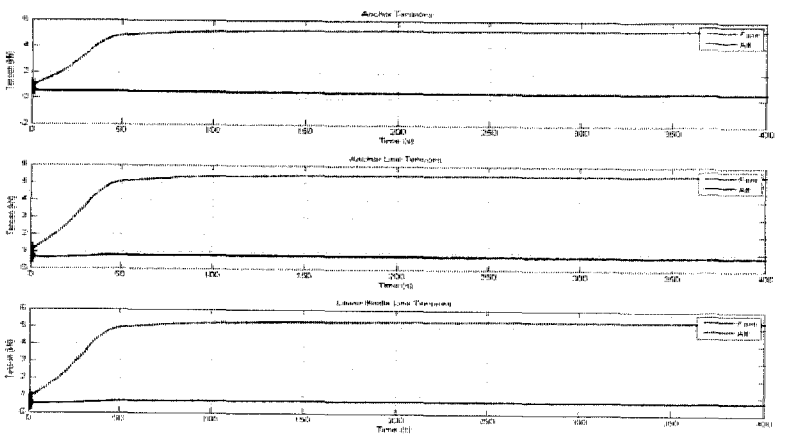

1.0 m/s

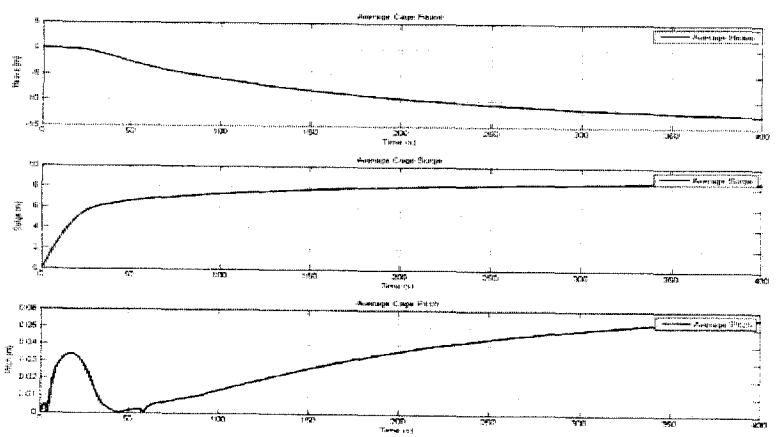

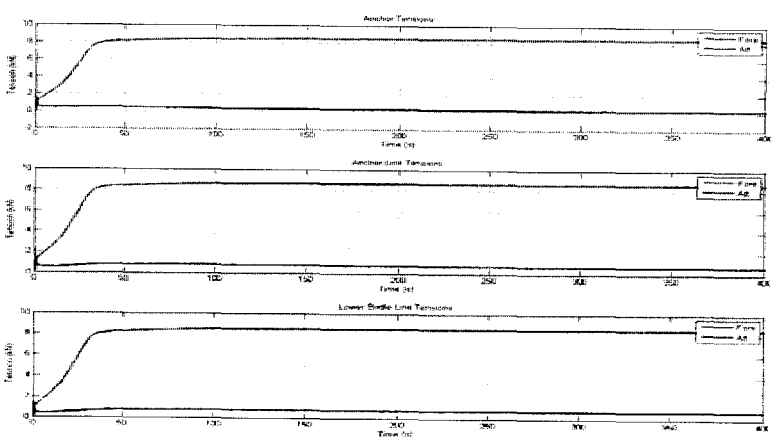

1.25 m/s

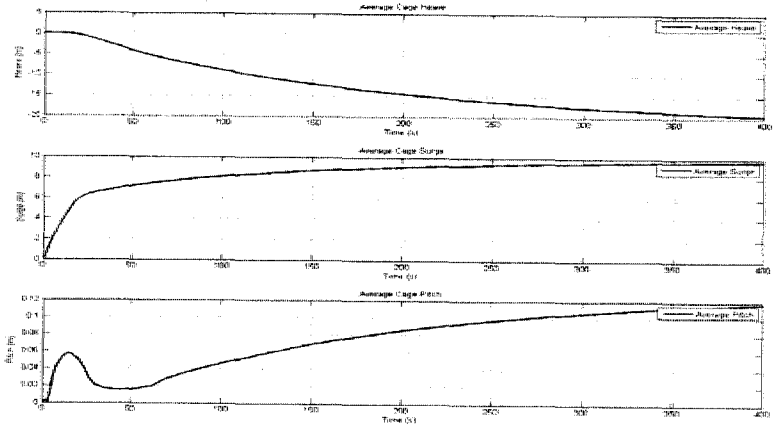

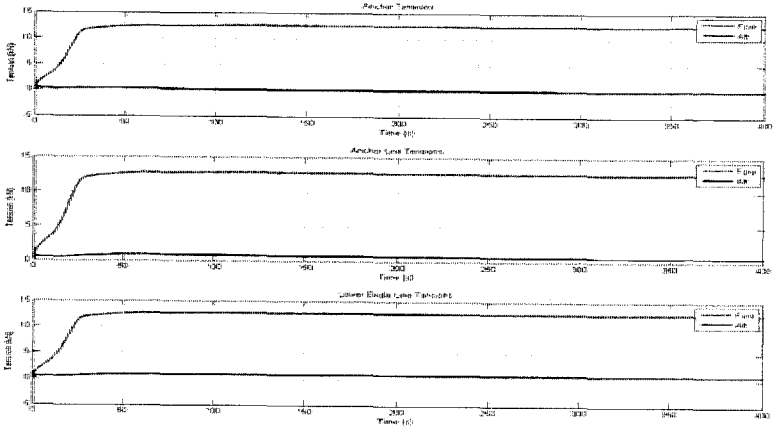

1.5 m/s

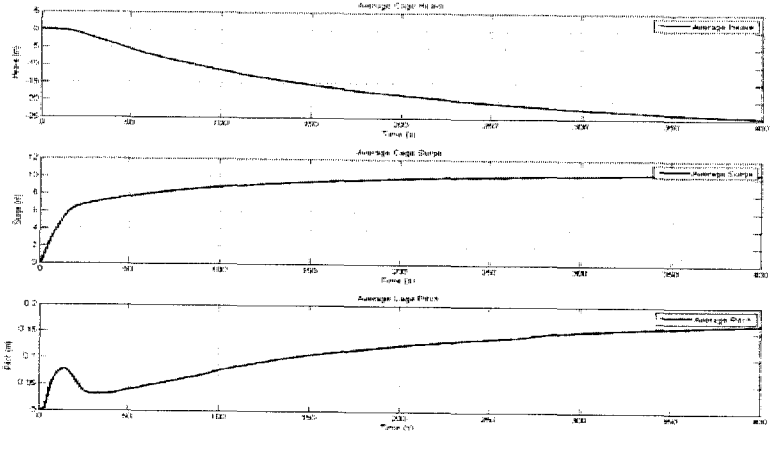

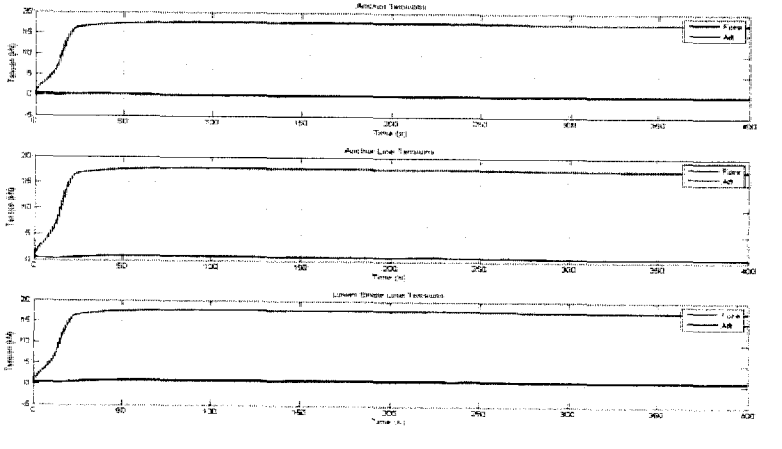

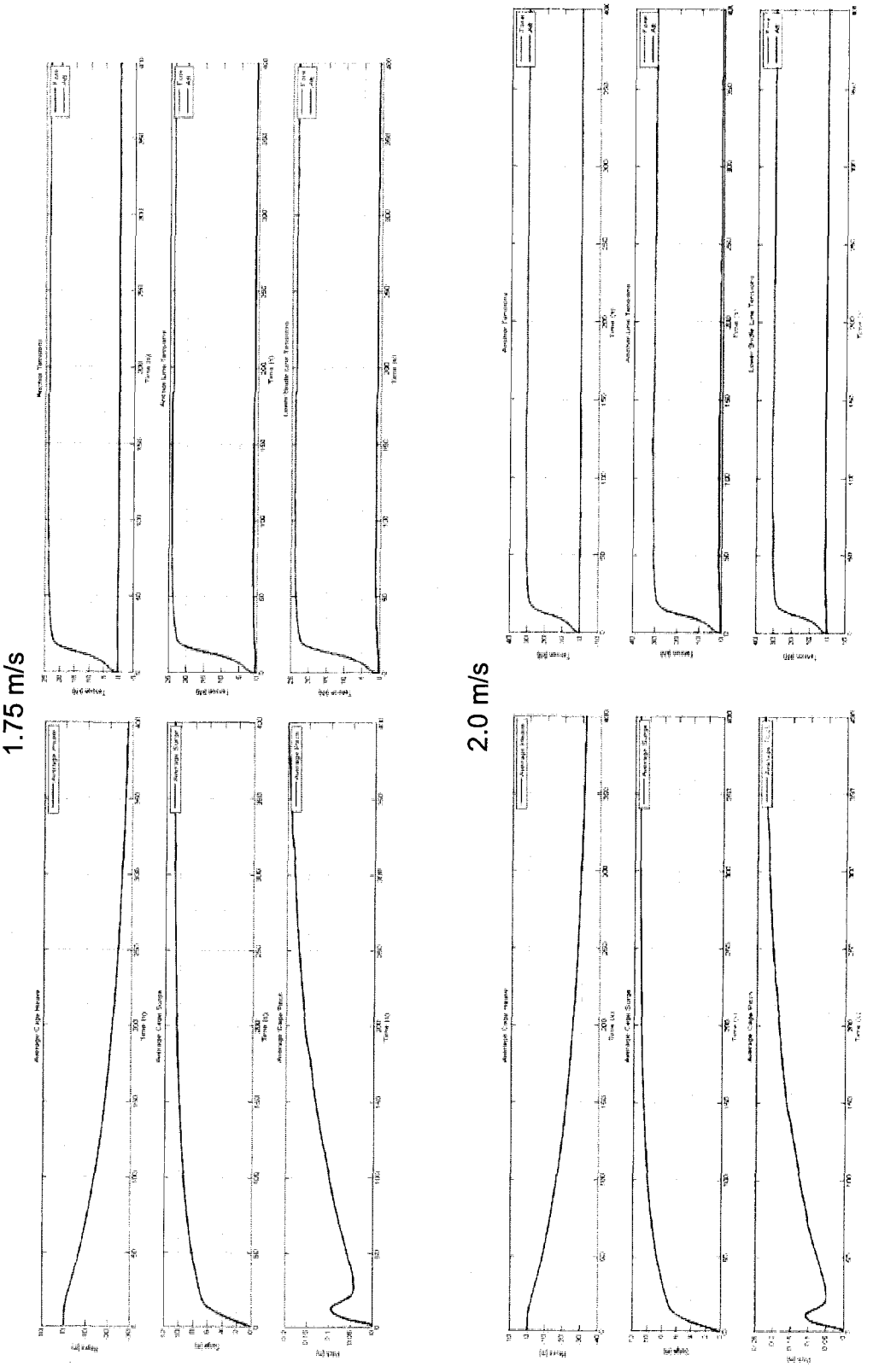
1.75 m/s
2.0 m/s

APPENDIX D - Motion Response and Tension Plots for the Single Cage Mooring: Transverse Loading

0.25 m/s

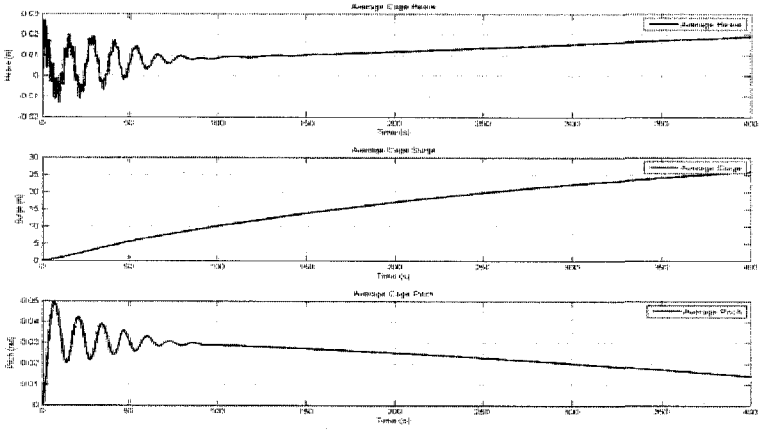

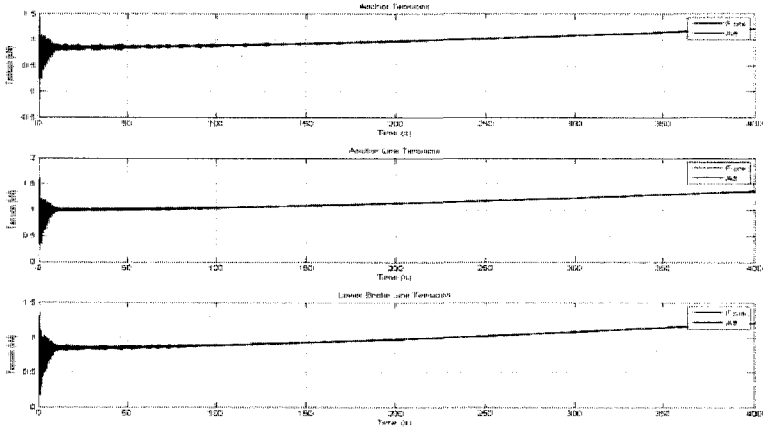

0.5 m/s

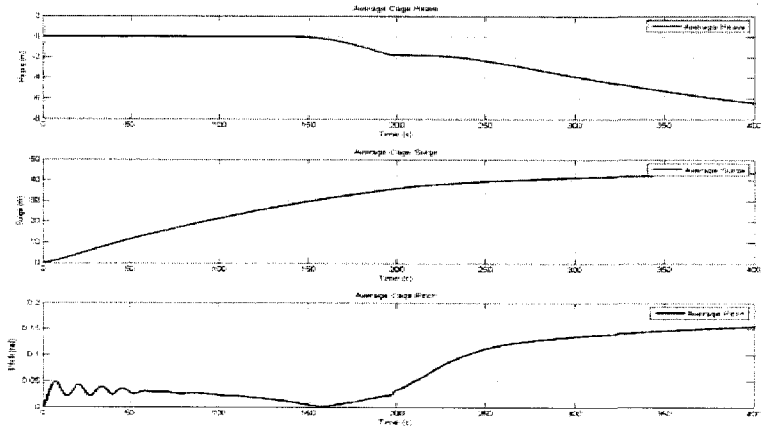

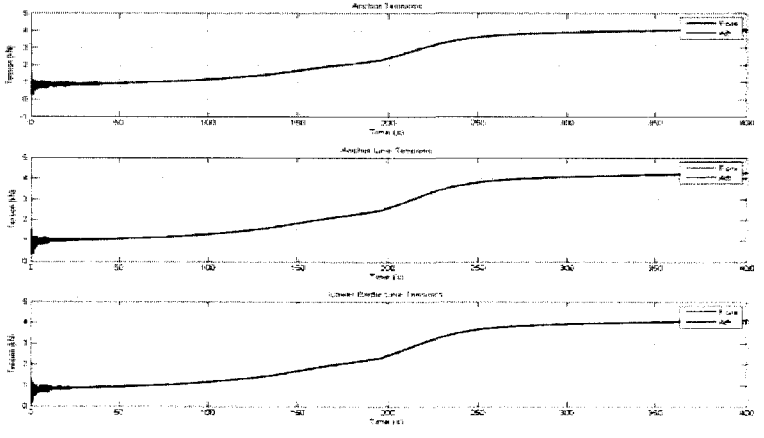

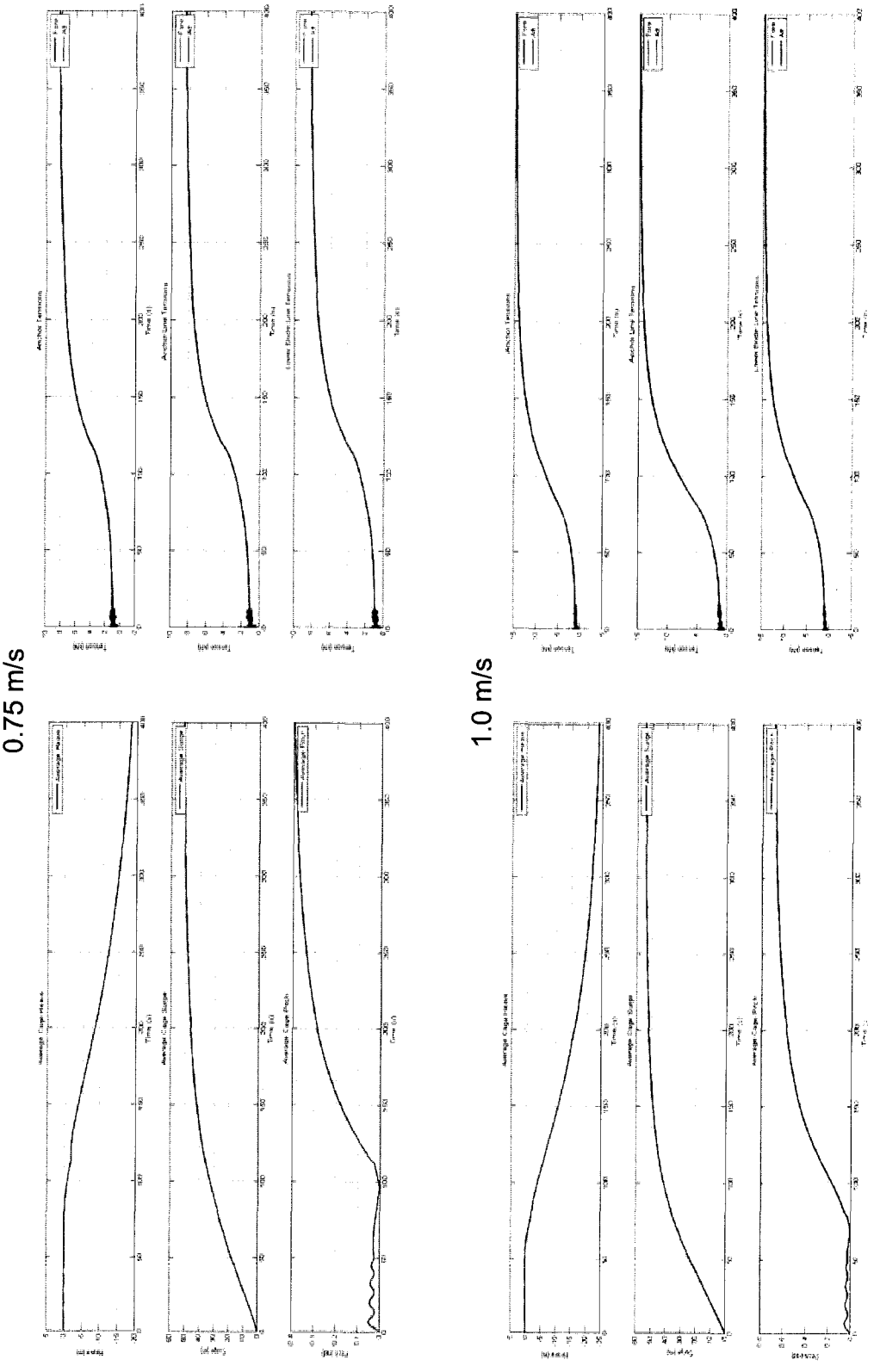
0.75 m/s
1.0 m/s

1.25 m/s

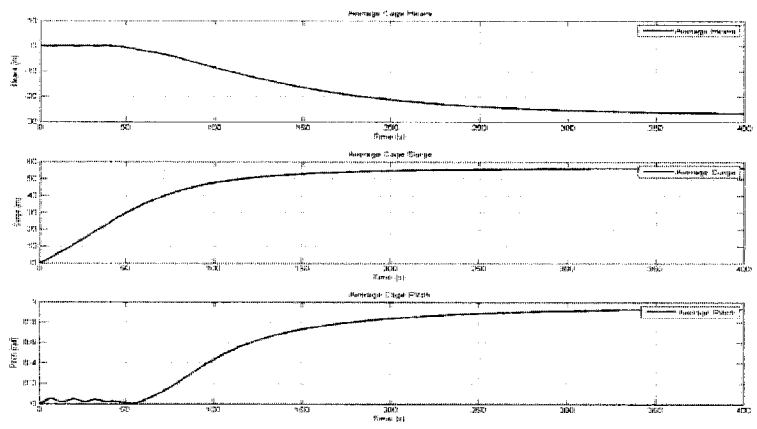

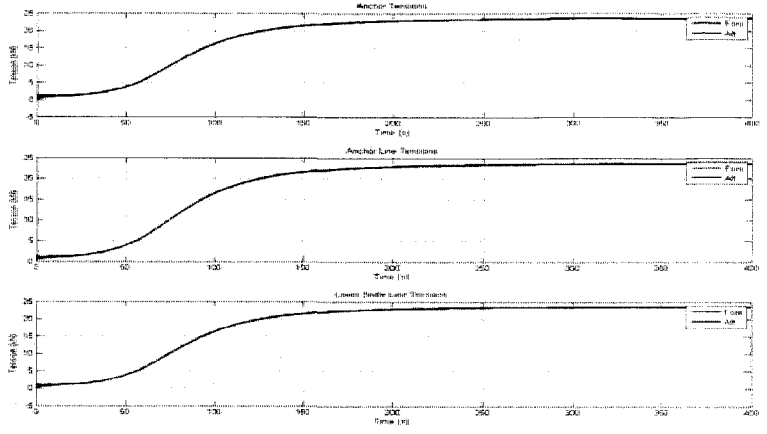

1.5 m/s

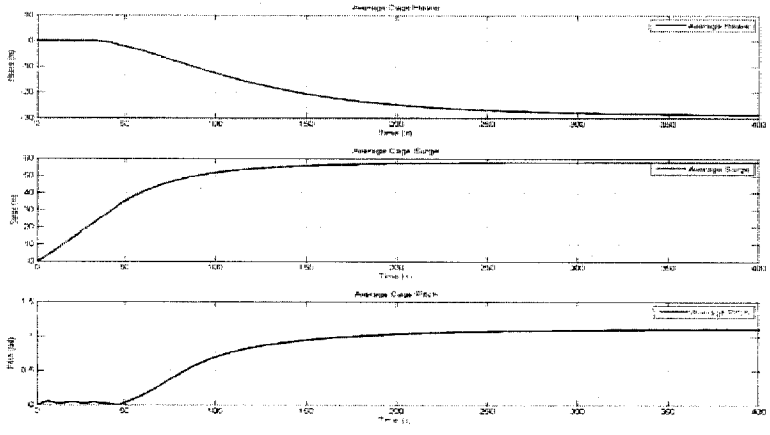

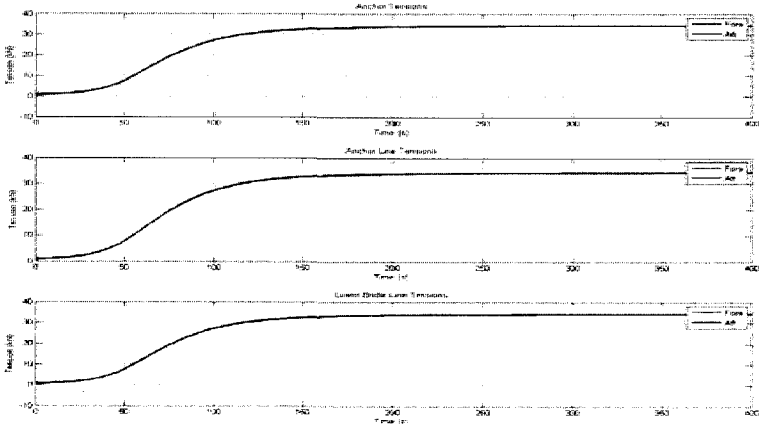

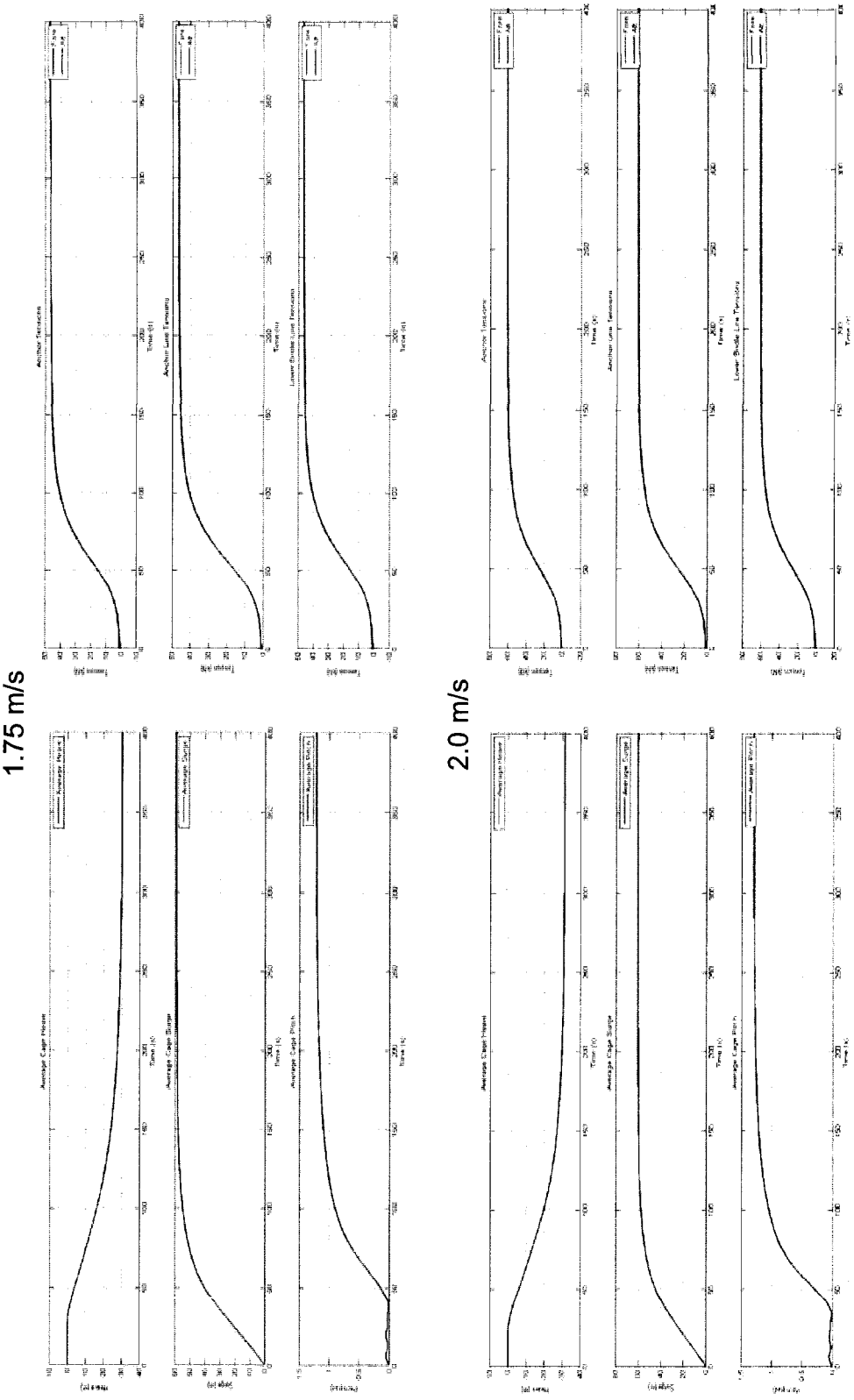
1.75 m/s
2.0 m/s

APPENDIX E - Motion Response Values for the Six Cage Mooring: In-line Loading

Current Velocity (m/s)		0.25	0.5	0.75	1.0	1.25	1.5	1.75	2.0
Heave (m)	1	-1.7606	-8.0436	-14.943	-19.874	-23.461	-26.216	-27.931	-30.188
	2	-0.01625	-2.5735	-9.0811	-14.772	-19.203	-22.726	-24.953	-27.95
	3	-0.02245	-0.46947	-4.8741	-10.377	-15.266	-19.391	-22.065	-25.753
	4	-0.02176	-0.16681	-2.4437	-6.8549	-11.747	-16.277	-19.334	-23.641
	5	-0.0211	-0.16861	-0.91869	-4.2885	-8.7418	-13.491	-16.87	-21.728
	6	-0.00538	-0.14847	-0.62672	-2.3387	-6.3546	-11.366	-15.095	-20.423
Surge (m)	1	5.7697	8.0925	9.8254	11.142	12.337	13.552	14.898	16.376
	2	5.7734	7.9289	9.773	11.37	12.889	14.458	16.203	18.121
	3	5.8041	7.9875	9.8239	11.568	13.324	15.171	17.236	19.51
	4	5.8292	8.0656	9.9336	11.736	13.641	15.691	17.998	20.542
	5	5.8475	8.12	10.019	11.858	13.837	16.015	18.483	21.208
	6	5.859	8.1501	10.066	11.883	13.863	16.083	18.615	21.416
Pitch (rad)	1	0.070281	0.10742	0.095916	0.075039	0.055981	0.039812	0.029887	0.01598
	2	0.013253	0.048145	0.066627	0.059412	0.046126	0.03212	0.023421	0.008897
	3	0.004561	0.004218	0.032639	0.039145	0.031965	0.020817	0.013066	0.000449
	4	0.005244	0.01551	0.002351	0.013571	0.011516	0.002325	0.00527	0.017778
	5	0.005843	0.023422	0.028006	0.019967	0.022618	0.034136	0.042915	0.055996
	6	0.018238	0.02304	0.066837	0.090651	0.12368	0.16069	0.18861	0.21192

APPENDIX E (cont) - Motion Response Values for the Six Cage Mooring: Transverse Loading

Current Velocity (m/s)		0.25	0.5	0.75	1.0	1.25	1.5	1.75	2.0
Heave (m)	1	0.035925	-9.6866	-17.999	-23.18	-25.068	-25.779	-26.672	-27.288
	2	0.003362	-4.2274	-13.701	-20.031	-22.36	-23.25	-24.38	-25.114
	3	0.002901	-2.0318	-11.543	-18.43	-20.976	-21.956	-23.213	-24.013
	4	0.003051	-2.0966	-11.629	-18.489	-21.024	-22.003	-23.254	-24.048
	5	0.004886	-4.5171	-13.962	-20.209	-22.506	-23.392	-24.506	-25.224
	6	-0.03219	-10.245	-18.435	-23.481	-25.319	-26.021	-26.885	-27.487
Surge (m)	1	33.533	47.218	53.947	59.237	64.004	68.949	74.139	79.355
	2	39.131	57.63	65.982	72.551	78.5	84.687	91.182	97.747
	3	41.42	62.764	71.971	79.21	85.793	92.647	99.844	107.13
	4	41.315	62.509	71.66	78.864	85.42	92.245	99.414	106.67
	5	38.773	56.869	65.058	71.523	77.394	83.5	89.916	96.388
	6	32.785	45.941	52.432	57.565	62.208	67.026	72.088	77.164
Pitch (rad)	1	0.020223	0.085613	0.22943	0.42194	0.62794	0.81261	0.96433	1.0749
	2	0.027139	0.073031	0.22941	0.43107	0.64317	0.83047	0.98324	1.0938
	3	0.028359	0.061589	0.22836	0.43622	0.65289	0.84232	0.99595	1.1072
	4	0.02834	0.062899	0.22915	0.43746	0.65447	0.84395	0.99709	1.1091
	5	0.026978	0.075035	0.23181	0.43431	0.64796	0.83617	0.98948	1.0981
	6	0.019672	0.088304	0.23269	0.42669	0.63475	0.82142	0.97331	1.0833

APPENDIX F - Motion Response and Tension Plots for the Six Cage Mooring: In-line Loading

0.25 m/s

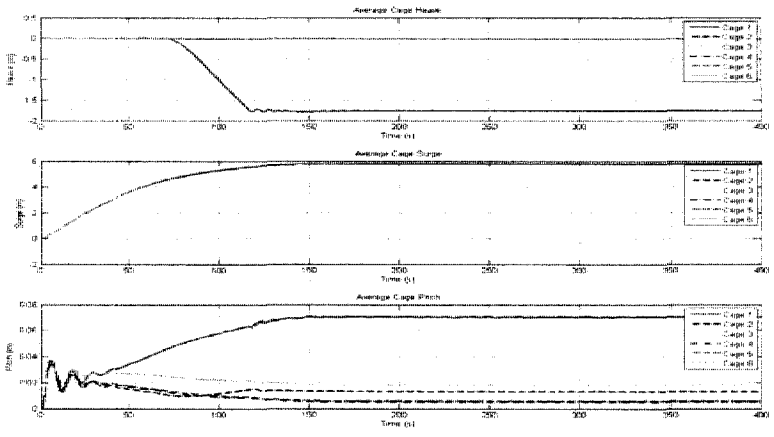

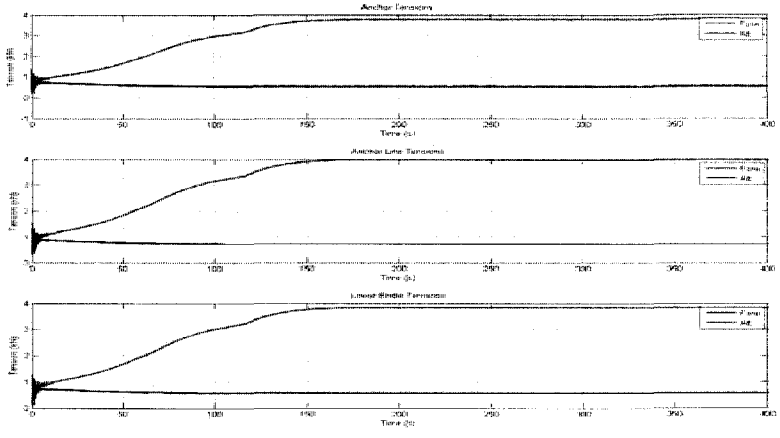

0.5 m/s

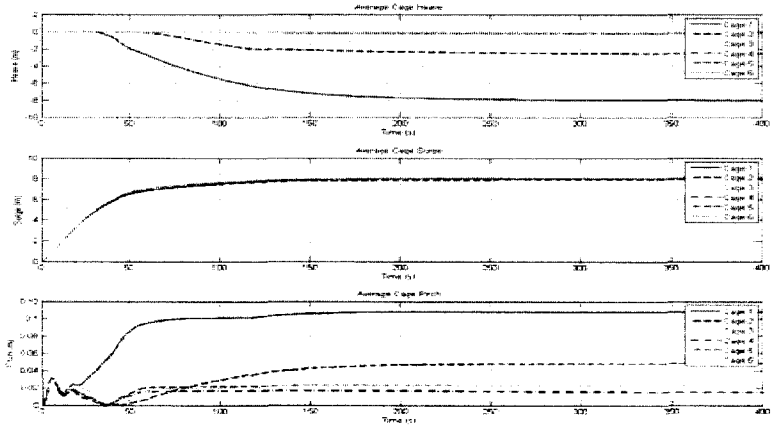

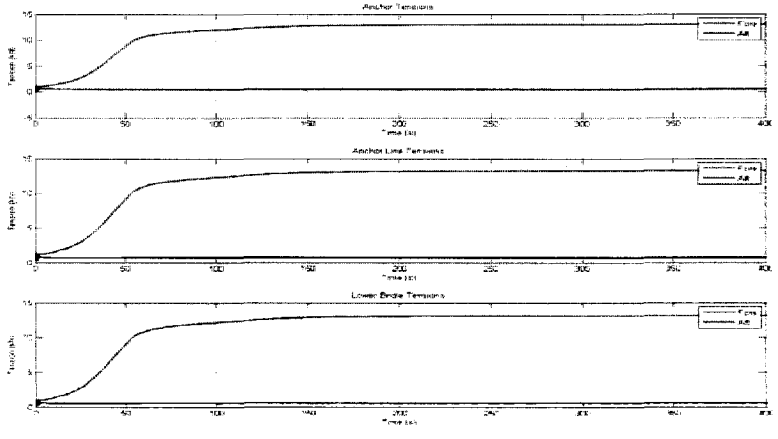

0.75 m/s

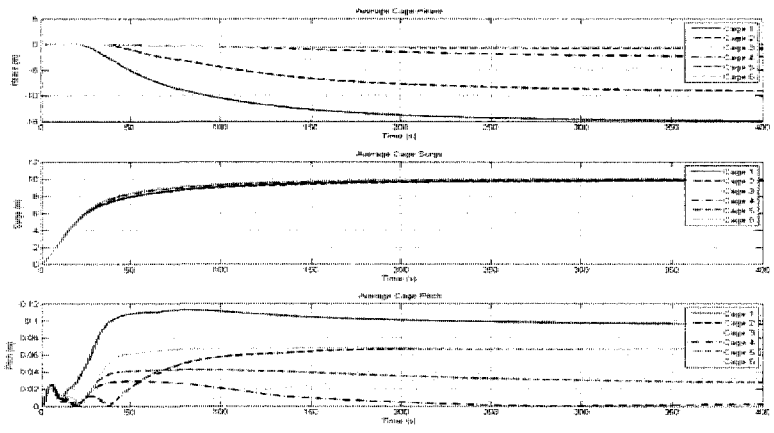

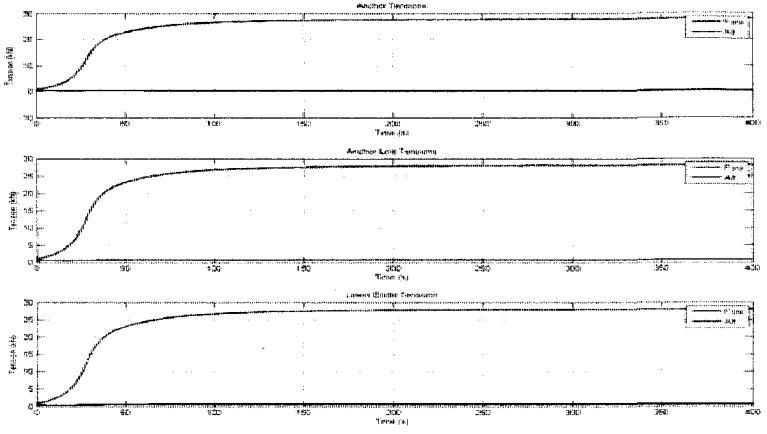

1.0 m/s

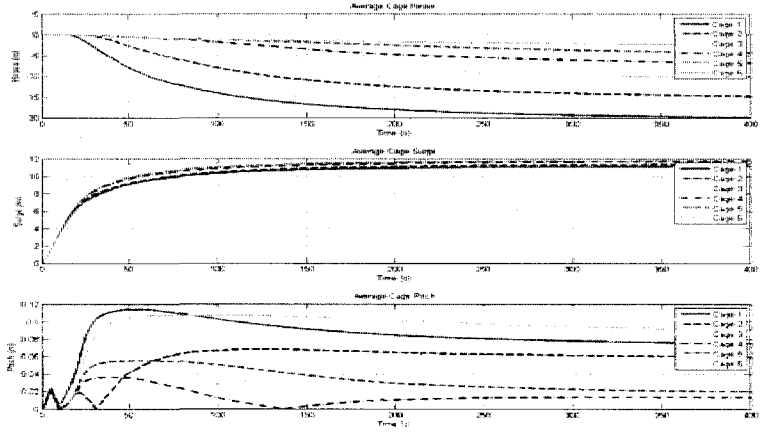

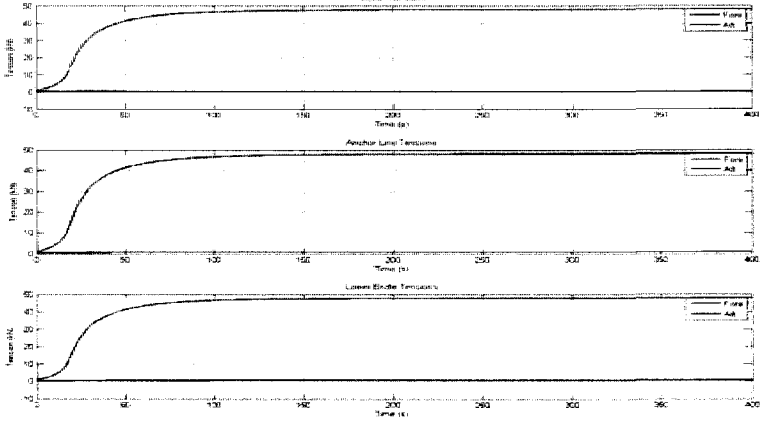

1.25 m/s

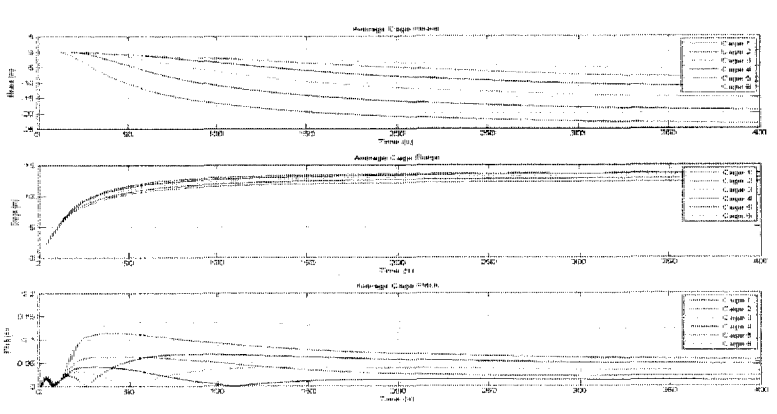

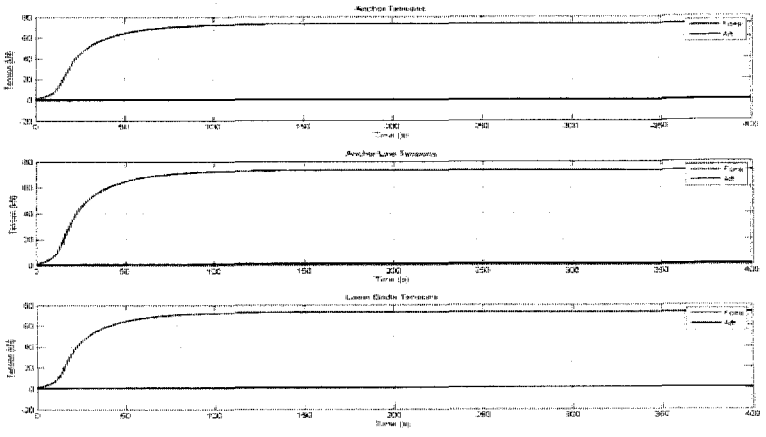

1.5 m/s

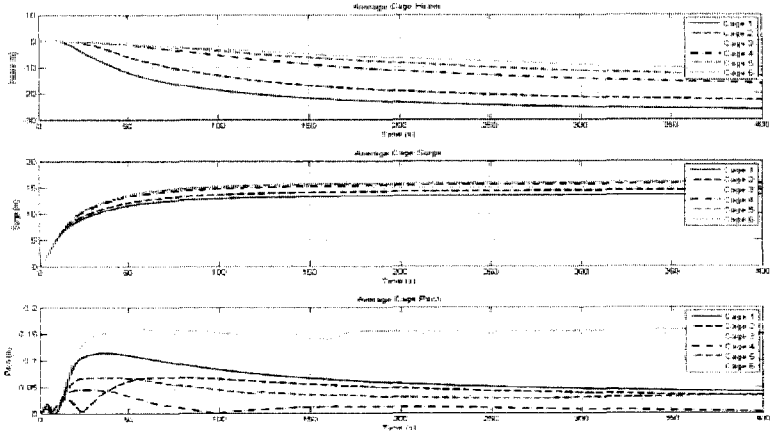

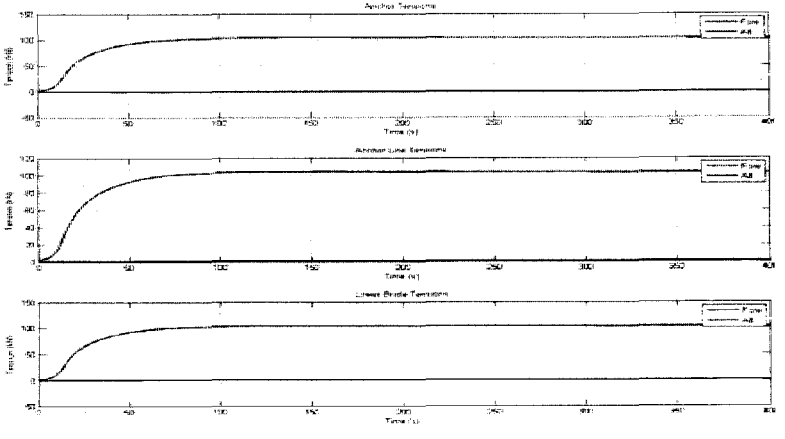

1.75 m/s

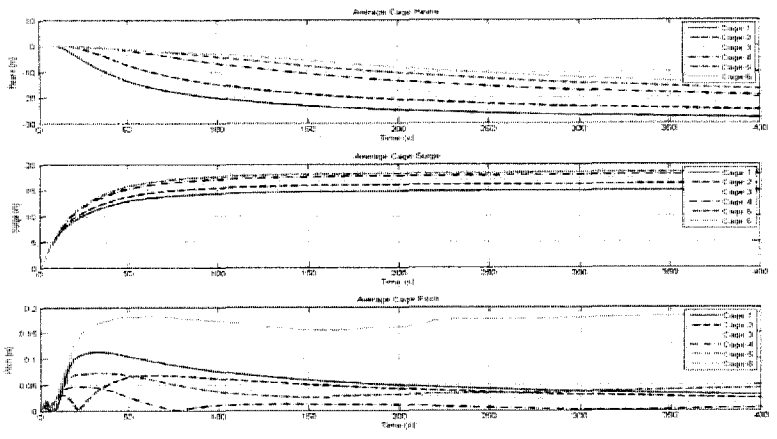

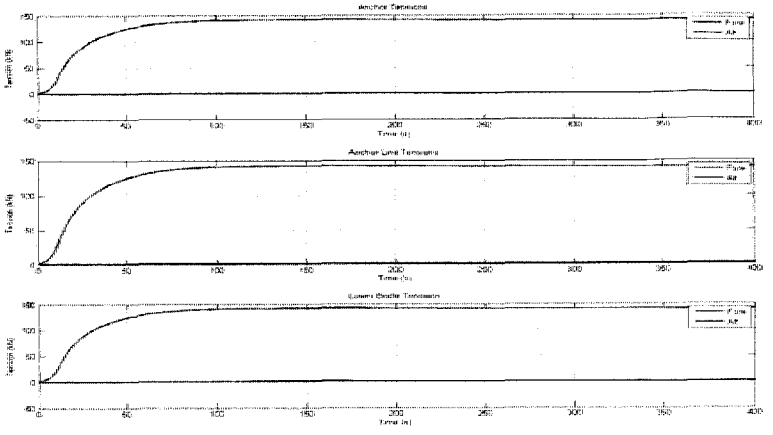

2.0 m/s

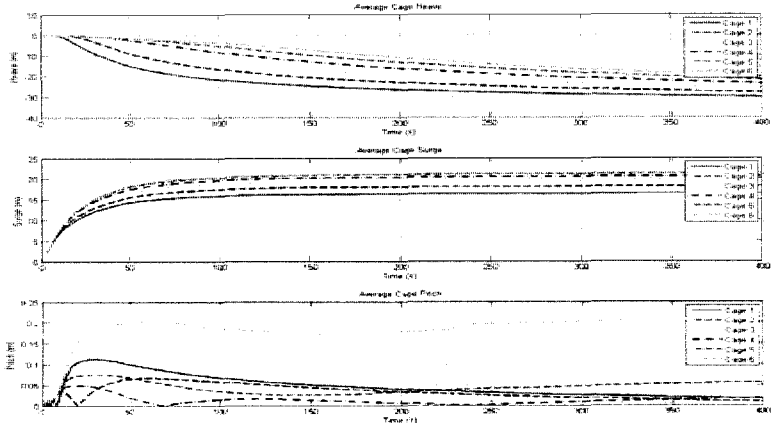

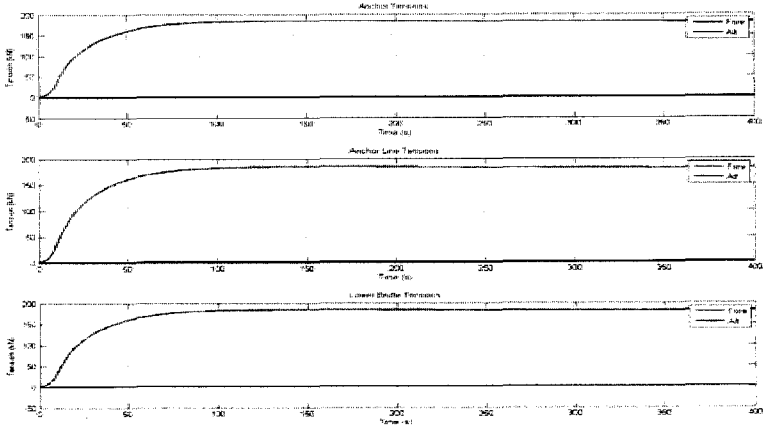

APPENDIX G - Motion Response and Tension Plots for the Six Cage Mooring: Transverse Loading

0.25 m/s

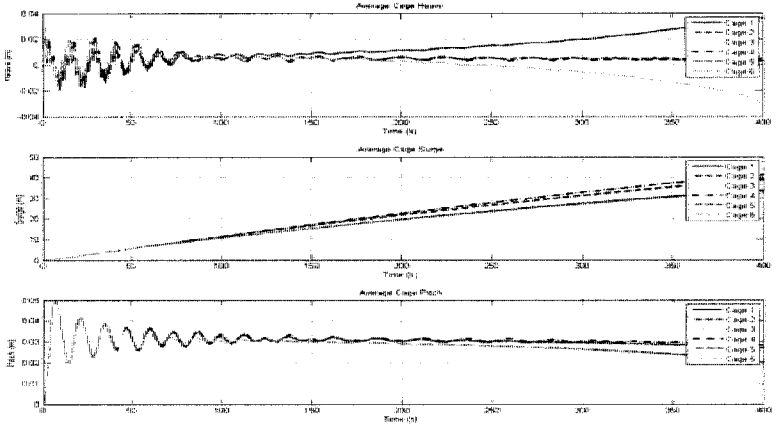

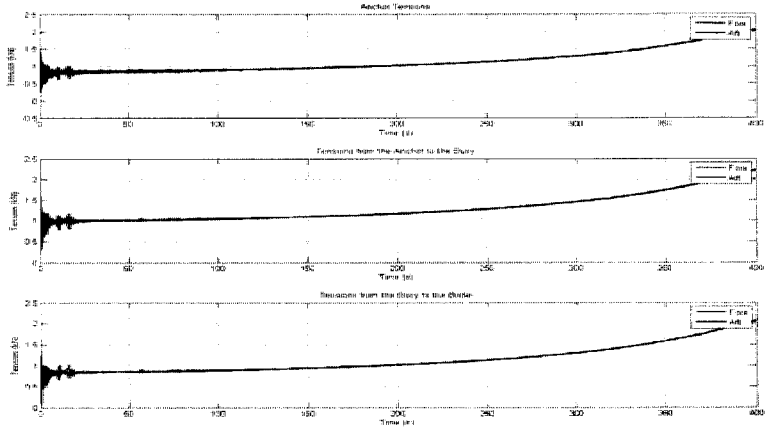

0.5 m/s

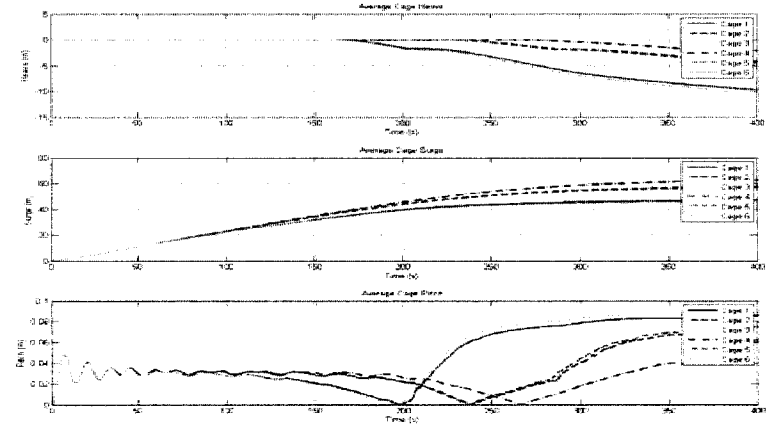

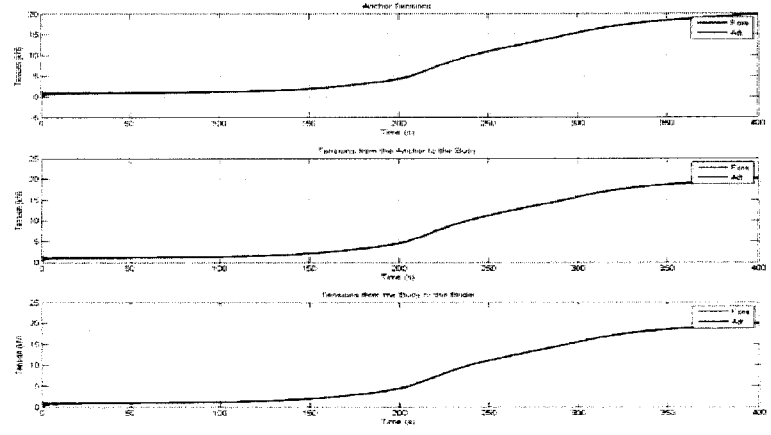

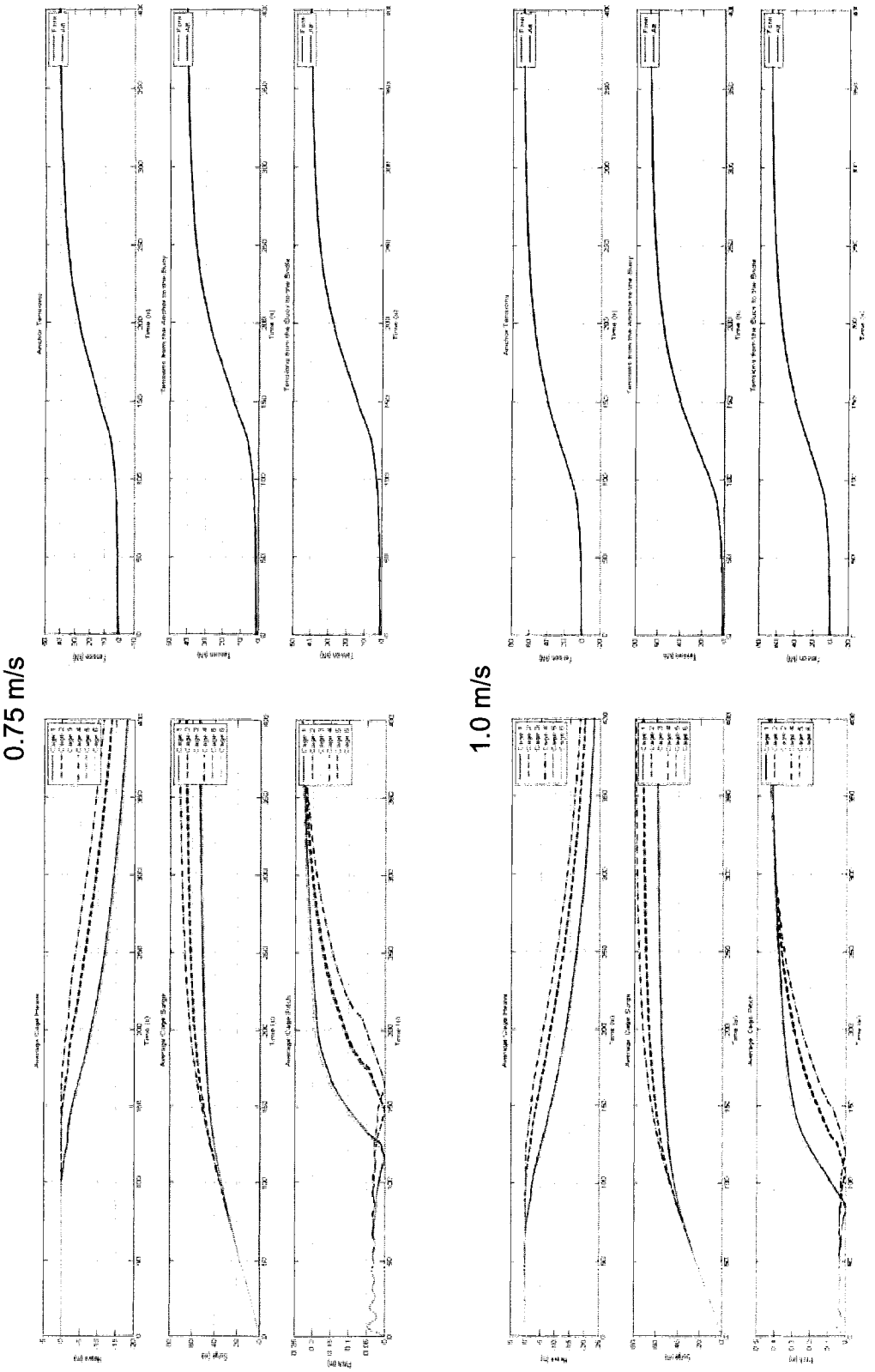
0.75 m/s
1.0 m/s

1.25 m/s

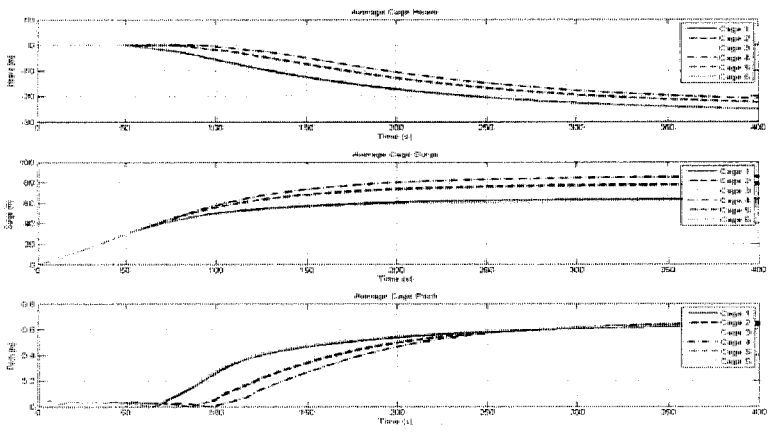

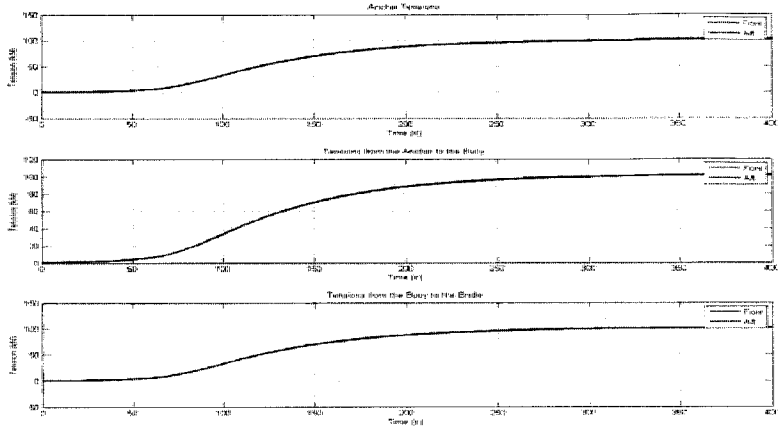

1.5 m/s

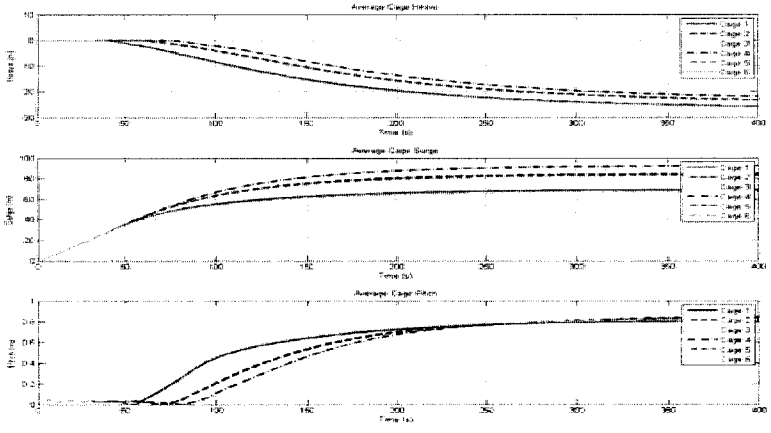

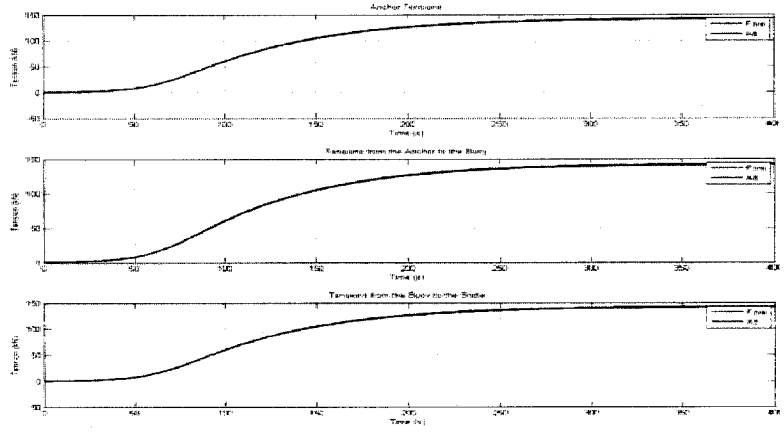

1.75 m/s

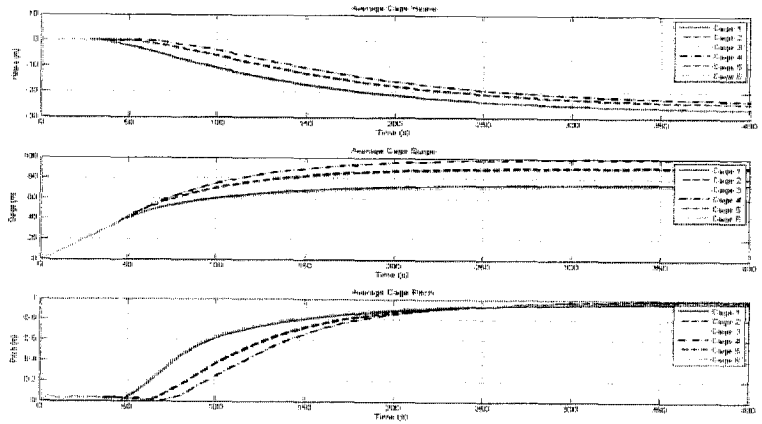

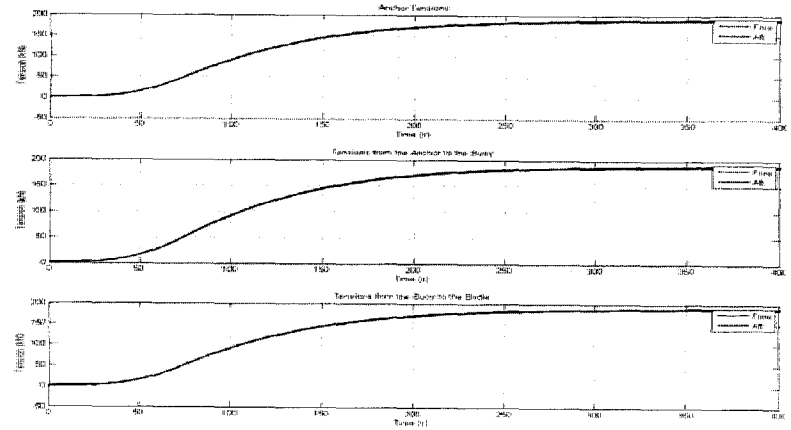

2.0 m/s

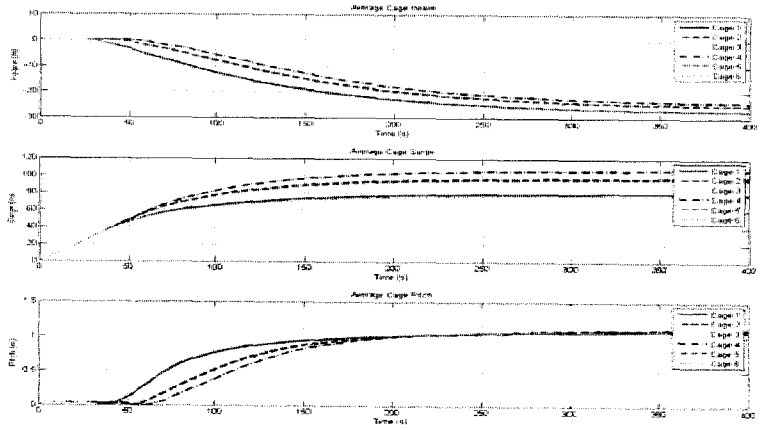

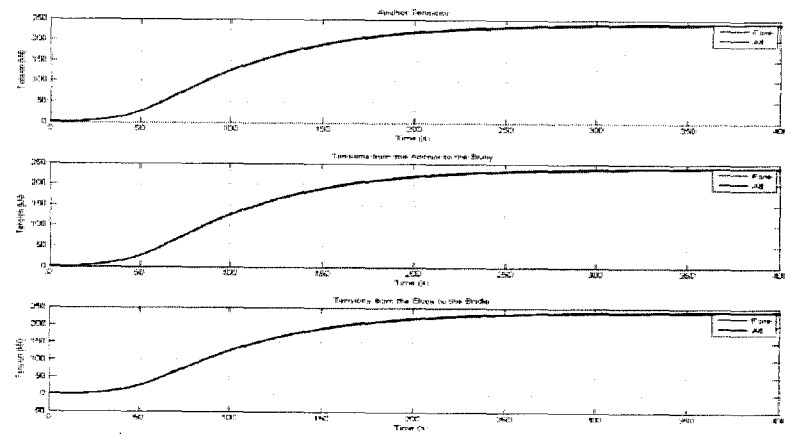

APPENDIX H – RAO Plots for the Single Cage Mooring

Heave RAO (in-line)

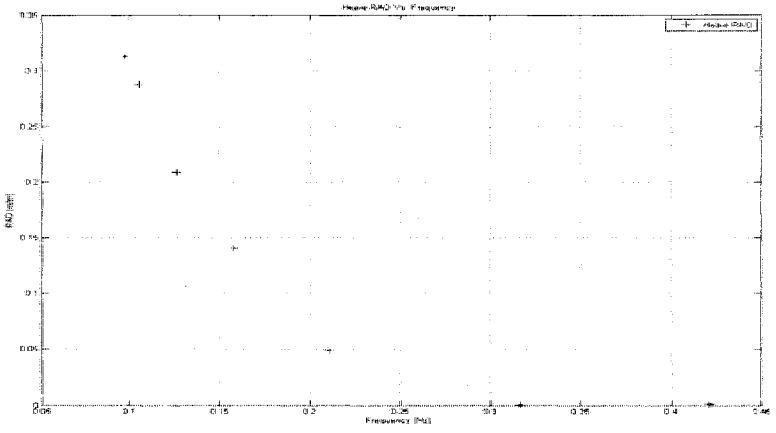

Surge RAO (in-line)

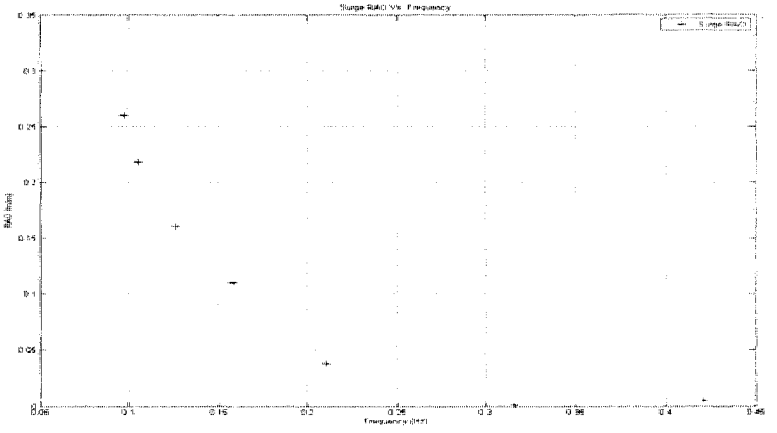

Pitch RAO (in-line)

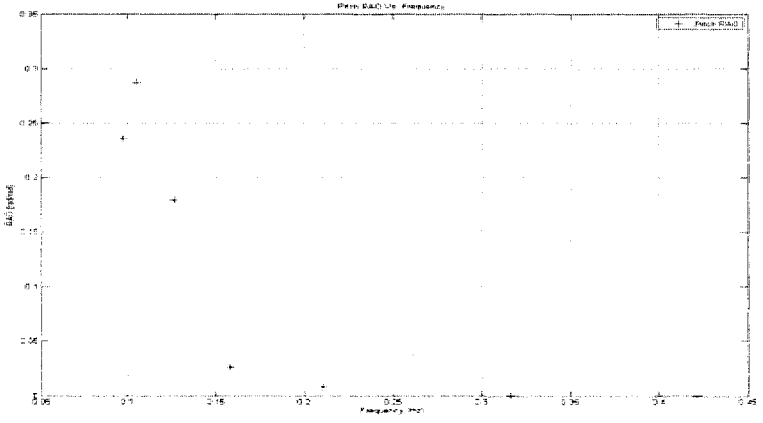

Tension RAO (in-line)

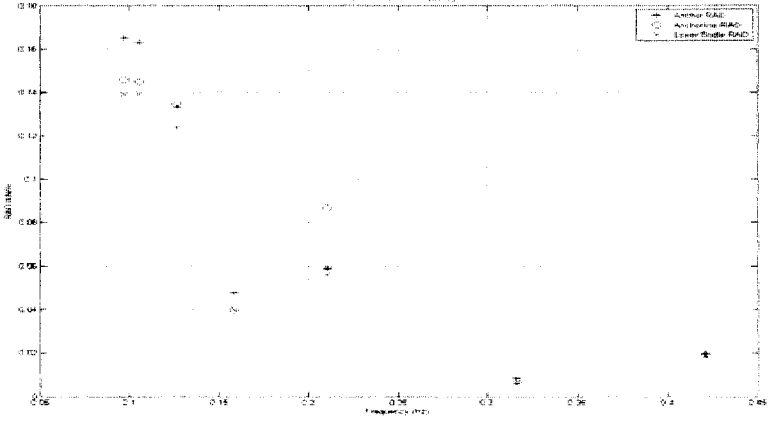

Heave RAO (transverse)

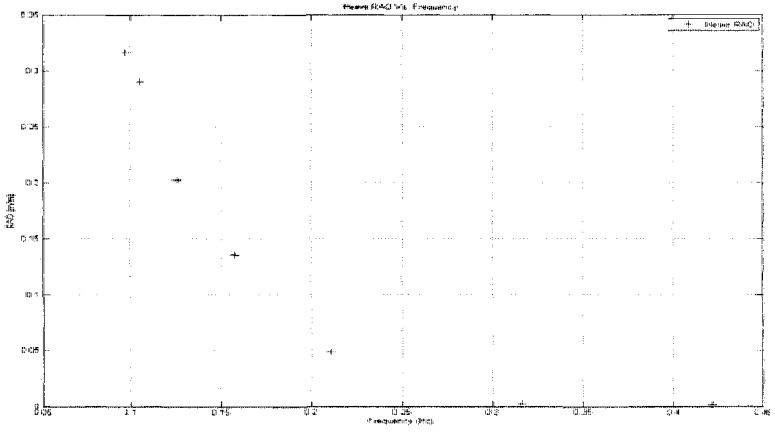

Surge RAO (transverse)

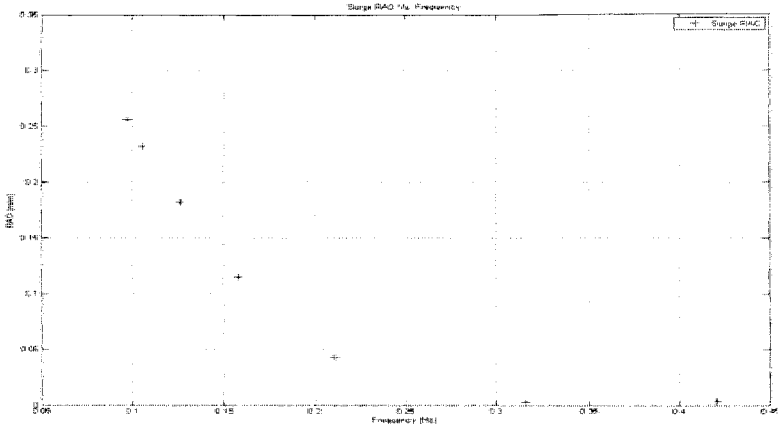

Pitch RAO (transverse)

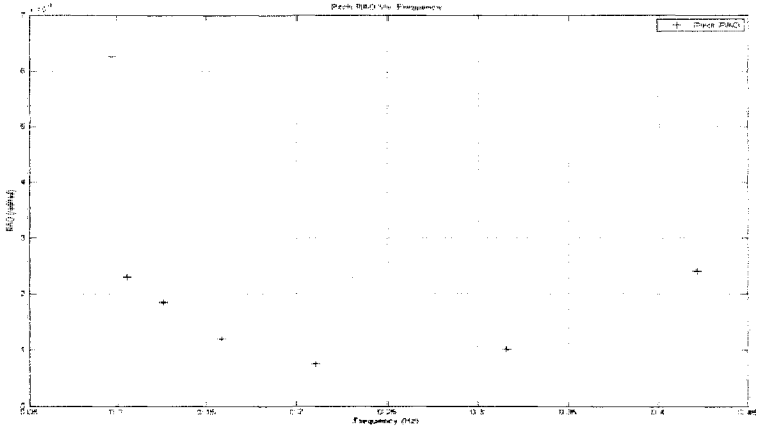

Tension RAO (transverse)

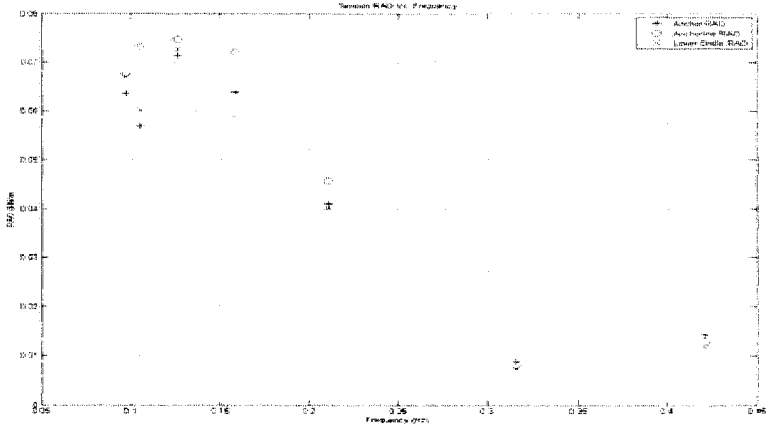

APPENDIX I – RAO Data for the Six Cage Mooring

In-Line Loading

Wave Regime		1	2	3	4	5	6	7
Heave RAO (m/m)	1	0.0013	0.0025	0.0499	0.1520	0.2057	0.2561	0.2586
	2	0.0021	0.0023	0.0501	0.1442	0.1835	0.2460	0.2553
	3	0.0023	0.0023	0.0526	0.1465	0.1888	0.2326	0.2501
	4	0.0021	0.0024	0.0503	0.1494	0.1961	0.2521	0.2517
	5	0.0014	0.0025	0.0511	0.1426	0.2062	0.2395	0.2481
	6	0.0013	0.0021	0.0538	0.1331	0.1997	0.2634	0.2812
Surge RAO (m/m)	1	0.0014	0.0013	0.0206	0.1364	0.1030	0.0676	0.0763
	2	0.0019	0.0015	0.0129	0.1081	0.0543	0.0565	0.0691
	3	0.0022	0.0010	0.0064	0.0860	0.0463	0.0114	0.0266
	4	0.0026	0.0011	0.0070	0.0901	0.0570	0.0369	0.0247
	5	0.0021	0.0011	0.0125	0.0656	0.0783	0.0149	0.0313
	6	0.0025	0.0017	0.0217	0.0404	0.0916	0.0972	0.1083
Pitch RAO (rad/rad)	1	0.0005	0.0011	0.0325	0.1656	0.3194	0.6467	0.8831
	2	0.0006	0.0016	0.0482	0.0598	0.3606	0.7918	1.0413
	3	0.0005	0.0015	0.0377	0.1706	0.3499	0.7940	0.9705
	4	0.0005	0.0017	0.0368	0.1492	0.3500	0.7528	1.0389
	5	0.0003	0.0013	0.0478	0.1206	0.3496	0.7871	1.0088
	6	0.0007	0.0016	0.0365	0.1424	0.2749	0.7176	0.9860
Anchor Tension RAO (kN/m)		0.0132	0.0071	0.0465	0.1038	0.1052	0.0487	0.0476
Anchor Line Tension RAO (kN/m)		0.0105	0.0049	0.0489	0.0879	0.1079	0.0638	0.0548
Lower Bridle Tension RAO (kN/m)		0.0104	0.0046	0.0540	0.0939	0.1536	0.0978	0.0715

APPENDIX I (cont) - RAO Data for the Six Cage Mooring:

Transverse Loading

Wave Regime		1	2	3	4	5	6	7
Heave RAO (m/m)	1	0.0012	0.0023	0.0472	0.1343	0.1868	0.2889	0.3150
	2	0.0021	0.0024	0.0492	0.1326	0.1862	0.2867	0.3186
	3	0.0016	0.0023	0.0476	0.1330	0.1870	0.2855	0.3075
	4	0.0019	0.0022	0.0490	0.1334	0.1873	0.2855	0.3168
	5	0.0019	0.0023	0.0491	0.1336	0.1857	0.2851	0.3097
	6	0.0013	0.0022	0.0472	0.1349	0.1865	0.2873	0.3100
Surge RAO (m/m)	1	0.0040	0.0026	0.0426	0.1143	0.1841	0.2330	0.2387
	2	0.0033	0.0026	0.0426	0.1144	0.1842	0.2327	0.2347
	3	0.0008	0.0026	0.0425	0.1145	0.1842	0.2332	0.2355
	4	0.0013	0.0025	0.0426	0.1147	0.1841	0.2332	0.2346
	5	0.0016	0.0026	0.0425	0.1143	0.1841	0.2330	0.2335
	6	0.0027	0.0026	0.0426	0.1144	0.1834	0.2313	0.2341
Pitch RAO (rad/rad)	1	0.0016	0.0004	0.0048	0.0100	0.0232	0.1047	0.1840
	2	0.0019	0.0004	0.0066	0.0208	0.0237	0.1020	0.1776
	3	0.0018	0.0004	0.0039	0.0210	0.0227	0.1077	0.1613
	4	0.0018	0.0004	0.0045	0.0224	0.0272	0.1040	0.1749
	5	0.0017	0.0005	0.0068	0.0203	0.0210	0.1108	0.1795
	6	0.0017	0.0004	0.0051	0.0142	0.0228	0.1127	0.1833
Anchor Tension RAO (kN/m)		0.0130	0.0089	0.0345	0.0557	0.0674	0.0569	0.0625
Anchor Line Tension RAO (kN/m)		0.0098	0.0084	0.0350	0.0580	0.0694	0.0581	0.0648
Lower Bridle Tension RAO (kN/m)		0.0097	0.0082	0.0389	0.0742	0.0718	0.0680	0.0737

APPENDIX J – RAO Plots for the Six Cage Mooring

Heave RAO (in-line)

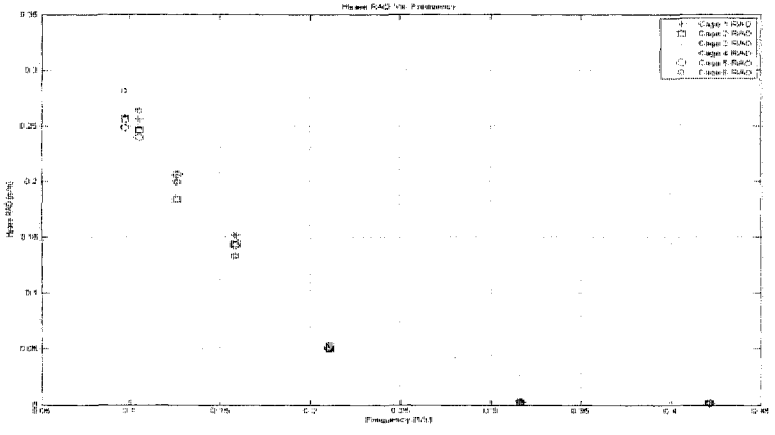

Surge RAO (in-line)

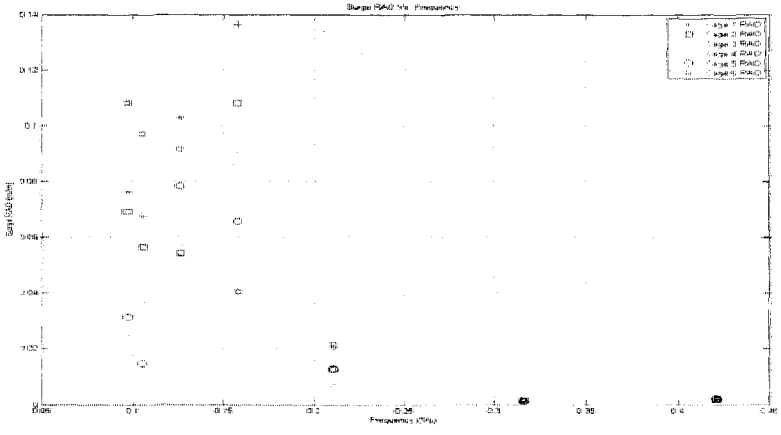

Pitch RAO (in-line)

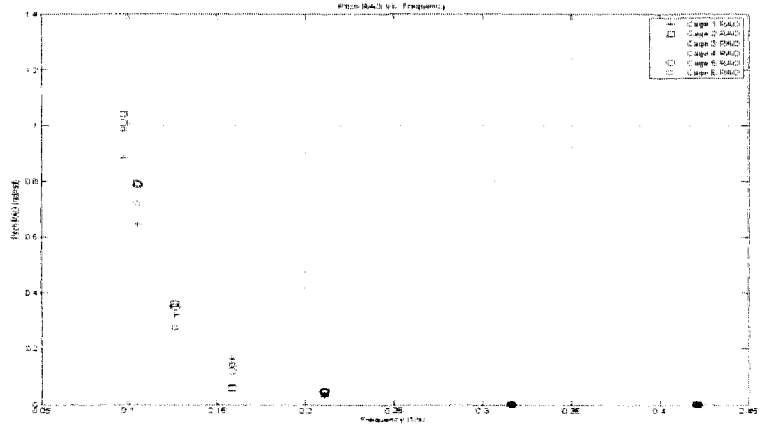

Tension RAO (in-line)

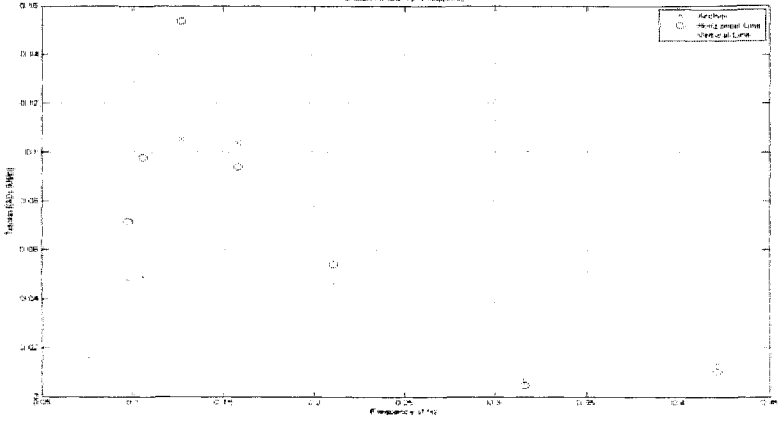

Surge RAO (transverse)

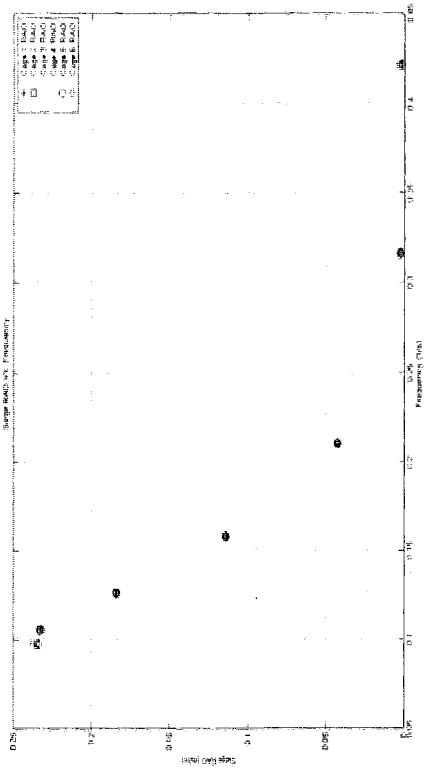

Tension RAO (transverse)

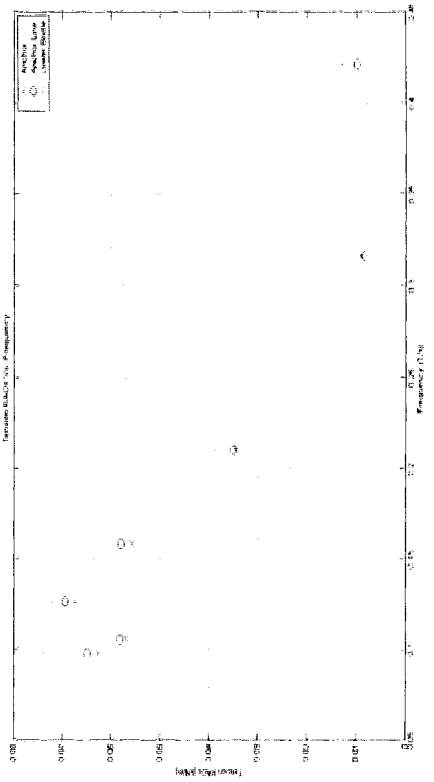

Heave RAO (transverse)

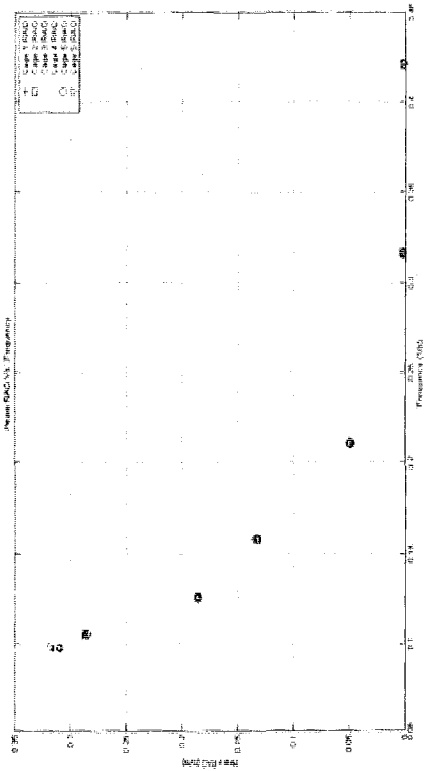

Pitch RAO (transverse)

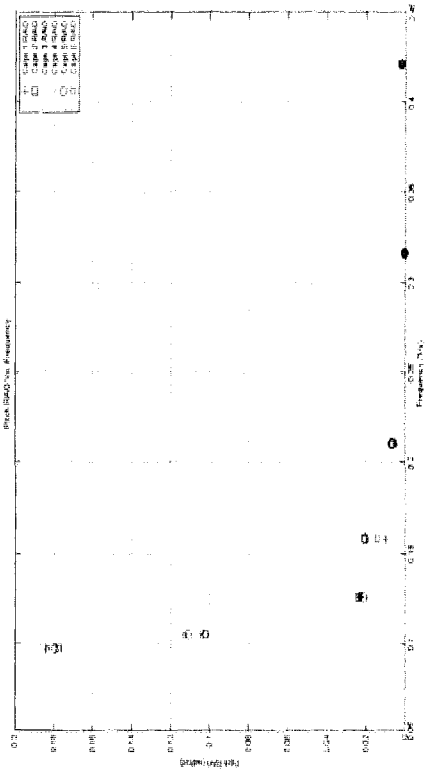

APPENDIX K – Duel Loading Current and Wave Motion Response and Tension Plots: Single Cage

Operational Loading (in-line)

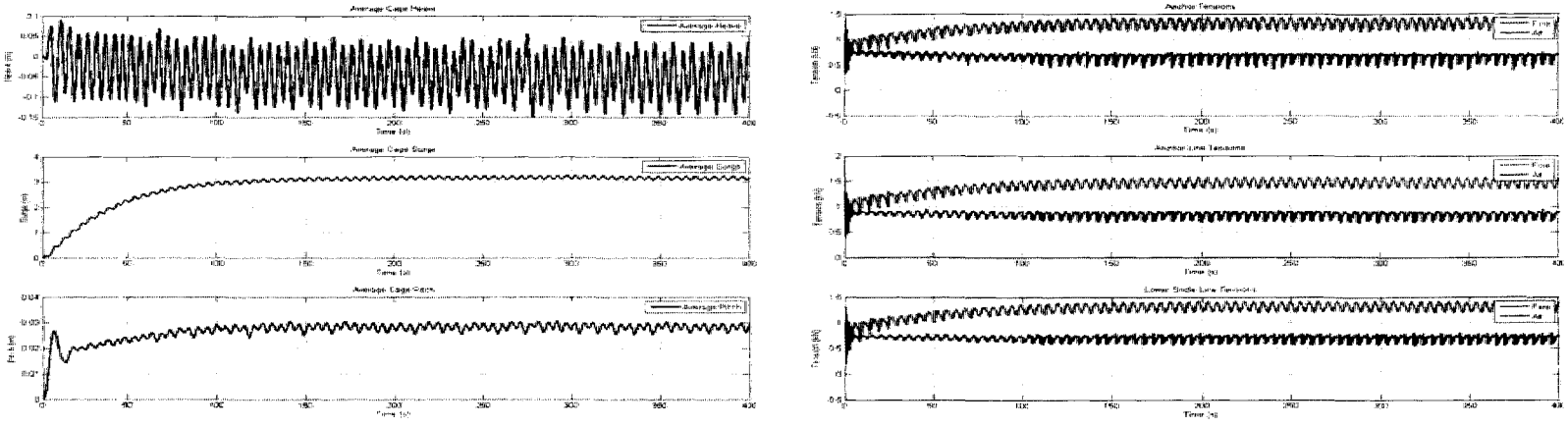

Storm Loading (in-line)

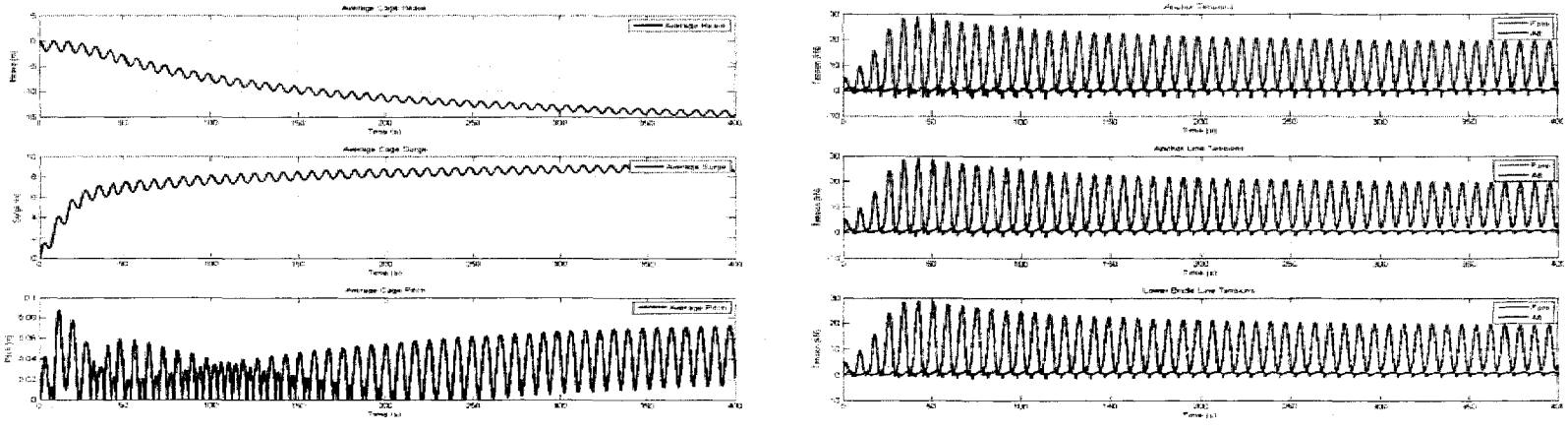

Operational Loading (transverse)

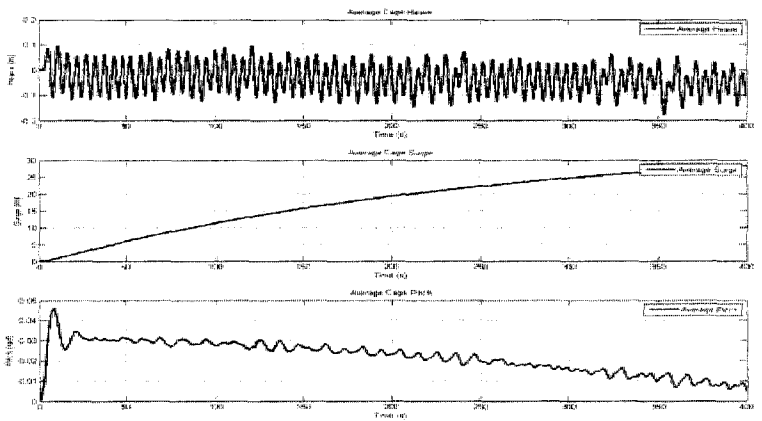

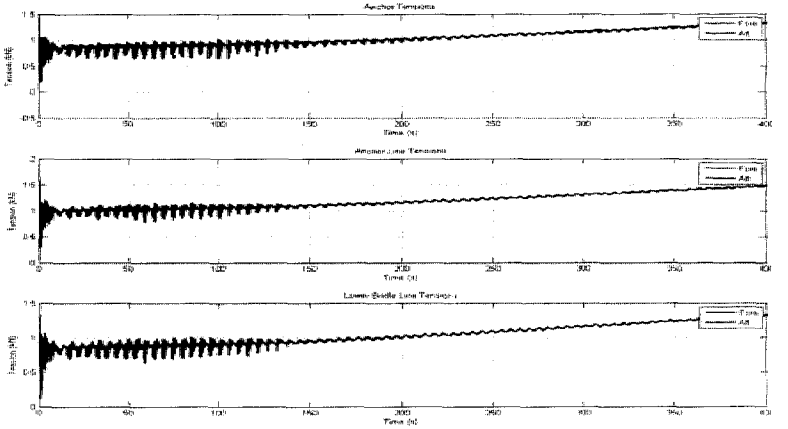

Storm Loading (transverse)

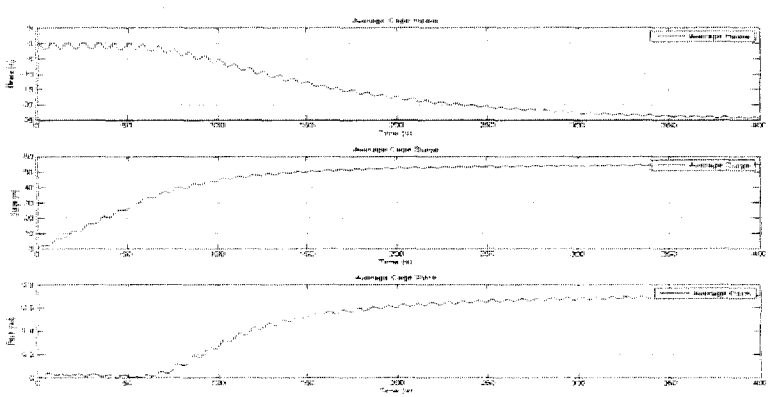

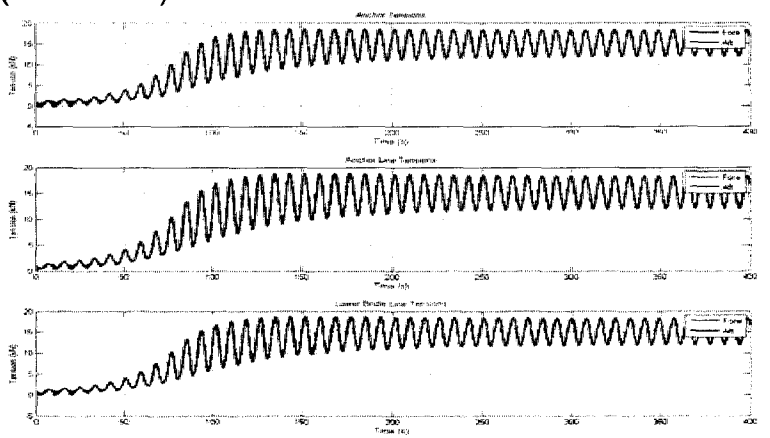

APPENDIX L – Duel Loading Current and Wave Motion Response and Tension Plots: Six Cage

Operational Loading (in-line)

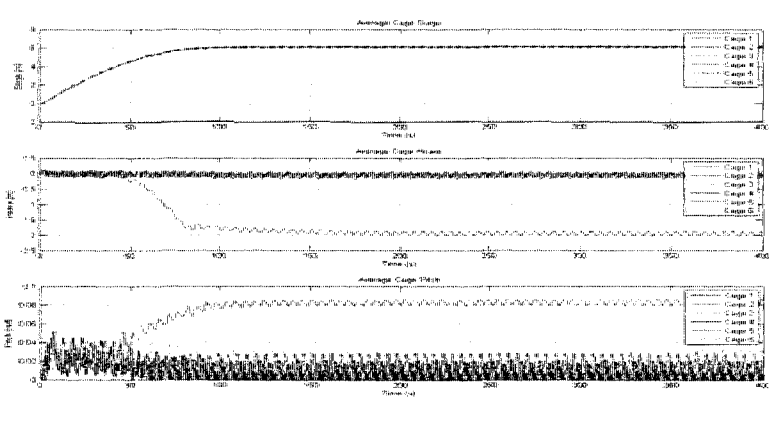

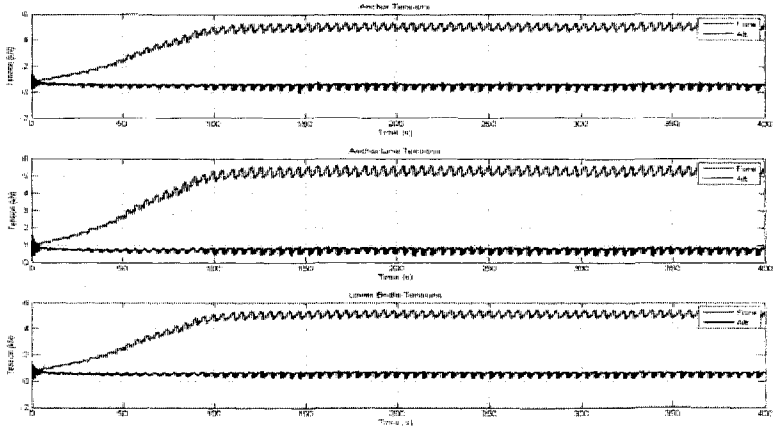

Storm Loading (in-line)

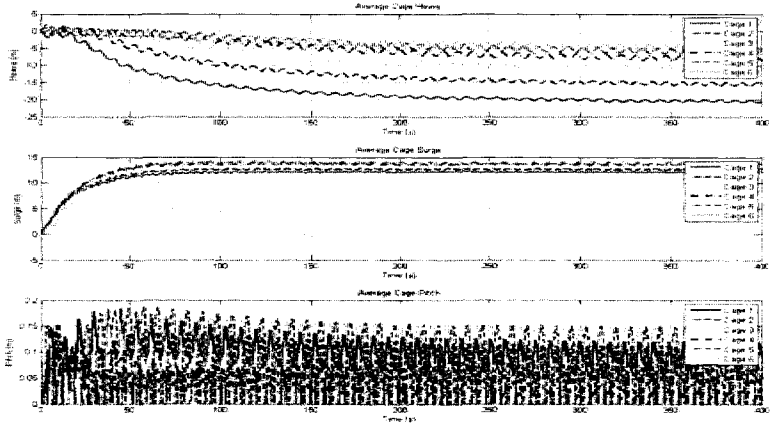

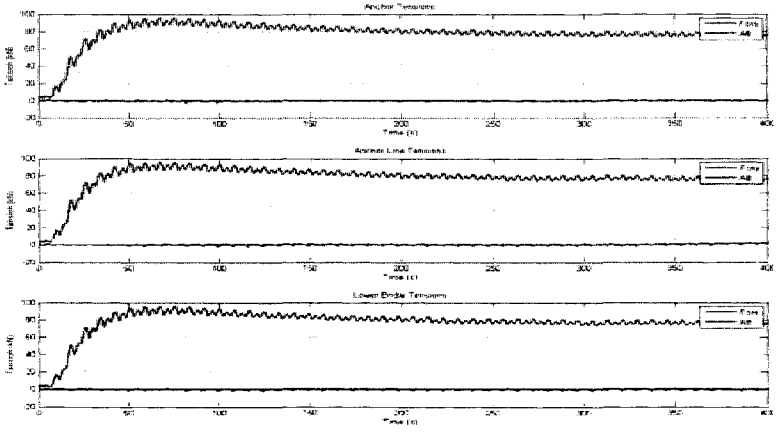

Operational Loading (transverse)

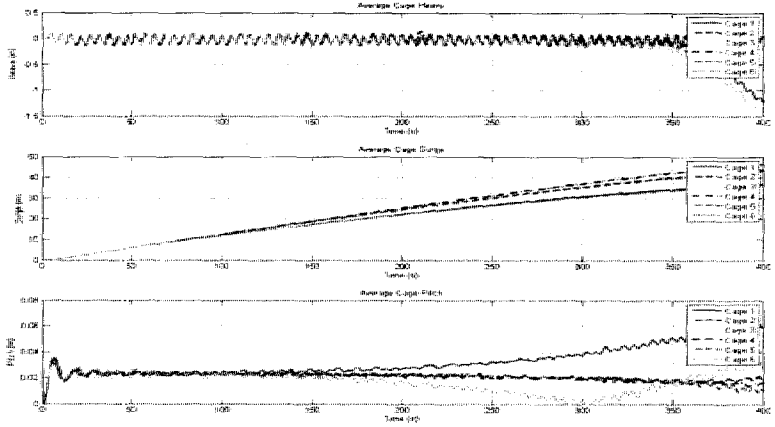

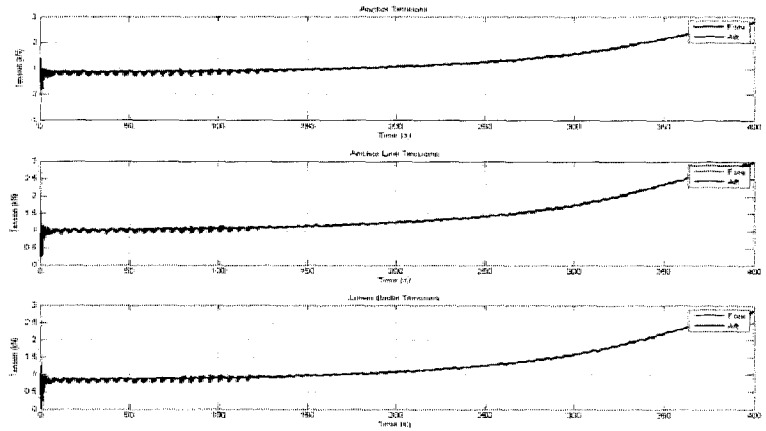

Storm Loading (transverse)

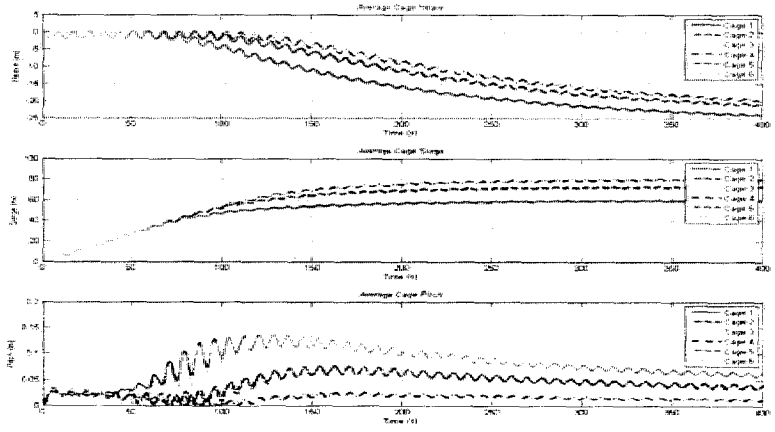

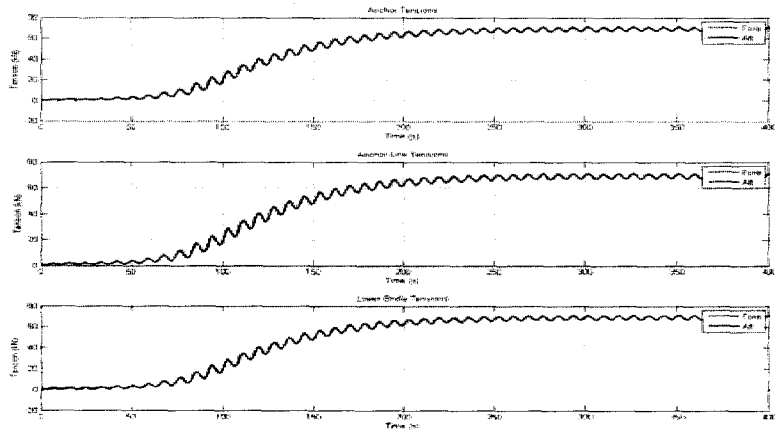

APPENDIX M – Correlation Tension Plots

Anchor Tension

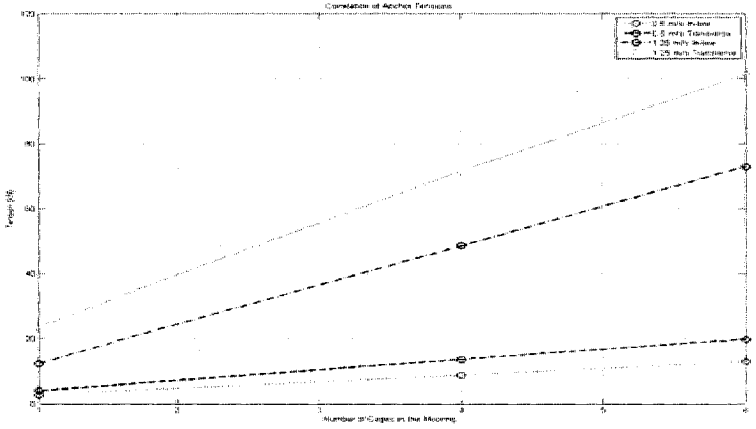

Anchor Line Tension

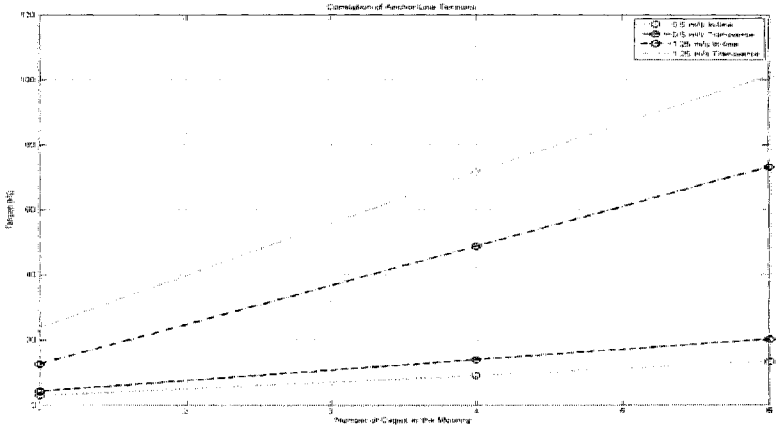

Lower Bridle Tension